Downloaded from orbit.dtu.dk on: Apr 29, 2024

DTU Library

Continuous Oxidative Biocatalysis

Lindeque, Rowan Malan

Publication date:
2020

Document Version
Publisher's PDF, also known as Version of record

Link back to DTU Orbit

Citation (APA):
Lindeque, R. M. (2020). *Continuous Oxidative Biocatalysis*. Technical University of Denmark.

General rights
Copyright and moral rights for the publications made accessible in the public portal are retained by the authors and/or other copyright owners and it is a condition of accessing publications that users recognise and abide by the legal requirements associated with these rights.

- Users may download and print one copy of any publication from the public portal for the purpose of private study or research.
- You may not further distribute the material or use it for any profit-making activity or commercial gain
- You may freely distribute the URL identifying the publication in the public portal

If you believe that this document breaches copyright please contact us providing details, and we will remove access to the work immediately and investigate your claim.

Continuous Oxidative Biocatalysis

Rowan Malan Lindeque

PhD Thesis

October 2020

DTU Chemical Engineering

Abstract

Enzymes have a number of characteristics that make them attractive as biocatalytic alternatives to conventional transition-metal based catalysts for the production of both high- and low-value products. These include, but are not limited to, mild operating conditions, high enantioselectivity and the possibility of modifying their properties to better suit a process. In particular, the use of oxidases to catalyze selective oxidations using molecular oxygen as an environmentally friendly oxidant, is gaining attention. However, as most industries are trending towards continuous processing to improve efficiency, biocatalysis must do the same. Since continuous biocatalysis is an emerging field, the goal of this thesis was to gain a deeper understanding of the limitations of oxidase-catalyzed reactions and then propose a practical reactor configuration to facilitate their industrial implementation.

Plug-flow is the preferred mode of continuous operation to allow good control of residence times and enable full conversion. However, the lack of mixing makes plug-flow reactors unsuitable for multiphase systems like gas-liquid biocatalytic oxidations. Therefore, operation in stirred tanks is proposed as a scalable alternative that affords better mass transfer. Even so, the biocatalytic oxidation of glucose was found to be predominantly oxygen limited in a continuous stirred tank reactor. This is due to the low water-solubility of molecular oxygen, which severely limits the driving force for gas-liquid mass transfer and results in ineffective use of the enzyme due to its comparatively low affinity towards oxygen. To raise its solubility, the partial pressure of oxygen in the reactor must be increased, either by raising the total pressure, which increases costs, or the oxygen content of the feed gas, which was found to potentially deactivate the enzyme above concentrations of 60-80%. A better alternative would thus be to employ protein engineering to improve the affinity of the enzyme towards oxygen. In the meantime, a model of the system was used to demonstrate that just one additional reactor in series with the first enables more effective enzyme use and the possibility of near-complete conversion.

The gas-liquid mass transfer coefficient, k_La, which is largely thought of as a reactor property, was found to be highly influenced by the composition of the reaction media. This is likely based on the complex interactions of the individual media components at the gas-liquid interface. Unfortunately, these influences could not be modelled with sufficient accuracy to allow reliable prediction of k_La. Since the k_La is a critical process parameter for the design, scale-up and operation of an oxygen-limited biocatalytic reaction, an alternative means of estimating its value that accounts for the reactor

operating conditions, as well as the reaction itself, is required. This was done by fitting the model of the system to experimental data. The estimated k_La values were significantly higher than those measured in pure water. Additionally, the k_La in the second reactor was higher than the first. This indicates that, in the case of gas-liquid biocatalytic reactions, the enzyme may be used more effectively with each successive stirred tank in a series, at least until the primary substrate becomes rate-limiting. The digital model of the system was further used to explore alternative strategies to improve reaction performance. If provided with economic constraints on each operating parameter, it would allow independent optimization of the reactors in a series to achieve near-complete conversion, as well as targets for improvements to the enzyme, through protein engineering, to be set.

Danske Resumé

Enzymer har en række egenskaber der gør dem attraktive, som biokatalytiske alternativer til konventionelle overgangsmetal-baserede katalysatorer, til produktion af både høj- og lavværdiprodukter. Disse inkluderer, men er ikke begrænset til, milde driftsbetingelser og høj selektivitet. Derudover er det mulighed for at ændre enzymers egenskaber for, at forbedre kompatibiliteten med en given proces. Der er stor opmærksomhed på brugen af oxidaser til selektivt at katalysere oxidationer, ved hjælp af molekylært ilt, som et miljøvenligt alternativ til katalysatorer baseret på overgangsmetaller.

Industrielt set er der i større grad fokus på kontinuerte processer, for at forbedre effektiviteten af processerne. Det er derfor vigtigt, at biokatalytiske processer udvikler sig i samme retning. Kontinuerte biokatalytiske processer er et relativt nyt og voksende felt inden for biokatalyse. Formålet med denne afhandling har derfor været fokuseret på, at skabe en dybere forståelse for begrænsningerne relateret til oxidase katalyserede reaktioner, samt foreslå en praktisk reaktorkonfiguration der vil kunne fremme industriel implementering af denne type biokatalytiske processer.

Plug-flow reaktorer er en af de foretrukne metoder til kontinuerlig drift, idet der normalt er god kontrol af opholdstider, god blanding, og det er muligt at have fuld omdannelse. Utilstrækkelig blanding i flerfasesystemer, gør denne type reaktor uegnet til biokatalytiske oxidationer (gas-væske systemer). Denne afhandling foreslår derfor at bruge kontinuerligt omrørte tankreaktorer, som et skalerbart alternativ med god massetransport. Alligevel viste det sig, at den biokatalytiske oxidation af glukose overvejende er iltbegrænset i en kontinuerligt omrørt tankreaktor. Dette skyldes den lave vandopløselighed af molekylært ilt. Hvilket alvorligt begrænser drivkraften for overførsel af ilt til væsken og resulterer i ineffektiv anvendelse af oxidase. For at øge mængden af opløst ilt i væskefasen i reaktoren kan mængden af opløst ilt i væskefasen øges ved at øge partialtrykket af ilt. Dette kan gøres ved at øge trykket i reaktoren, hvilket vil resultere i markant øgede omkostninger, eller ved at øge iltindholdet i fødegassen til reaktoren. Det blev observeret at oxidasen potentielt blev deaktiveret ved iltkoncentrationer over 60-80%. Det bedste alternativ til denne løsning, vil derfor være at modificere oxidasen, ved protein modifikation, for at øge oxidasens resistens overfor høje iltkoncentrationer. Indtil der er modificeret og udviklet en optimeret oxidase, blev en model af systemet brugt til at demonstrere, at 2 reaktorer i serie muliggør mere effektiv enzymbrug og potentiel bedre konvertering.

Gasoverførselskoefficient, kLa, der i vid udstrækning betragtes som en reaktoregenskab, viste sig at være stærkt påvirket af sammensætningen af reaktionsmediet. Dette er sandsynligvis forårsaget af komplekse interaktioner mellem de enkelte mediekomponenter ved gas-væske spændingsfladen. Desværre kunne disse påvirkninger ikke modelleres med tilstrækkelig nøjagtighed til, at give pålidelig forudsigelse af kLa. Idet kLa er en kritisk procesparameter til design, opskalering og drift af en iltbegrænset biokatalytisk reaktion, er der behov for en alternativt måde, at estimere dens værdi. Dette alternativ skal tage højde for reaktorens driftsbetingelser og selve reaktionen. Dette blev gjort ved at tilpasse modellen til eksperimentelle data fra systemet. Det viste sig at de beregende kLa-værdier var signifikant højere end dem målt i rent vand.

Derudover var kLa i den anden reaktor højere end i den første. Dette indikerer, for gas-væske baserede biokatalytiske reaktioner, at enzymet kan anvendes mere effektivt med kontinuerligt omrørte tankreaktorer i serie. Dette vil gøre sig gældende, indtil det primære substrat bliver den hastighedsbegrænsende faktor. Ydermere, blev modellen af systemet brugt til, at udforske alternative strategier for at forbedre reaktionens ydeevne. Dette vil kunne bruges til, hvis de økonomiske begrænsninger kendes for hver driftsparameter, uafhængig optimering af reaktorerne i en serie for at opnå næsten fuldstændig konvertering, samt sætte mål for forbedringer af oxidasen gennem protein modificering.

Acknowledgements

I would like to express my sincere gratitude to my supervisor, Professor John Woodley. While our philosophies were not always aligned, I appreciate that you trusted me to independently work through the trials and tribulations of research, while always making sure I had a clear view of the bigger picture. I hope that the small contribution I have made to our field provides a stepping stone for future members of your research group. My thanks go also to my peers Murray, Mafalda and Angela, through whom I was able to gain deeper insights into the intricacies of biocatalysis. And to Leander, who managed to communicate advanced modelling techniques in a way that even I, an avowed experimentalist, could not only comprehend, but also implement towards the betterment of my research.

To Tiago and Carina, I cannot express how grateful I am for your friendship and counsel, which always prevented me from straying too far down the rabbit hole. To my parents, Malan and Pauline, thank you for being so patient while I've been on the other side of the world these past 5 years. I hope you both know that Namibia will always be the place I belong. And a special thanks to my brother, Colin, for treating me like an expert, even when I sometimes feel like an imposter. Finally, I must thank my best friend, Tristan, for always providing me with a window into the world beyond engineering and academia.

Contents

Abstract i

Danske Resumé iii

Acknowledgements v

Abbreviations viii

Nomenclature ix

Chapter 1: Introduction 1

1.1 Biocatalysis 1

1.2 Oxidative Biocatalysis 4

1.3 Continuous Processing 8

1.4 Scope 9

1.5 Outline 9

Chapter 2: Reactor selection for continuous biocatalysis 11

2.1 Introduction 11

2.2 Reactor Types 11

2.3 Batch vs. Continuous 14

2.4 Residence Time Distribution 16

2.5 Enzyme Kinetics 19

2.6 pH Control and Multiphase Systems 23

2.7 Reactor Selection Methodology 27

2.8 Immobilization 30

2.9 Conclusions 31

Chapter 3: Experimental methods 33

3.1 Introduction 33

3.2 Continuous oxidation reactions 33

3.3 GOx stability 38

3.4 k_La determination 38

Chapter 4: Glucose oxidation in a CSTR 41

4.1 Introduction 41

4.2 Results and Discussion 43

4.3 Conclusions 52

Chapter 5: Glucose oxidation in dual CSTRs 53

5.1 Introduction 53

5.2 Single vs. Multiple CSTRs 54

5.3 Results and discussion 58

5.4 Conclusions 60

Chapter 6: Mass transfer coefficient 61

6.1 Introduction 61

6.2 Results and discussion 62

6.3 Conclusions 71

Chapter 7: Estimation of process parameters 73

7.1 Introduction 73

7.2 Model description 74

7.3 Results and Discussion 77

7.4 Conclusions 88

Chapter 8: Identifying constraints on operating conditions 89

Chapter 9: Conclusions 95

Chapter 10: Future perspectives 99

References 101

Abbreviations

API	Active pharmaceutical ingredient
BSTR	Batch stirred tank reactor
CPBR	Continuous packed-bed reactor
CPFR	Continuous plug-flow reactor
CSTR	Continuous stirrend tank reactor
DO	Dissolved oxygen
GOx	Glucose oxidase
ISPR	*In situ* product removal
ISSS	*In situ* substrate supply
KPi	Potassium phosphate
OCR	Oxygen consumption rate
ODE	Ordinary differential equation
OPR	Oxygen production rate
OTR	Oxygen transfer rate
RTD	Residence time distribution
SFR	Segmented flow reactor

Subscripts

CAT	Catalase
E	Enzyme
F	Feed
G	Glucose
GA	Gluconic acid
GOx	Glucose oxidase
HP	Hydrogen peroxide
max	Maximum
O	Dissolved oxygen
R	Reactor
req	Required

Nomenclature

a	Interfacial area	m^{-1}
C	Concentration	mM
C_O^*	Saturation oxygen concentration	mM
C_O^m	Measured oxygen concentration	mM
F_{S0}	Inlet molar flowrate of substrate	$mol.s^{-1}$
H	Henry's constant	$mmol.L^{-1}.Pa^{-1}$
k_{cat}	Specific rate constant	$\mu mol.min^{-1}.mg^{-1}$
K_I	Product inhibition constant	mM
k_L	Liquid-side mass transfer coefficient	$m.h^{-1}$
k_La	Volumetric mass transfer coefficient	h^{-1}
K_M	Substrate affinity constant	mM
P_G/V	Gassed power input	$W.m^{-3}$
p_{O2}	Partial pressure of oxygen	Pa
Q	Volumetric flowrate	$m^3.s^{-1}$
t	Reaction time	s
U	Enzyme activity	$\mu mol.min^{-1}.mg^{-1}$
V	Reaction volume	m^3
v	Reaction rate	$mmol.L^{-1}.h^{-1}$
V_{max}	Maximum reaction rate	$mmol.L^{-1}.h^{-1}$
v_s	Superficial gas velocity	$m.s^{-1}$
X	Fractional substrate conversion	
η	Effectiveness factor (v/V_{max})	
μ	Dynamic viscosity	Pa.s
τ	Mean residence time	s
τ_R	Probe response time	s

Chapter 1

Introduction

1.1 Biocatalysis

Biocatalysis is here defined as the use of enzymes to catalyze chemical reactions for the production of commercially valuable products. Enzymes are specialized proteins that are naturally produced by all living organisms. However, for industrial use, they are generally expressed recombinantly in a handful of well-understood, fast-growing and non-toxic bacterial, yeast or fungal strains. Thereafter, the cells containing the enzymes can be employed directly as biocatalysts, provided they are prevented from growing, thus differentiating biocatalysis from fermentation. On the one hand, whole-cell biocatalysis affords the enzymes some protection from harsh conditions outside the cell and allows exploitation of natural enzyme cascades within the cell, particularly for regeneration of critical cofactors.[1] On the other hand, the presence of cellular membranes increases the likelihood of mass transfer limitations, the cells must be supplied with nutrients for cell maintenance and they are still susceptible to lysis/deactivation under harsh conditions. The alternative is to isolate the enzymes of interest from the cell, either for application as a crude cell-free extract or in more purified forms.[2] This has the benefit of decoupling enzyme activity from enzyme expression to afford greater flexibility and freedom during process design, but incurs additional costs and complicates catalyst recovery/recycle due to the solubility of enzymes. In both cases, the stability of a biocatalyst under industrial operating conditions (elevated temperatures, extreme pH, organic solvents, high shear) may be low. To counter this, biocatalysts are often immobilized to a solid support or within a polymer matrix, but this adds to their cost and may compromise activity.[3]

In the last few decades, biocatalysts have been shown to have a number of advantages over their conventional chemical counterparts. For instance, biocatalysts operate under natural conditions (ambient temperature, atmospheric pressure and neutral pH) which are generally mild in comparison to those frequently encountered in the traditional chemical industry, and they are produced through microbial fermentation of renewable sugars, rendering them more sustainable than catalysts that rely on rare metals with dwindling natural reserves.[4] These advantages are predominantly attractive to sectors that produce extremely large volumes of simple commodity chemicals which incur larger

carbon footprints and have extremely small profit margins due to the low value of their products. For example, high fructose corn syrup has long been produced at industrial scale using immobilized glucose isomerase[5] and lipases are increasingly being used for commercial biodiesel production[6]. In these industries, reducing the cost of operation and waste treatment through the implementation of biodegradable enzymes at milder operating conditions is extremely attractive. However, high enzyme activity and stability are imperative to reduce the cost of the enzyme for such large scales of production.[7]

Through millennia of evolution, countless enzymes, unique to every living organism, have developed exceptional enantio-, regio- and stereoselectivity towards the vast majority of chemicals encountered in nature.[8] While these properties are less relevant for the production of simple commodity chemicals, they are absolutely crucial for the production of more complex, high-value molecules, such as pharmaceuticals.[9] For example, a variety of enzymes are already implemented for the commercial production of treatments for diabetes (Saxagliptin and Sitagliptin), central nervous system disorders (Pregabalin) and autoimmune diseases (Atazanavir), to name a few.[10] In contrast, the poor selectivity of conventional catalysts necessitates the use of lengthy reaction sequences[11], including numerous protection and deprotection steps[12], to ensure the desired product specifications can be met. Each reaction in the sequence increases the complexity and cost of the overall process, while reducing its yield. Furthermore, each conventional catalyst in a multi-step sequence may have widely different optimal operating conditions, requiring each reaction to be spatially or temporally separate from one another. Since most enzymes typically operate within a similar, narrow range of operating conditions, it enables multiple sequential biocatalytic reactions to be carried out simultaneously in the same reactor, mimicking the biocatalytic cascades found throughout nature.[13] Operating in this way avoids the need for intermediate purification steps, saving both time and resources.[14] This is especially attractive if some intermediates in the system are unstable or toxic, as they are produced and subsequently consumed with no need for intermediate storage.[15] For this reason, the system is also less likely to become inhibited by accumulation of intermediates. Likewise, accumulation of potentially inhibitory by-products is limited by the high selectivity of the enzymes. Finally, the use of a biocatalytic cascade allows for one or more of the reactions in the sequence to be energetically unfavorable, provided the overall thermodynamics of the sequence remain favorable.[16]

Nonetheless, the greatest advantage of enzymes over conventional catalysts undoubtedly stems from their complex structures. Even the slightest modification of their amino acid sequences may have a

significant impact on the properties and performance of the enzyme, as evidenced by their evolution in nature. With the advent of recombinant DNA technologies and automated high-throughput robotics, it is now possible to direct and accelerate their evolution by generating vast mutant libraries through random mutagenesis and screen them for mutants with attractive properties.[17] These include; improved stability under industrial conditions, increased activity towards a broader range of substrates or even entirely new chemistries.[18] Additionally, continuous improvements to our understanding of, and ability to model, the crystal structures of enzymes and how they interact with substrates is allowing more rational approaches for deciding which amino acid substitutions to make.[19] It may even be possible to design enzymes entirely from scratch with the aid of computational tools.[20] Our inability to modify the properties of simple chemical catalysts has historically constrained process engineering around what is catalytically possible. As such, overcoming process limitations has been dependent on technological innovation. But, as the field of process engineering continues to mature, technological breakthroughs occur less frequently. The ability to engineer enzymes themselves creates the potential for the catalyst to be designed to better suit the process, a paradigm shift that may open up many new possibilities in the field of chemical engineering. For example, it enables the retrosynthesis of pharmaceuticals, both new and old, via shorter reaction pathways that were previously impossible or unfeasible.[21] As such, technological limitations can now also be used to set targets for enzyme engineers.

Mutations to the amino acid sequence of an enzyme may have both positive and negative influences on performance. Therefore, it is important for protein engineers to be conscious of the dominant limitation of a particular process, often attributed to the largest cost contributor, so as to prioritize screening efforts.[22] For instance, high upstream costs can be reduced by increasing the activity of the enzyme to achieve a higher volumetric productivity ($g_{product}.L^{-1}.h^{-1}$). This enables the use of smaller reactors or less enzyme to reduce capital or operating costs, respectively. High downstream processing costs can be reduced by ensuring that the enzyme can operate at higher product concentrations ($g_{product}.L^{-1}$) without becoming inhibited. This improves driving forces for separation and reduces the amount of water that has to be removed during product isolation. If the substrate is the dominant operating cost, it is important to improve the selectivity and efficiency of the enzyme to maximize the process yield ($g_{product}.g_{substrate}^{-1}$). Finally, if the biocatalyst itself is the largest cost contributor, the stability of the enzyme must be improved to raise the biocatalyst yield ($g_{product}.g_{enzyme}^{-1}$). This reduces the number of times the enzyme needs to be replenished. The target values for each of these process metrics differ,

depending on the value of the desired product.[23] Other metrics, such as E-factor ($g_{waste}.g_{product}^{-1}$) and atom efficiency ($MW_{product}.MW_{substrate}^{-1}$), exist for assessing the sustainability of a process and are particularly important when waste treatment represents the primary operating cost.[24] The aforementioned examples demonstrate that some biocatalytic reaction chemistries (isomerization, transesterification, esterification, reductive amination, transamination, resolution etc.) have already been made feasible for commercial application. However, the complete biocatalytic toolbox has yet to be fully realized at industrial scale.

1.2 Oxidative Biocatalysis

Over the last few decades, oxidation has been one of the largest processes in the chemical industry, second only to polymerization.[25] In 1992, it was estimated that oxidation reactions accounted for roughly 30% of total chemical production.[25b] At the time, the use of stoichiometric oxidants, such as permanganates or chromium salts, was common practice for the production of fine chemicals, but these were found to be expensive, toxic and generated large quantities of heavy-metal wastes.[25-26] As a result, industries began to shift in favor of heterogeneous catalytic oxidation to enable the use of more environmentally friendly oxidants.[25, 27] The most attractive oxidizing agent is molecular oxygen since it is solely comprised of active oxygen and thus produces no by-products. Hydrogen peroxide and ozone are also attractive since their by-products (H_2O and O_2 respectively) are environmentally friendly. Other commonly applied oxidants include sodium hypochlorite, tert-butyl hydroperoxide, 4-methylmorpholine 4-oxide, potassium peroxymonosulfate and iodosylbenzene.[25a] However, these tend to result in the production of potentially toxic by-products and can be expensive. Less than a decade later, in 2001, more than 60% of all catalytically synthesized chemicals and intermediates were estimated to be products of oxidation reactions.[25a] This is unsurprising, given that aldehydes, alcohols, ketones, organic acids and epoxides can all be produced via catalytic oxidation. Nevertheless, conventional transition metal-based catalysts tend to be poorly selective, resulting in the formation of undesired by-products.[25a] Conversely, oxidative biocatalysts are highly selective and use molecular oxygen, in the form of air, as an inexpensive, benign and abundant oxidant.

There are two enzyme subclasses that catalyze selective oxidations using molecular oxygen, namely oxygenases[28] and oxidases[29]. Oxygenases incorporate one or two atoms of molecular oxygen into a substrate, but require a nicotinamide cofactor (NADH or NADPH) as an electron donor. These cofactors are far too expensive to be supplied to a reaction in stoichiometric amounts.[30] Therefore, the cofactor needs to be continuously regenerated by a secondary reaction to make these enzymes

economically feasible, which adds additional co-substrates and co-products that complicate downstream processing.[31] In contrast, oxidases do not require nicotinamide cofactors, instead utilizing molecular oxygen as an electron acceptor and producing water or hydrogen peroxide as a by-product.[9a] This makes them more attractive for industrial implementation and so they will be the focus of the following chapters. For instance, oxidases have already been industrially implemented for the production of Islatravir[13c, 32], an HIV treatment, as well a crucial intermediate for the production of cephalosporin antibiotics[33]. Oxidases have also been shown to enable the production of enantiopure compounds, including ligands, amino acids and amines, either through asymmetric synthesis (galactose oxidase, monoamine oxidase)[34] or resolution of racemic mixtures (D-amino acid oxidase, cyclohexylamine oxidase)[35]. Additionally, pyrroles, which are attractive pharmaceutical ingredients, have been synthesized from pyrrolines with a combination of nicotine oxidase and monoamine oxidases.[36]

In order to assess the industrial feasibility of continuous oxidase-catalyzed reactions, glucose oxidase (GOx) was selected as a case study for the following reasons:

- **High activity:** During the early stages of development for biocatalytic processes, the biocatalyst itself is often the rate-limiting step. In these cases, very little can be done from a process engineering standpoint to improve performance. In contrast, GOx is a highly active enzyme towards its native substrate, which enables reaction rates that are high enough to reveal process limitations.
- **Stability:** Low enzyme stability, both under quiescent and industrial operating conditions, can impede the study of oxidases during continuous operation. Many laboratory formulations of enzymes are prone to low stability due to the presence of proteases in cell lysates or the absence of any stabilizers or preservatives. GOx is readily available in commercial formulations that are highly stable.
- **Well-defined:** GOx is a well-researched enzyme. As a result, its rate law and kinetic parameters have been characterized. This facilitates model development in parallel with experimentation to identify process limitations or gaps in understanding.

The reaction catalyzed by GOx, shown in Scheme 1.1, follows a ping-pong bi-bi rate law (Equation 1.1), in which the reaction rate is dependent on the concentrations of GOx (C_{GOx}), glucose (C_G) and dissolved oxygen (C_O).[37] The mechanism of this rate law (Scheme 1.2) is comprised of a

double-displacement reaction.[38] In the first step, glucose binds with the free enzyme and is oxidized to form gluconolactone. Next, oxygen binds to the reduced enzyme and is converted to hydrogen peroxide, freeing the enzyme to repeat the cycle.

$$v_{GOx} = \frac{k_{cat,GOx} C_{GOx} C_G C_O}{C_G C_O + K_{MO} C_G + K_{MG} C_O} \tag{1.1}$$

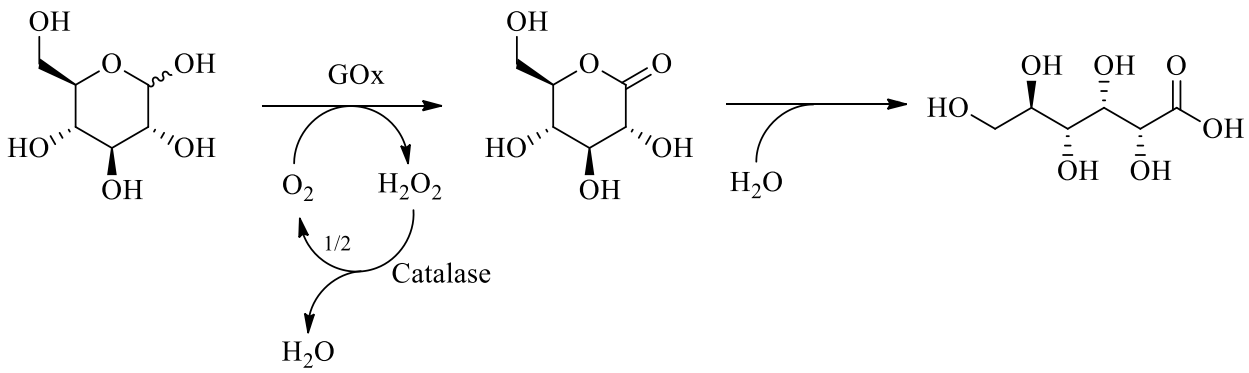

Scheme 1.1. GOx-catalyzed conversion of D-glucose to D-glucono-δ-lactone, which spontaneously hydrolyzes to form gluconic acid. Catalase is used to recover some oxygen from the potentially harmful hydrogen peroxide by-product.

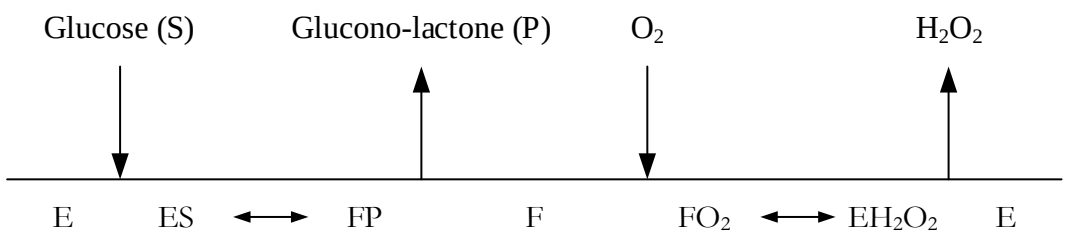

Scheme 1.2. The ping-pong bi-bi reaction mechanism of glucose oxidase showing conversion of the substrate (S) into the product (P) and subsequent regeneration of the free enzyme (E) from its reduced form (F)

The rate constant of the enzyme (k_{cat}) and its affinity constants towards glucose (K_{MG}) and oxygen (K_{MO}) have been determined in a specially adapted tube-in-tube reactor and are shown in Table 1.1.[39]

The small diameter of the tube-in-tube reactor used in this study (0.23 mm) gave an extremely large specific surface area (17391 m^{-1}) and very short diffusion distances. Additionally, it could be operated at pressures up to 10 bar. These features allow DO concentrations of up to 12 mM to be reached, making the reactor ideal for measuring the kinetic parameters of oxygen-dependent enzymes. The reason for this is that, while molecular oxygen has many attractive properties, it presents some limitations for biocatalytic oxidations, owing to its poor solubility in water (0.26 mM in equilibrium with air at 25°C and 1 atm, based on its Henry's Law constant[40]), which is low compared to the K_{MO} of most oxidases, according to data available in the BRENDA database.[41] Hydrogen peroxide produced as a by-product of oxidase-catalyzed reactions, which can deactivate the enzyme if allowed to accumulate[42], is normally removed by coupling the oxidase with catalase. Conveniently, catalase converts hydrogen peroxide into water and oxygen, which can be consumed by the oxidase. Nevertheless, as shown in Scheme 1.1, the stoichiometry of the catalase reaction does not allow the coupled enzyme system to become self-sufficient and so external supply of oxygen is still required.

Table 1.1. Kinetic parameters of GOx[39]

Kinetic parameter	Value	Unit
$k_{cat,GOx}$	17.8 ± 1.39	$\mu mol.min^{-1}.mg_{GOx}^{-1}$
K_{MG}	75.2 ± 9.38	mM
K_{MO}	0.51 ± 0.09	mM

The spontaneous hydrolysis of gluconolactone to gluconic acid, which are structurally distinct from one another, is fortunate, since it limits the likelihood of gluconic acid inhibiting the system by competing with glucose for a place in the active site of the enzyme. The same, however, cannot be said for hydrogen peroxide, which has been found to competitively inhibit GOx.[43] Thus, Equation 1.1 must be modified as follows

$$v_{GOx} = \frac{k_{cat,GOx} C_{GOx} C_G C_O}{C_G C_O + K_{MO} C_G \left(1 + \frac{C_{HP}}{K_I}\right) + K_{MG} C_O} \tag{1.2}$$

where C_{HP} is the concentration of hydrogen peroxide and K_I is an inhibition constant. Unfortunately, it has been found that the inhibition constant for glucose oxidase is approximately equal to its K_{MO}, which implies that GOx has roughly the same affinity towards binding with hydrogen peroxide as it does dissolved oxygen.[43] This also indicates that the enzyme can be significantly inhibited by hydrogen peroxide at concentrations as low as 0.51 mM. Therefore, it is especially important to ensure the complete depletion of hydrogen peroxide to avoid inactivation as well as inhibition of GOx. This is more challenging than it seems, since the rate of catalase is dependent on the concentration of hydrogen peroxide, as shown in Equation 1.3. Thus, hydrogen peroxide can never be removed entirely using catalase. As such, catalase is typically supplied in excess to reduce the peroxide concentration as much as possible. Alternatively, hydrogen peroxide can be decomposed by contact with gold, iron, copper or activated carbon[44], but this may result in the formation of reactive oxygen species that could potentially damage the enzymes[45].

$$v_{CAT} = \frac{k_{cat,CAT} C_{CAT} C_{HP}}{K_{MHP} + C_{HP}} \tag{1.3}$$

1.3 Continuous Processing

Continuous processing is frequently used for the production of commodity chemicals, where extremely large production volumes and low profit margins demand economic efficiency.[46] However, continuous processing is also becoming increasingly attractive for the production of fine chemicals. To illustrate this, let us examine the pharmaceutical industry, where product quality, not process economics, has historically been the major driving force due to the high value and extreme complexity of its products.[46] As a result of this, the industry is tightly regulated to ensure quality specifications can be met and failure to comply can often lead to drug shortages.[46] Pharmaceuticals are also produced in much lower quantities than commodity chemicals and so production has typically been limited to batch operation, which allows flexible switching between products.[46] On top of this, a recent shift towards personalized medicine as well as the ever-increasing potency of drugs demands even smaller production volumes.[46-47] As such, it would seem that there is no need for continuous production. However, the pharmaceutical landscape is changing in ways that are causing both regulators and drug manufacturers to embrace it nonetheless. For instance, the chance of discovering new blockbuster

pharmaceuticals is becoming smaller and competition due to the manufacture of generics is rising, increasing the need for cost-effective production.[47] Additionally, emerging markets demand more affordable pharmaceuticals that further emphasize the need for reducing operating costs.[47] This requires production processes to be flexible, not only in terms of product range but capacity as well.[47] Batch processing suffers from long hold-up times, which reduces productivity and necessitates large equipment that limits capacity changes.[47] In contrast, higher productivity can be achieved through continuous operation, allowing reduced equipment and facility sizes.[47-48] In fact, continuous processing is generally more efficient than batch for a variety of reasons. Smaller equipment improves heat and mass transfer and allows more precise residence time control.[48] Multi-step reaction sequences can be telescoped, shortening processing times by eliminating hold-ups between steps.[48] Continuous processes are also easier to control, which improves their safety. This enables shorter and more direct reaction sequences to be used, as hazardous intermediates no longer have to be avoided, since they are produced and consumed *in situ* without any need for storage between steps.[48] Fewer reaction steps and the possibility of inline separations also help to avoid yield losses and improve sustainability by reducing waste generation.[48]

1.4 Scope

The scope of this thesis is to demonstrate continuous operation of a biocatalytic oxidation in conventional and scalable reactor technologies, and assess whether this could be a feasible means of carrying out selective oxidation in industry. To this end, the main objective is to gain better understanding of the oxygen-dependent kinetics of oxidases during continuous operation through the use of laboratory experiments as well as kinetic and mechanistic digital models. Herein, only *in vitro* application of enzymes as homogenous catalysts will be examined.

1.5 Outline

This thesis is divided into 10 chapters, the contents of which are summarized as follows:

Chapter 1 introduces the advantages of biocatalysis with regards to the manufacture of pharmaceutical intermediates or active ingredients, with a particular focus on oxidation reactions. The benefits of continuous processing are also introduced.

Chapter 2 explores the applicability of various reactor configurations towards continuous biocatalysis for pharmaceutical production. A reactor selection methodology is also proposed, based on which the most appropriate reactor configuration for multiphase biocatalytic oxidations is selected.

Chapter 3 outlines the experimental methods used throughout the thesis.

Chapter 4 investigates the kinetic behavior of glucose oxidase through experiments in a continuous stirred tank reactor, with emphasis on the trade-off between productivity and effective use of the enzyme.

Chapter 5 utilizes basic modelling to determine the most practical and effective configuration of continuous stirred tank reactors for biocatalytic glucose oxidation, the results of which are compared to experimental data.

Chapter 6 studies the effect of media composition on gas-liquid mass transfer to identify whether this can be used for its accurate prediction.

Chapter 7 further develops the digital model of the system to estimate parameters. The model is also used to assess the outcomes of changes to the operating conditions or the kinetic parameters of the enzymes.

Chapter 8 discusses the prerequisite knowledge required to select operating conditions in a stirred tank reactor for a biocatalytic oxidation to be feasible.

Chapter 9 presents the main conclusions of the thesis.

Chapter 10 proposes additional avenues of research that could facilitate the implementation of oxidative biocatalysis into industry.

Chapter 2

Reactor selection for continuous biocatalysis

This chapter forms the basis of a recently published journal article: Lindeque, R. M.; Woodley, J. M., Reactor Selection for Effective Continuous Biocatalytic Production of Pharmaceuticals. *Catalysts* 2019, 9 (3), 262.

2.1 Introduction

Until recently, biocatalytic reactions were predominantly limited to batch operation due to the low activity of wild-type enzymes towards substrates of commercial interest, as well as their low stability under industrial operating conditions. This often precluded their use for the continuous production of commodity chemicals but not for the selective production of higher value chemicals, such as pharmaceuticals, for which batch manufacturing was standard practice. However, as even these industries are now beginning to shift away from batch operation to embrace the many advantages of continuous processing[49], so too must the field of biocatalysis if it is to remain relevant. Fortunately, as discussed in Chapter 1, the advent of recombinant DNA technologies, which have enabled protein engineering through directed evolution or rational design, now allows the tailoring of enzymes to better suit industrial application.[50] Furthermore, since the fine chemical industry is by no means the first manufacturing sector to have made this transition, a variety of continuous reactor technologies are already widely available, with unique configurations specialized to overcome a broad range of process limitations. As continuous biocatalysis is a relatively new field, reactor selection can be a daunting task in the absence of any standardized methodologies. Fortunately, all chemical reactors can be modeled as a combination of three ideal reactor types, described in the following section. Thus, to streamline the development and implementation of biocatalysis for continuous processing, one simply has to understand how enzymes behave in each of these fundamental reactor types and determine which of these behaviors is best suited towards the unique needs of the target industry.

2.2 Reactor Types

Figure 2.1 shows schematic diagrams of the three ideal reactor types, namely the batch stirred tank reactor (BSTR), the continuous stirred tank reactor (CSTR) and the continuous plug-flow reactor

(CPFR). The characteristics of these reactors are well-researched.[51] Design equations for each of the reactors, shown in Figure 2.1, can be used to determine the concentration of enzyme (C_E) required to achieve a desired fractional conversion of substrate (X) for a given initial or feed substrate concentration (C_{S0}). In a BSTR, the time of reaction (t) and reaction volume (V) are also required, whilst for CSTRs and CPFRs the volumetric flowrate through the reactor (Q) is needed. K_M is the affinity constant of the enzyme towards the substrate and k_{cat} is its rate constant.

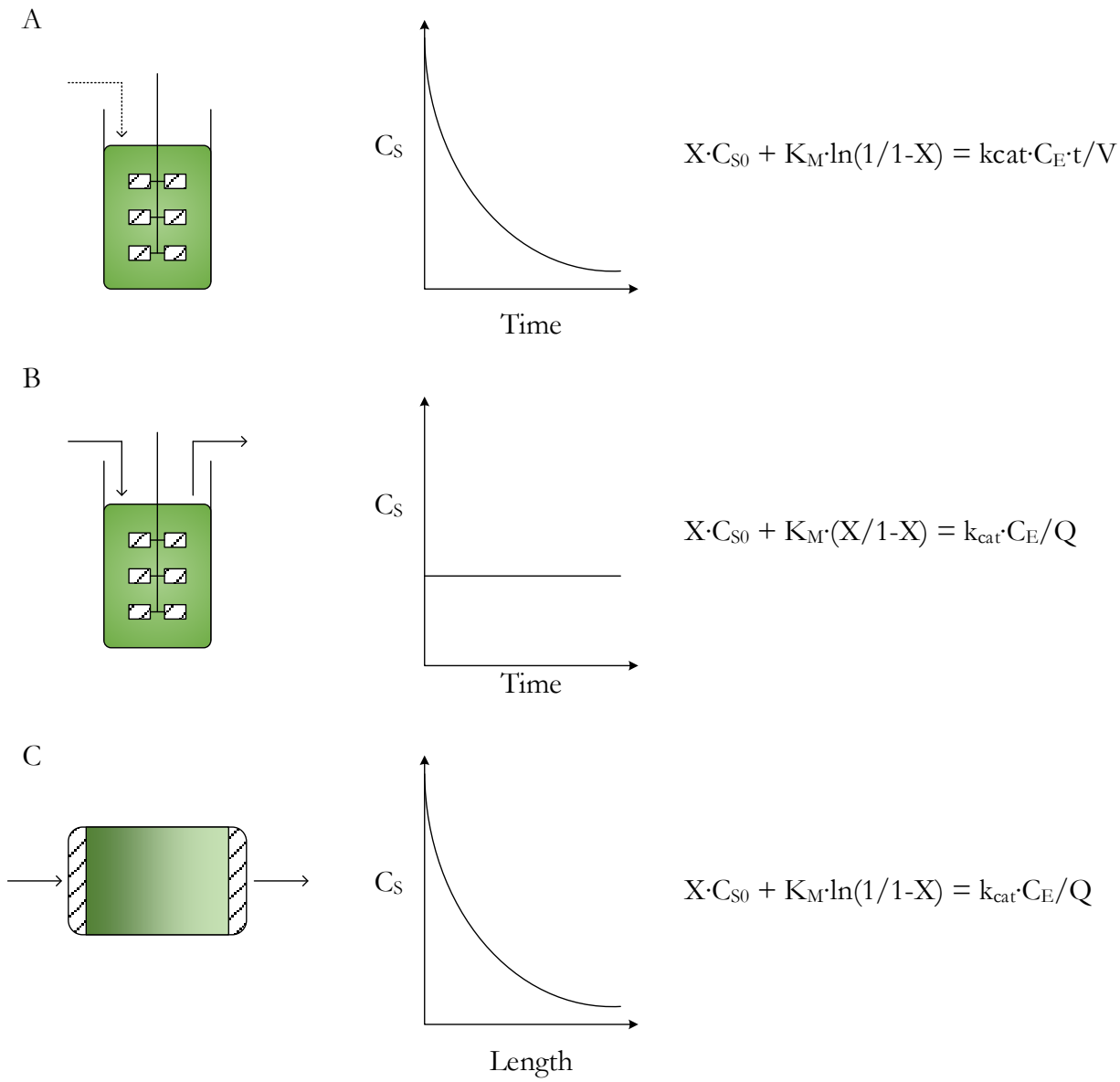

Figure 2.1. Reactor schematics, substrate concentration (C_S) profiles and design equations for single-substrate biocatalytic reactions in A) batch stirred tank reactor (BSTR), B) continuous stirred tank reactor (CSTR) and C) continuous plug-flow reactor (CPFR).

In a BSTR, the mechanically stirred vessel is first filled with substrate and enzyme, to initiate the reaction, after which no material is removed until the reaction is stopped. BSTRs are well-mixed reactors, meaning that concentrations are the same regardless of location within the reactor. Typical enzyme kinetics follow Michaelis–Menten behavior, where rate is independent of substrate (zero order) at high concentrations but becomes proportional to the amount of substrate (first order) at lower concentrations, with a transition in between. This means that in a BSTR the substrate is initially consumed quickly, whilst later in the reaction, as it enters the first order regime, the reaction rate slows, as illustrated by the substrate concentration profile in Figure 2.1A. However, given sufficient time in the reactor, complete conversion can be achieved, provided the equilibrium is favorable. BSTRs are commonly used for biocatalytic reactions[52] due to their simplicity and flexibility. For instance, substrate concentrations can be kept below toxic or inhibitory levels by adopting a fed-batch approach[53] where substrate is fed to the reactor, resulting in a reaction volume that increases with time. Additionally, pH changes caused by the biocatalytic reaction can be neutralized through the addition of an acid or base to maintain the optimal pH of the enzyme.

The design of a CSTR is similar to that of a BSTR, except that material is continuously added to, and removed from, the reactor, such that the working volume remains constant. In this case, the biocatalyst must either be fed continuously to the reactor (to make up for loss of catalyst in the effluent) or it must be retained within the reactor by immobilization and/or partially permeable membranes. Like BSTRs, CSTRs are well-mixed and so the reactor contents and effluent are homogenous. However, since there must be enough substrate in the reactor to achieve an adequate reaction rate, the effluent will always contain some substrate and so full substrate conversion is not possible[22a]. This trade-off between reaction rate and conversion is an important characteristic of CSTRs. Furthermore, since the reactor contents are homogenous, the substrate concentration, and subsequently the reaction rate, throughout the reactor remain constant with respect to time, as shown in Figure 2.1B.

In a CPFR, reactants are pumped into a long tubular reactor where, unlike stirred tanks, material flowing through does not mix with any material flowing ahead of it, or behind it. This results in concentration gradients over the length of the reactor, identical to the concentration gradients over time in a BSTR. Therefore, if the reactor is sufficiently long, the substrate can be fully converted. For this reason, in Figure 2.1C the concentration profile is given with respect to length, since the time material spends in a CPFR is simply a function of the reactor length and volumetric flowrate. Although

it is possible to operate a CPFR with a soluble catalyst, biocatalysts are typically immobilized onto the reactor wall or on particles of a carrier material, which are then packed into a tube to form a continuous packed-bed reactor (CPBR)[54] that still exhibits plug-flow behavior. However, this can potentially introduce mass transfer limitations and large pressure drops over the reactor[55].

2.3 Batch vs. Continuous

There are many considerations which need to be evaluated when selecting the type of reactor to use. However, even for simple single-product reactions in a single liquid phase, two considerations which are always of relevance are the residence time distribution (RTD) and the kinetics of the enzyme catalyzed reaction. BSTRs and CPFRs have identical kinetic behavior and both afford good control over RTDs. Consequently, it would appear that there is little motivation to invest in the shift from batch operation to continuous since both give the same result. However, much research has highlighted the benefits of continuous biocatalysis over batch processing, for both production as well as research and development, and these are summarized in Figure 2.2[37a, 56]. Nonetheless, it has also been shown that, for single-phase homogenous reactions, the differences in performance between batch and continuous reactors at the laboratory scale are negligible[57]. Therefore, in such instances, shifting from batch to continuous would appear to be a time-consuming and resource-intensive process that yields few improvements. But, at production scales, where mixing and heat transfer in large batch reactors are less efficient, shifting to continuous operation could be beneficial. Additionally, steady-state operation of a continuous reactor affords simpler control and greater consistency than a dynamic batch process at large scale. These advantages facilitate process intensification, which is critical to improve the economic feasibility of biocatalytic processes, especially those producing simple commodity chemicals.[58]

For complex fine chemicals, economics are often not the primary driving force during process design, due to their high values. Nevertheless, such chemicals are often the products of numerous reaction steps. Some of these reaction steps, especially those involving optically active compounds, may be biocatalytic, but many reactions are still more efficient using chemical catalysts. Chemocatalytic reactions are frequently operated continuously to benefit from rapid mixing and heat transfer[59], particularly in the case of exothermic reactions, or to avoid the storage of unstable or toxic intermediates. Therefore, when selecting a reactor for a biocatalytic reaction that may have to be integrated into a combined chemo/biocatalytic reaction sequence[60], opting for a continuous approach would be more practical, potentially allowing for end-to-end manufacturing that could even include

downstream processing and formulation[11b]. For this reason, it may also make more sense to use continuous reactors for research and development in fine chemical industries, as it simplifies the transition to production scale through the process of scale-out/parallelization/numbering up. For pharmaceutical production, this could provide a means of reducing time-to-market.[61]

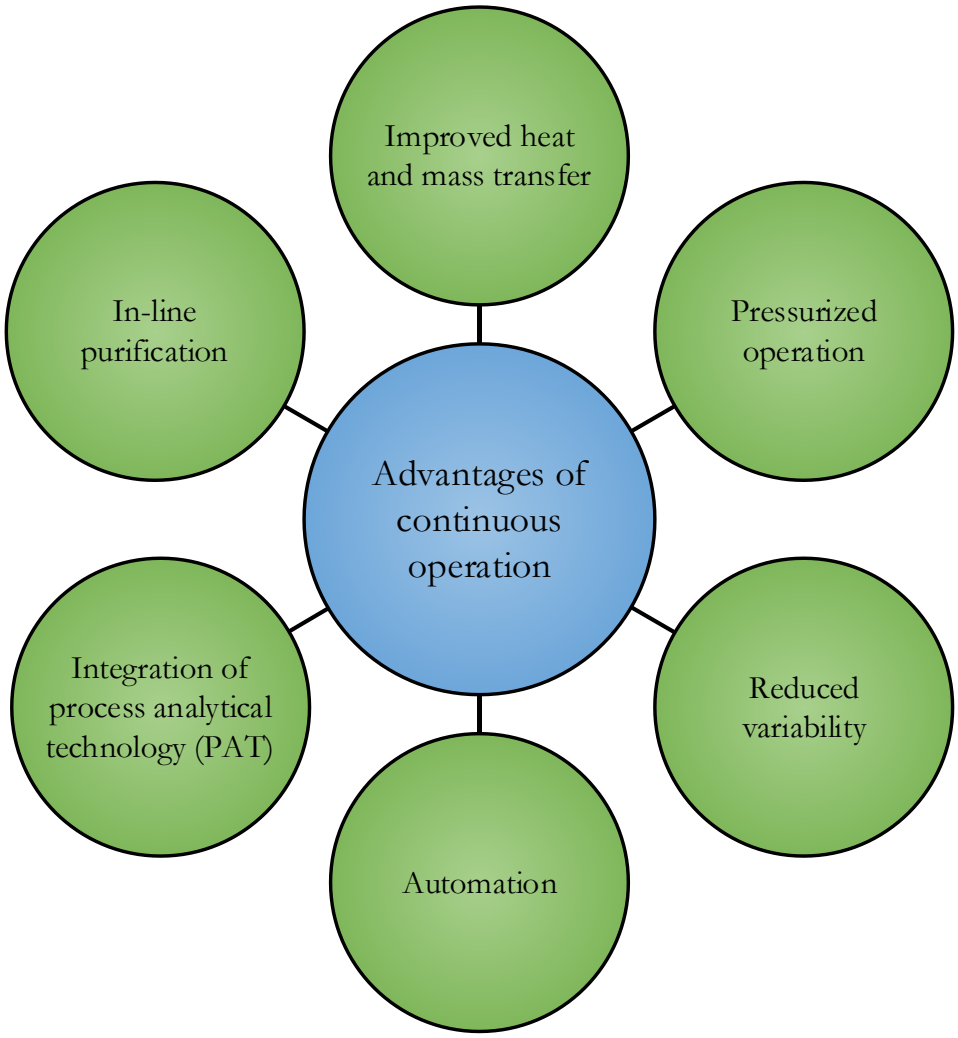

Figure 2.2. Benefits of shifting towards continuous biocatalysis.

Finally, continuous operation is generally more efficient than batch operation, which is plagued with lengthy start-up and shutdown times, before and after each reaction, and mandatory downtimes as the reactors need to be routinely cleaned. Of course, there are still some cases where BSTRs may be the most appropriate reactor to use. For instance, if the reaction rates of an enzyme are very low, then continuous operation in a CPFR would require very low flowrates or an impractically long reactor. In such a case, it would be beneficial to simply run the reaction in a BSTR for a long period of time until

the reaction reaches completion. However, even in such cases where BSTRs are in use it is still beneficial to simulate continuous behavior. For example, this could be done by operating three BSTRs in parallel, but with each at a different stage in the process (i.e., start-up, operation, shutdown).

2.4 Residence Time Distribution

Residence time defines the length of time material is in a reactor. For an ideal BSTR it is simply the time from the addition of the final reagent (usually biocatalyst) to the quenching time of the reaction. In other words, all material is in the reactor for the same length of time and can be said to have a defined residence time. If this time is sufficiently long, then all the reactant will have been converted to product. Therefore, in the production of fine chemicals, batch reactors have frequently been used simply because complete conversion was achievable. Moreover, if some substrate remains at the end of the reaction, more catalyst can be added to complete the conversion. This flexibility is very attractive. Even in cases where reaching equilibrium prevents complete conversion of substrate to product, all material has an identical residence time and thereby the reaction mixture has a defined conversion. For more complex reactions (with multiple reactants, products or phases) this is critical, because otherwise what might leave the reactor is a variable mixture of compounds that complicates downstream processing. For instance, active pharmaceutical ingredients (APIs) are complex, and their production is strictly regulated (e.g., by the Federal Drug Administration or European Medicines Agency). For this reason, there is a demand for precision chemistry in the pharmaceutical industry to achieve high product quality in a reproducible manner, ensuring the safety of the patient. It is for this reason that enzymes are particularly attractive due to their high selectivity[62], compared to most conventional catalysts, which minimizes by-product formation. Additionally, they operate at mild conditions[63] which also greatly reduces the occurrence of spontaneous degradation of reactants, intermediates or products. This allows for the precise production of APIs with simpler downstream processing steps. However, to truly capitalize upon this, the reactor should also give a precise residence time. In other words; a precision catalyst used in a precision reactor. In this way the benefit of continuous biocatalysis becomes clear.

Residence time is an important characteristic of any reactor. It is desirable to have a well-defined residence time for accurate control of reactions. In an ideal CPFR, where no back-mixing occurs, material exits the reactor in the same order as it enters with a single residence time (τ) which can easily be calculated from the working volume of the reactor and the volumetric flowrate (Equation 2.1).

$$\tau = \frac{V}{Q} \tag{2.1}$$

The ideal BSTR and CPFR are the only two cases where a reactor has a single residence time. For all other reactor types and configurations, multiple residence times exist and so residence times are typically expressed as a function of time, known as the residence time distribution. For instance, the RTD of the ideal BSTR (or ideal CPFR) is represented mathematically by the following Dirac delta function, shown graphically in Figure 2.3

$$\mathrm{RTD}(t) = \delta(t - \tau) \tag{2.2}$$

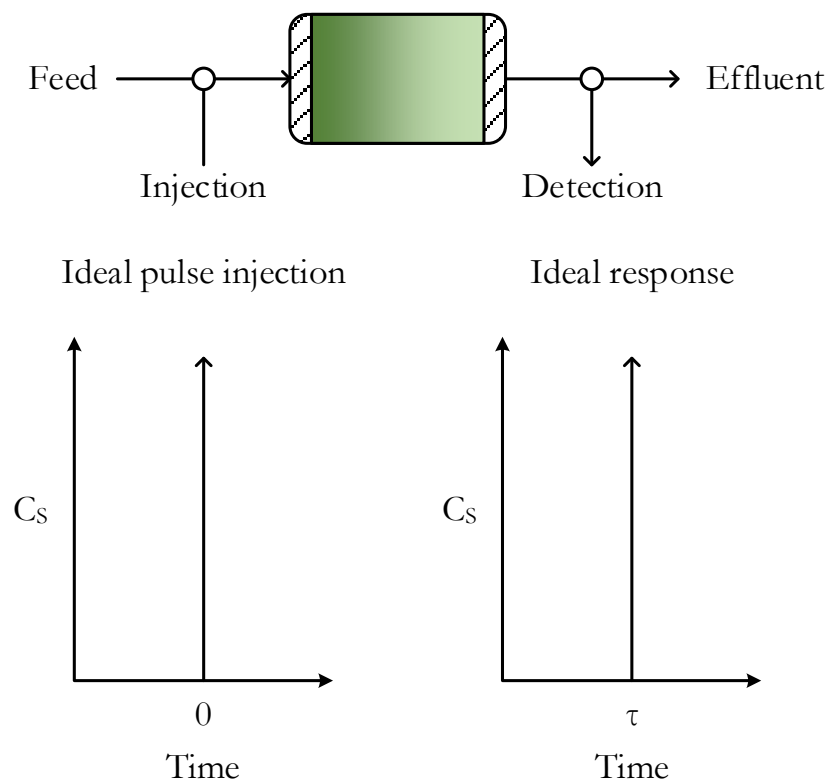

Figure 2.3. Response of a CPFR to a pulse injection under ideal conditions.

In an ideal CSTR it is assumed that mixing is complete and instantaneous, such that the composition of the entire reactor volume and the reactor outlet are homogenous. As a result, some of the feed molecules exit the reactor immediately, since fluid is constantly being removed at the outlet, whilst others remain in the reactor almost indefinitely. Therefore, the RTD can be represented by an exponential decay function (Equation 2.3), illustrated in Figure 2.4, although the mean residence time can still be calculated using Equation 2.1.

$$\mathrm{RTD}(t) = \frac{1}{\tau} e^{\left(\frac{-t}{\tau}\right)} \tag{2.3}$$

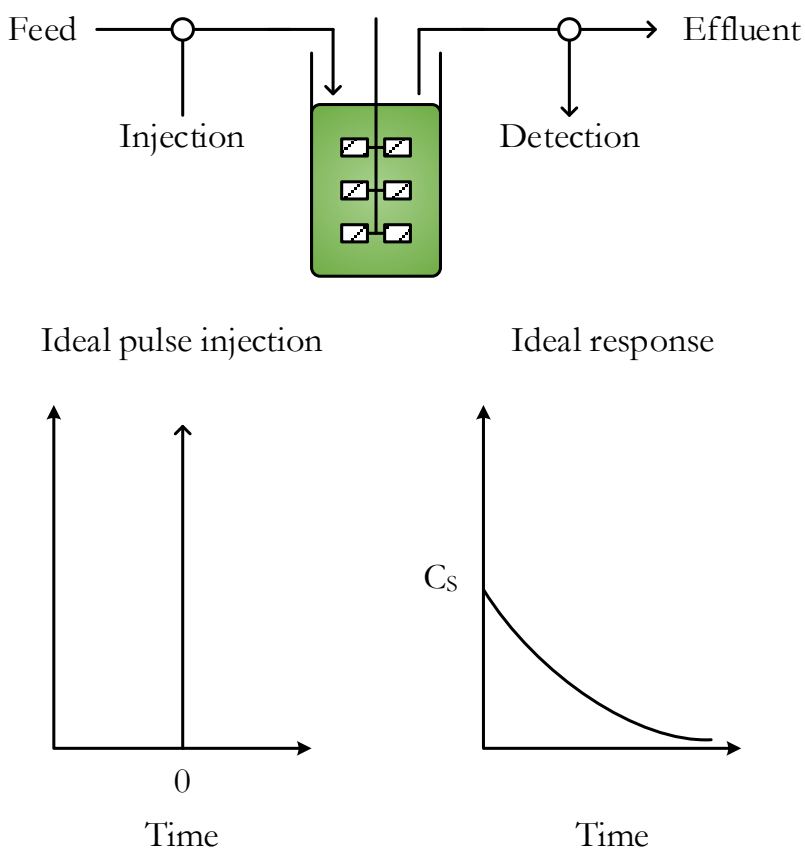

Figure 2.4. Response of a CSTR to a pulse injection under ideal conditions.

2.5 Enzyme Kinetics

Enzyme kinetics are often modeled using the basic Michaelis–Menten equation (Equation 2.4). Modified versions of this equation also exist to describe more complex systems, such as those with substrate or product inhibition, as well as multiple substrates or products.

$$v = \frac{V_{max} C_S}{K_M + C_S} \tag{2.4}$$

$$V_{max} = k_{cat} C_E \tag{2.5}$$

Equation 2.4 relates the reaction rate (v) to the substrate concentration. The maximum rate of the enzymatic reaction (V_{max}) is dependent on the concentration of the enzyme and its rate constant (Equation 2.5). The affinity constant of the enzyme towards a specific substrate, K_M, corresponds to the substrate concentration at which the initial rate will be half of the maximum rate. Therefore, to approach the maximum rate of an enzymatic reaction, and so use the enzyme effectively, the substrate concentration must be sufficiently high (relative to its K_M) that the rate equation approximates the following zero order form

$$\begin{gathered} C_S \gg K_M \\ v \approx V_{max} = k_{cat} E \end{gathered} \tag{2.6}$$

If an enzyme has a very high affinity towards a particular substrate, characterized by a very low K_M, the maximum rate of the enzymatic reaction can be achieved at low substrate concentrations. This is a highly desirable scenario because it means that the enzyme can likely be used effectively regardless of reactor type. This can be illustrated by dividing the design equation of a CSTR (Figure 2.1B) with that of a CPFR (Figure 2.1C) to determine the ratio of enzyme concentrations ($C_{E,CSTR}/C_{E,CPFR}$) required to reach a desired fractional conversion, illustrated in Figure 2.5. To reach high fractional conversions, much higher enzyme concentrations are required in a CSTR than a CPFR unless the

substrate concentration in the feed is a few orders of magnitude higher than the affinity constant of the enzyme. For this reason, protein engineering efforts should be focused on increasing the affinity of enzymes towards industrially attractive molecules[22b, 64]. In the meantime, however, enzymes generally have low affinities towards complex, non-native substrates, like many pharmaceutical intermediates. Thus, in these instances, the choice of reactor can greatly affect the reaction rates that can be achieved in a biocatalytic reaction.

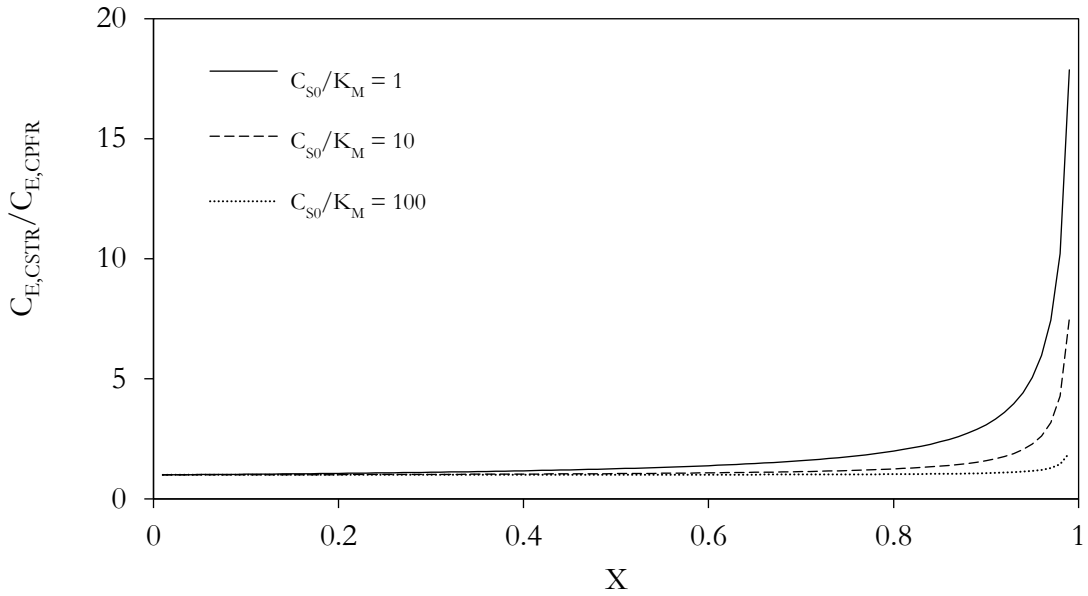

Figure 2.5. Enzyme concentrations required in a CSTR versus a CPFR to achieve a desired fractional conversion of substrate.

For instance, in a CSTR, substrate is fed into a much larger, well-mixed volume. This means the reaction takes place at a single, constant substrate concentration far more dilute than that of the feed, resulting in reduced rates throughout the reactor. In contrast, the substrate concentration in a CPFR is equal to that of the feed at the inlet, where the enzyme can operate closer to its maximum rate, and progressively decreases across the length of the reactor, as does the reaction rate. This is typically a more effective way of using the catalyst. As previously expressed, this kinetic behavior is identical to that of a biocatalytic reaction in a BSTR[51].

Enzyme inhibition by substrate or product is also very important to consider when selecting a reactor for biocatalysis. On the one hand, if the enzyme is inhibited by high concentrations of the substrate,

the substrate dilution that occurs in a CSTR may be desirable, whereas the high initial substrate concentration in a CPFR could have a negative impact. On the other hand, if the enzyme is inhibited by the product, operating in a CSTR is undesirable as the homogeneity guarantees inhibition throughout the reactor unless a much larger, more dilute reaction volume is used, which would increase capital costs as well as the cost of downstream processing. Conversely, in a BSTR, product inhibition would only become problematic towards the end of the reaction. Likewise, in a CPFR, the rate would only be severely inhibited towards the end of the reactor, whilst maintaining a smaller, more concentrated and cost-effective volume. The concentrations of substrate and product throughout the reactor also influence the thermodynamic equilibrium of the reaction[65].

The difference in capital costs between a CSTR and CPFR is best demonstrated with an example. One of the most successful instances where a biocatalytic reaction has been implemented in industry in recent years is the use of a highly engineered transaminase in the production of sitagliptin, the active ingredient in an anti-diabetic medication[66]. The kinetic parameters of this enzyme have not been published. However, another transaminase from *Halomonas elongata*, which has been characterized, was recently used for the continuous production of amines at laboratory scale[67]. The turnover number of this enzyme was found to be 0.094 s^{-1}, and its K_M values were 2.57 mM and 0.56 mM towards (*S*)-1-phenylethylamine (amino donor) and pyruvate (amino acceptor), respectively, for the production of acetophenone at 25°C [68]. Due to the higher affinity of the enzyme towards pyruvate, it will be assumed that pyruvate can be supplied in sufficient excess such that the reaction rate is only dependent on the concentration of (*S*)-1-phenylethylamine, according to Equation 2.4. Equation 2.7 shows how the Michaelis–Menten expression can be transformed into a function of the fractional conversion, where F_{S0} is the inlet molar flowrate of substrate.

$$v = \frac{k_{cat} C_E \frac{F_{S0}}{Q}(1 - X)}{K_M + \frac{F_{S0}}{Q}(1 - X)} \tag{2.7}$$

Assuming an enzyme concentration of 1 $g.L^{-1}$, desired annual production target of 100 kg and a final product concentration of 10 $g.L^{-1}$, Figure 2.6 shows the Levenspiel plot for this reaction, which can be used to determine the reactor volume required to achieve a desired conversion in a continuous

reactor with these conditions[69]. For a CSTR, the required volume is equal to the area of a rectangle with a height of F_{S0}/v and a width of X, whereas for a CPFR, the required volume is the area under the curve. It is clear from Figure 2.6 that a similar volume would be required for both reactors to achieve most fractional conversions. In fact, only 2.5 L more volume would be required in a CSTR than a CPFR to achieve 80% substrate conversion. However, in most biocatalytic reactions the only difference between the substrate and product is a single functional group, which can make separating them extremely challenging. Therefore, to avoid adding more complexity to the downstream process it is best to aim for complete conversion of the substrate and this is where the gap between the CSTR and the CPFR becomes apparent. From Figure 2.6, it can be calculated that, to achieve 99% substrate conversion, a CPFR with a volume of 38 L would be sufficient, but a CSTR would require a volume of 134 L, nearly 4 times larger. This problem becomes significantly worse if a conversion of 99.9% is desired, in which case a CSTR would require 23 times more volume than a CPFR, greatly increasing capital and downstream processing costs. These are perfectly reasonable targets for reaction conversion in the pharmaceutical industry, based on what is already achievable.[70]

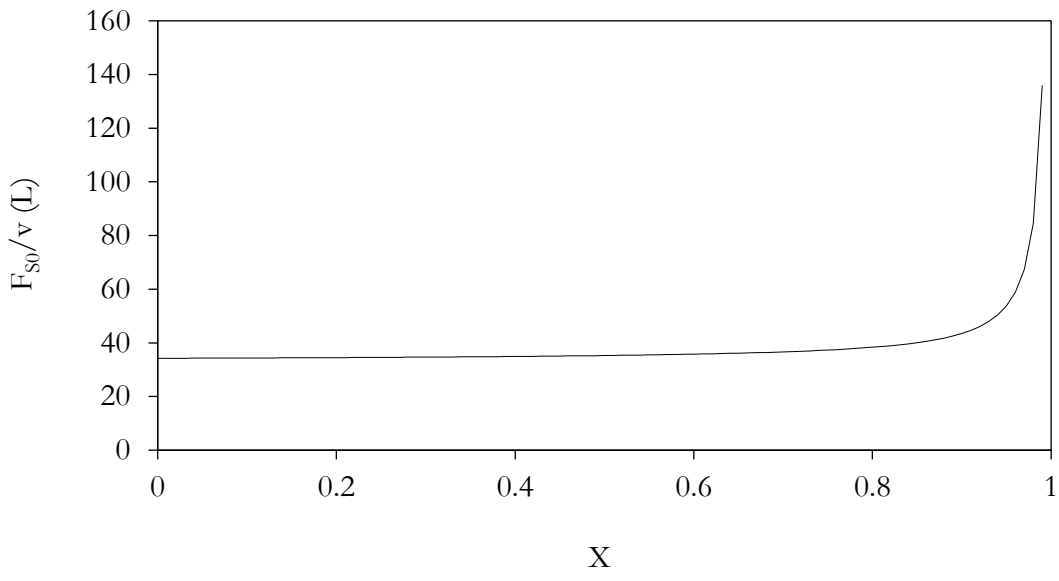

Figure 2.6. Levenspiel plot for the production of acetophenone from (*S*)-1-phenylethylamine and pyruvate by an amine transaminase from *Halomonas elongata*.

2.6 pH Control and Multiphase Systems

Much of the previous discussion has shown that CPFRs are generally better suited for continuous biocatalysis than CSTRs, particularly for the production of high-value molecules. Nevertheless, CPFRs and CPBRs do have some limitations that may preclude their use with certain systems. For instance, although residence time and temperature are easily controlled in these reactors, control of pH across the length of the reactor is often more challenging due to the concentration gradients that arise from the lack of mixing[22c]. To overcome this problem, engineered enzymes that can tolerate the range of pH expected to occur across the reactor would be required. Alternatively, the effluent from the CPFR can be recycled through a CSTR where acid or base can be added to adjust the pH back to the optimal value, as illustrated in Figure 2.7. Here, the well-mixed behavior of a CSTR is extremely beneficial to quickly counteract pH changes. Another possibility is to operate multiple shorter CPFRs in series since the performance will be the same as a single long CPFR. This allows additional pH adjustments to be made in between CPFRs, as shown in Figure 2.8. This configuration could also allow intermediate substrate feeding to avoid substrate inhibition.

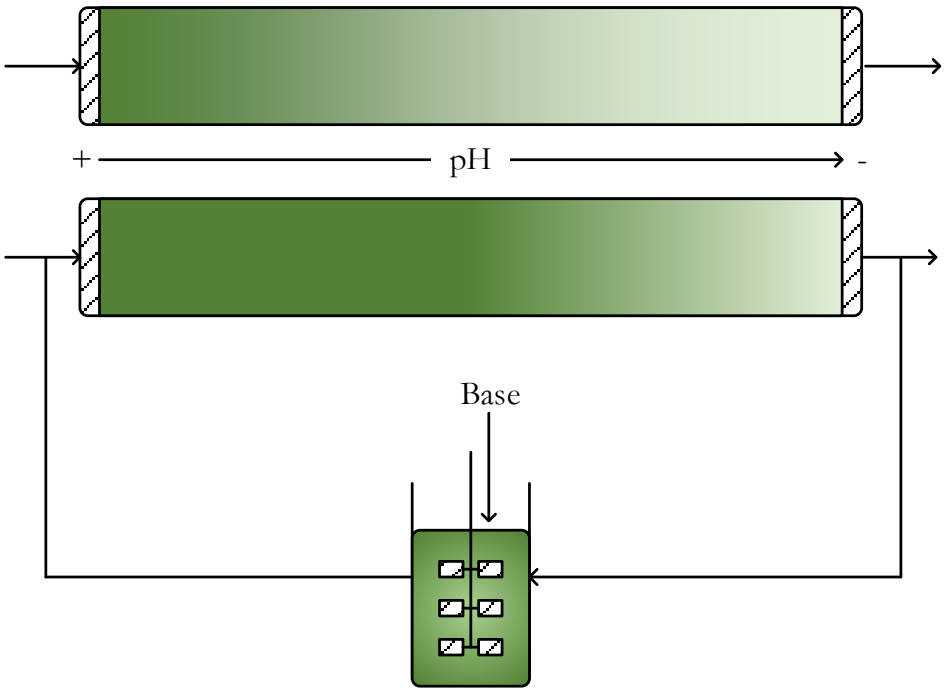

Figure 2.7. Comparison of pH profiles in a CPFR when pH is controlled via the feed stream and when coupled to a CSTR with base addition through a recycle loop.

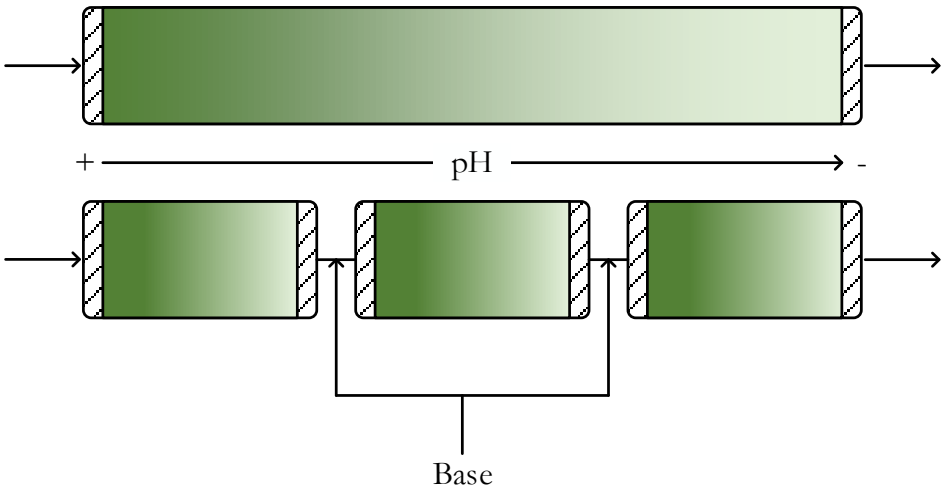

Figure 2.8. Operating multiple CPFRs in series allows intermediate pH adjustment without increasing the total reactor volume required to reach the desired conversion.

Another instance where CPFRs are generally ill-suited for use is with multiphase systems, commonly encountered in the field of industrial biocatalysis, as channeling often occurs due to the lack of mixing[71]. In fact, multiphase biocatalytic systems are often limited by mass transfer between phases, such as the supply of molecular oxygen to biocatalytic oxidation reactions or when using a water-immiscible organic solvent as a means of *in situ* substrate supply (ISSS) or *in situ* product removal (ISPR) to combat inhibition[72]. In such systems, it is imperative to maintain large interfacial areas between the immiscible phases to facilitate mass transfer. For small-scale applications, microfluidic reactors are being used increasingly because their high surface-to-volume ratios afford excellent mass transfer rates between immiscible phases[73]. However, for large scale applications, surface-to-volume ratios tend to be much lower and so mechanical mixing is required to speed up mass transfer. As such, CSTRs would appear to be much better suited than CPFRs for handling multiphase systems. Nonetheless, as previously discussed, they also have many disadvantages. One way of overcoming these limitations would be to operate a series of CSTRs, which approximates plug-flow behavior, as shown in Figure 2.9. This approach may also be generally attractive to the fine chemical industry as very few modifications would have to be made to existing batch infrastructure to switch to continuous operation.

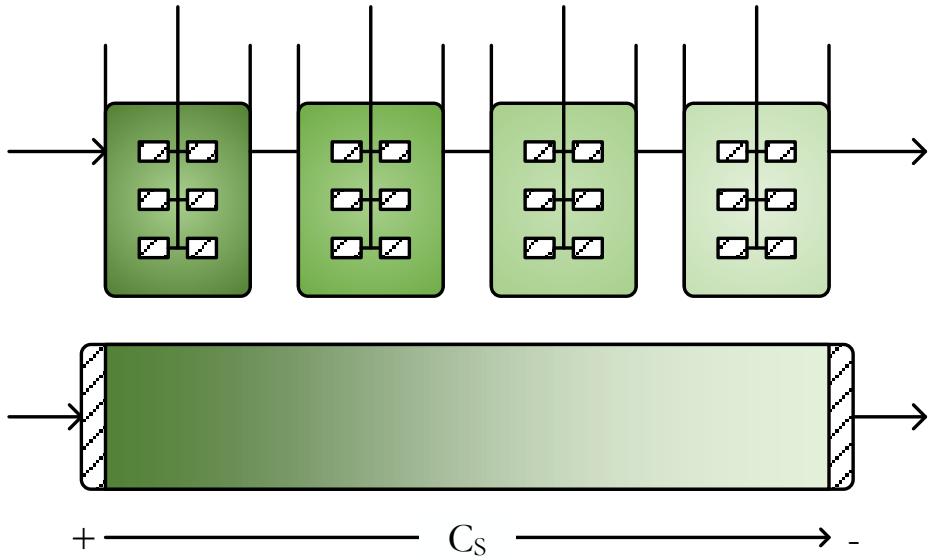

Figure 2.9. A series of CSTRs approximates the plug-flow behavior of a CPFR, but also allows intermediate addition of substrates, pH adjustment and improved mass transfer in multiphase systems.

Gas-liquid Mass Transfer

Gaseous molecular oxygen can be supplied to a continuous reaction in many ways e.g. through a gas permeable membrane in a tube-in-tube configuration[74] (Figure 2.10A), by flow of alternating gas and liquid segments in a single tube[75] (Figure 2.10B) or simply by bubbling the gas into a stirred tank.

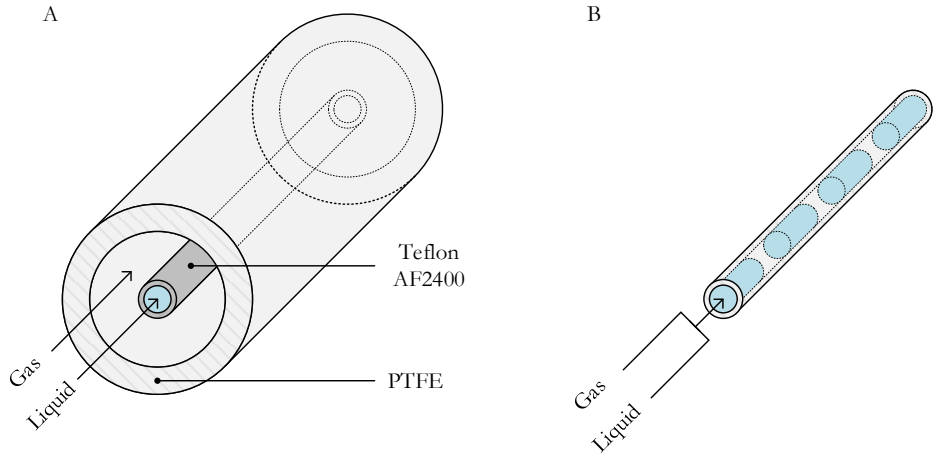

Figure 2.10. A) Tube-in-tube and B) segmented flow microreactors for gas-liquid reactions.

Regardless of how the gas is supplied, the important factor to consider is the interfacial area between the gas and liquid phases over which gas-liquid mass transfer occurs. This is represented by the specific

surface area of the reactor, in this case the area of gas-liquid interface per liquid volume. The larger the specific surface area, the faster oxygen can be supplied to the oxidation reaction occurring in the bulk of the liquid phase, enabling higher reaction rates. Unfortunately, while tubular reactor configurations are generally attractive for continuous operation, their specific surface areas are determined by the tube dimensions. Specifically, in a tube-in-tube configuration, the area of the gas-liquid interface is equivalent to the inner surface area of the tube in contact with the reaction media while, in a segmented flow configuration, the tube diameter dictates the size of the gas bubbles in contact with the reaction media. Therefore, on the one hand, at small tube diameters the surface-to-volume ratios are high, resulting in large specific surface areas that enable rapid gas-liquid mass transfer. However, small diameter tubes are subject to large pressure drops and, furthermore, can easily become clogged, which limits their use in industrial applications. On the other hand, increasing the diameter of a tubular reactor dramatically decreases its specific surface area, as shown in Figure 2.11.

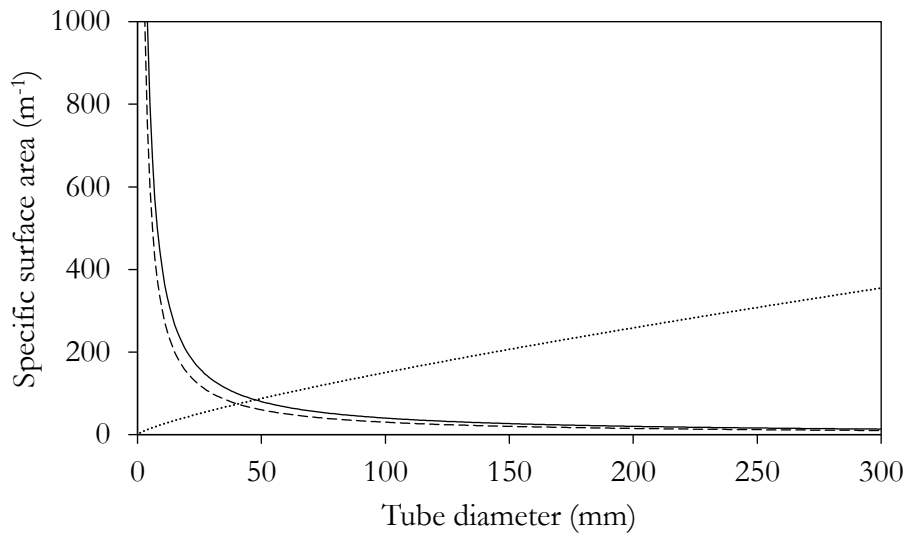

Figure 2.11. Gas-liquid interfacial areas of tube-in-tube reactor (solid line) and segmented flow reactor (SFR) (dashed line) at different diameters (length = 1 m), as well as a continuous stirred tank reactor (CSTR) of equivalent volume (dotted line). For the SFR, equidistant spherical bubbles with diameters equal to that of the tube were assumed. For the CSTR, specific surface area was estimated using correlations for volumetric mass transfer coefficient (k_La)[76] and liquid-side mass transfer coefficient (k_L)[77]. Detailed calculations can be found in Chapters 6 and 11 of the Handbook of Industrial Mixing[78].

In contrast, interfacial areas in stirred tanks (bubbled with air or any gas containing oxygen) of equivalent volume typically increase with scale[79]. This is very attractive for streamlining industrial implementation of continuous biocatalytic oxidations, since the design, scale-up, operation and control of stirred tank reactors is well researched.[80] Furthermore, batch stirred tank reactors are already widely applied in many industrial production processes[81] and can easily be retrofitted to operate continuously, especially since aerated batch reactors already operate continuously with respect to the gas phase.

2.7 Reactor Selection Methodology

While not widely discussed in the scientific literature, the analyses of reactor configurations in the previous sections are established. This analysis was arranged into a reactor selection methodology so that decisions about continuous biocatalytic reactors can be made on a rational basis. However, before the reactor selection process can begin, a number of prerequisites should be satisfied, namely that the kinetic parameters for the enzyme of interest have been characterized, the operating conditions (temperature, pH, co-solvents etc.) have been set and the enzyme has been shown to be stable at these conditions for a sufficient duration, which is case-dependent. Additionally, it is recommended that the main limitations of the enzyme[82] are identified and its performance is compared with relevant economic targets[23a], as discussed in Chapter 1.

Figure 2.12 shows a proposed workflow for selecting a continuous reactor configuration. Initially, it is important to assess whether the enzyme or downstream purification is likely to be the dominant operating cost of the process, since the objectives in each case are different. For example, if an expensive enzyme is required then it is crucial to select a reactor configuration that will make the most effective use of the enzyme kinetics. However, if the enzyme is inexpensive, relative to product isolation and purification, the kinetics become less important since higher enzyme concentrations can always be used to increase reaction rates. In such a case, it would instead be desirable to simplify downstream processing by ensuring that effluent concentrations do not vary significantly, so as to maintain the necessary driving force for separation. This can be achieved by having a well-defined residence time. Additionally, if possible, the substrate should be fully converted to avoid difficult separations.

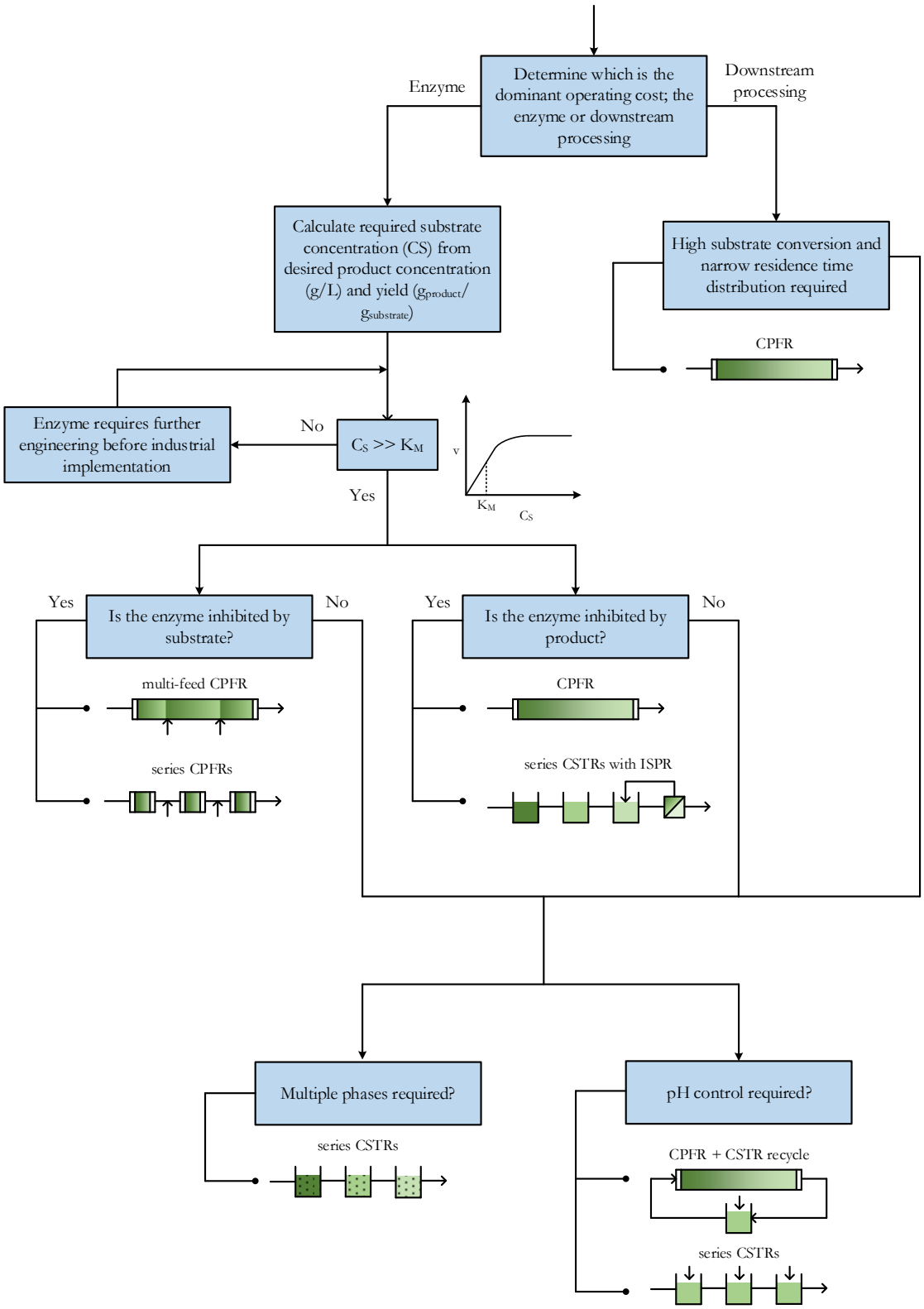

Figure 2.12. Methodology for selection of continuous biocatalytic reactor configurations.

If the enzyme is determined to be the dominant operating cost, the next step is to calculate the required substrate concentration from the desired product concentration and reaction yield. For instance, in the case of high value products, a product concentration of at least 60 $g.L^{-1}$ is generally required to be economically feasible[23a]. Once the substrate concentration is determined it should be compared to the affinity constant of the enzyme to assess whether it is high enough for the enzyme to operate close to its maximum rate. Since enzymatic reactions typically take place in aqueous environments, the water solubility of the substrate may be a limiting factor, especially for large, complex, organic molecules. Therefore, organic solvents may be required to increase substrate solubility. Protein engineering has recently been applied to allow enzymes to operate in the presence of organic solvents[83] without becoming inactivated. However, the ideal scenario would be to have enzymes operating in neat substrate, completely solvent-free[84]. If the substrate concentration is not above the affinity constant, it means that the enzyme is guaranteed to operate at less than half of its maximum rate, which is far too ineffective for many industrial processes given the cost of enzymes. Consequently, it would be better to continue engineering the enzyme to reduce its K_M until it is below the required substrate concentration.

If the substrate concentration is sufficient for good rates, the next step is to determine whether the enzyme is inhibited by the substrate or product. If the enzyme is inhibited at substrate concentrations close to the desired feed concentration, a CPFR can be used if it is fed with a lower substrate concentration at multiple points along the reactor. However, the lack of mixing could make it difficult to radially disperse the substrate in reactors with larger diameters, especially if the substrate is fed from one side of the reactor. Therefore, a better alternative may be to operate a series of shorter CPFRs, using the same total reaction volume, but with a substrate feed between each reactor.

If the product inhibits the enzyme at the desired product concentration, a CPFR can be used to ensure that product inhibition is only severe towards the end of the reactor. Alternatively, plug-flow behavior can be approximated with a series of CSTRs, each having a higher product concentration than the previous. In this way, only the last reactors should be severely inhibited. Nevertheless, the last reactor in the series should be equipped with a means of selectively removing the product to prevent complete inhibition in the reactor and avoid substrate in the effluent.

If downstream processing is found to have a higher overall cost contribution than the enzyme, plug-flow behavior is critical for approaching full conversion; so too having good control over the residence

time, and consequently the concentration profiles at the outlet. Therefore, a CPFR would be the most appropriate reactor configuration.

Finally, the need for pH control and/or multiple phases should be considered. In both of these cases, good mixing is required to neutralize pH changes or generate high interfacial areas between phases. For multiphase reactions, a series of CSTRs should be used to approximate plug-flow behavior while still allowing sufficient dispersion of the phases. This configuration would also be beneficial for pH control because it provides multiple acid/base feed points. Alternatively, a CPFR can be coupled with a recycle loop through a CSTR where pH can be controlled, although the presence of a recycle complicates the process.

2.8 Immobilization

Due to the high cost of enzymes, it is desirable to recycle them for continuous operation, provided they are stable enough for repeated use. Isolation of the enzyme downstream of the reactor, using selectively permeable membranes, is one possibility, but introduces an additional unit operation and further complexity to the process. A better alternative is to retain the enzyme within the reactor. This can be done by placing membranes at the reactor outlet, however, fouling of the membrane and concentration polarization are likely to become problematic[85]. For this reason, the most common method of retaining enzymes within a reactor is by binding them to larger carrier particles that are easier to separate from the reactor effluent than the soluble enzyme. For instance, the use of paramagnetic nanoparticles as supports has recently received much attention due to their high specific surface areas and simple retention within the reactor by a magnetic field[86]. But, numerous other methods and support materials have also been described for the immobilization of a wide variety of enzymes[4c]. Depending on the support material used, immobilization can improve the stability of an enzyme towards harsher operating conditions, such as elevated temperatures or the presence of organic co-solvents[87], since bonds are formed between the enzyme and the support. However, in some cases, these bonds, particularly strong covalent bonds, may prevent the enzyme from adopting a more stable conformation or one that is required to catalyze the desired reaction and so, immobilization of an enzyme can also negatively affect its stability or activity[88]. Physical adsorption is an alternative for immobilizing enzymes without forming such strong bonds[89] but this makes it easier for the enzyme to leach off the support during reactor operation. Affinity immobilization, whereby enzymes are engineered to contain specific tags[90] that bind very selectively to ligands on specialized support materials, minimizes leaching and maintains the flexibility of the enzyme so that activity loss is reduced.

This method of immobilization also ensures that only the desired enzyme binds to the support instead of other proteins or impurities that may be present in crude cell extracts.

In stirred tank reactors, whether they are operated in batch or continuously, the use of immobilized biocatalysts is often limited because the catalyst loading in the reactor is restricted to about 10% (v,v), compared to 60% (v,v) in a CPBR[51]. This is because the shear forces from stirring[91] may break apart the carrier material, making the biocatalyst difficult to separate from the reaction media and potentially contaminating the effluent. Loss of biocatalyst in the effluent would also reduce the productivity of a CSTR. Cross-linked enzyme aggregates (CLEAs)[92] are a more suitable form of immobilization for use in stirred tank reactors[93] due to their smaller size compared to typical carrier-bound biocatalysts.

Although immobilization has proven to be advantageous in some cases, it is important to recognize that the support and immobilization process add additional cost to the biocatalyst and this should always be taken into consideration when assessing the feasibility of a process. Furthermore, although most immobilization supports allow for high protein loadings due to their large specific surface areas, internal diffusion limitations frequently make such high loadings ineffective[94]. As a result, immobilization often limits the amount of enzyme that can be loaded into a reactor, compared to soluble enzymes. Fortunately, as protein expression and engineering continue to improve, the costs of enzymes may decrease until eventually it becomes feasible to utilize soluble enzymes in continuous processes[95]. This would be especially attractive for fine chemical industries, where the high value of the products can help offset the cost of the biocatalyst, to simplify production. Additionally, the enzyme would only need to be stable at the desired operating conditions for the length of the residence time in the reactor.

Due to the high variability and case-dependence of immobilization techniques and materials, as well as the absence of any rational selection methodology, the identification of an optimal immobilization strategy is extremely time- and resource-intensive. As such, immobilization was not implemented in this work. Instead, soluble enzymes were continuously supplied to reactors during experiments. While this may not yet be economical at industrial scale, it simplifies the laboratory-scale study of enzyme kinetics under continuous operation.

2.9 Conclusions

CPFRs are attractive for continuous biocatalysis because they exhibit well-defined residence time distributions and enable complete conversion, which greatly simplifies downstream processing.

Moreover, they make effective use of enzymes by avoiding excessive substrate dilution throughout the reactor, especially in cases where product inhibition is a concern. However, plug-flow operation inherently results in a low degree of mixing, which is essential for reactions that require pH control or multiphase reactions that are limited by interphase mass transfer. In these instances, effective plug-flow operation is limited to the microscale, where high surface-to-volume ratios and short diffusion distances counteract the lack of mixing. While it may be possible to scale out these reactors for industrial application, the sheer number of reactors required to operate in parallel to achieve industrial productivities would likely create many practical limitations with respect to process monitoring and fluid distribution. Upon scale-up, the performance of these reactors begins to drop drastically. Therefore, a more scalable alternative would be to operate multiphase reactions in CSTRs, where mechanical mixing is used to facilitate mass transfer and pH control. Thus, the CSTR appears to be the most suitable reactor configuration for biocatalytic oxidation of glucose to gluconic acid using molecular oxygen. As such, reactor configurations comprised of single or multiple CSTRs will be the focus of the following chapters.

Chapter 3

Experimental methods

3.1 Introduction

In Chapter 2, it was found that CSTRs may be the most suitable reactor type for carrying out continuous biocatalytic oxidations, despite their limitations, since the use of mechanical mixing enables high gas-liquid oxygen transfer rates. Additionally, unlike microscale reactors, whose large surface-to-volume ratios do the same, CSTRs are more readily scalable. This allows their immediate implementation into industry, especially since many manufacturers already employ batch stirred-tank reactors that could easily be retrofitted to operate continuously. As such, experiments were carried out in CSTR configurations, the results of which are discussed in Chapters 4, 5 and 6. The experimental methods employed in these chapters are described in the following sections.

3.2 Continuous oxidation reactions

The glucose oxidase (GOx) used in experiments (Novozym® 28166) was kindly donated by Novozymes A/S, Denmark. All other chemicals and catalase were purchased from Sigma-Aldrich, Denmark. Reactions were carried out in 150 mL (liquid volume) my-Control stirred tank reactors (Applikon Biotechnology B.V., Netherlands), illustrated in Figure 3.1. An Ismatec Reglo Independent Channel Control peristaltic pump (Cole-Parmer, USA) was used to supply the reactor with an enzyme feed (0.2-2 $g.L^{-1}$ GOx, 0.2-2 $g.L^{-1}$ bovine liver catalase, 100 mM pH 7 potassium phosphate buffer) and a substrate feed (2 M glucose, 100 mM pH 7 potassium phosphate buffer), each at a rate of 1.5 $mL.min^{-1}$, as well as pump the mixed reactor contents out of the vessel at a rate of 3 $mL.min^{-1}$. Therefore, overall feed concentrations into the reactor were 1 M glucose and 0.1-1 $g.L^{-1}$ GOx and catalase with a dilution rate of 1.2 h^{-1}. These same concentrations were used to initiate each reaction.

As discussed in Chapter 1, catalase is often coupled to oxidases as a means of removing hydrogen peroxide, a by-product of the oxidation reaction, to avoid inhibition and/or deactivation. The activity of an enzyme is measured in Units (U), defined as the amount of enzyme required to convert 1 μmol of substrate per minute. According to the manufacturer specifications, the activity of the GOx and catalase are 6.5 $U.mg_{pure\ enzyme}^{-1}$ and 2000 $U.mg_{protein}^{-1}$, respectively, at 25°C and pH 7.[96]

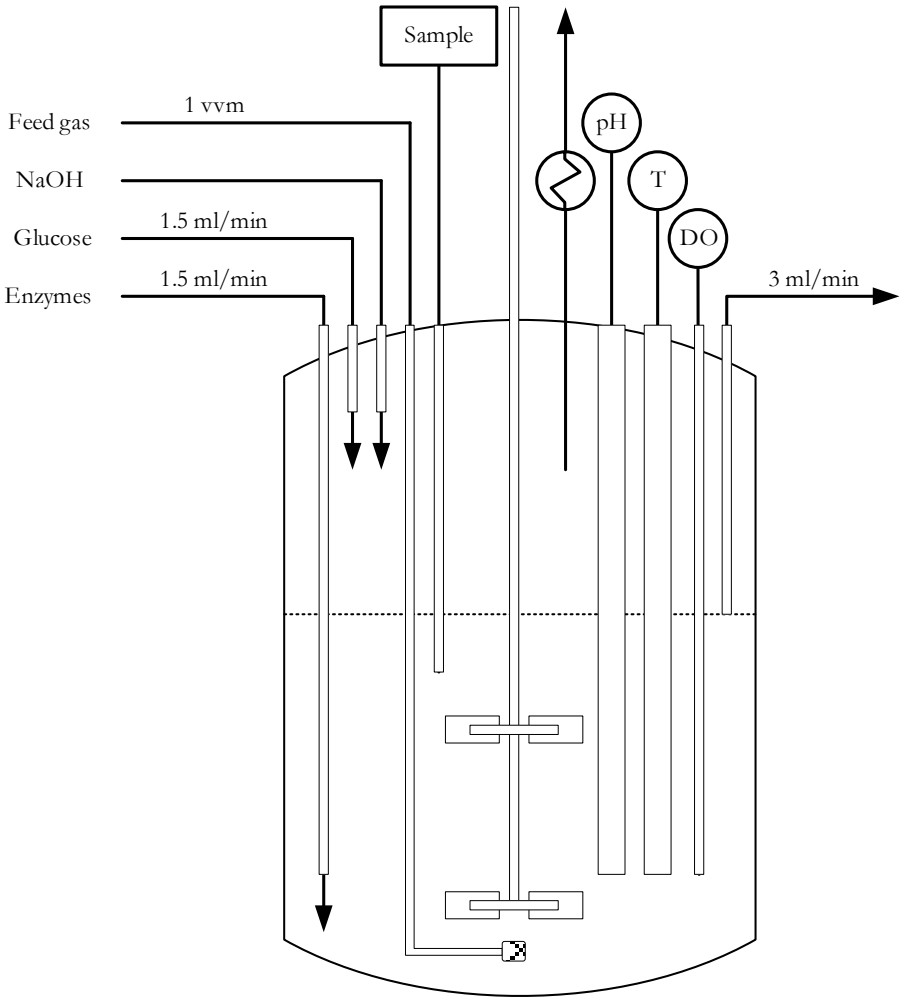

Figure 3.1. CSTR setup for continuous biocatalytic oxidation of glucose to gluconic acid. Two flights of Rushton impellers were used for mixing. Due to the small liquid volume (150 mL) and number of internals, no additional baffles were included.

However, the overall activity of the lyophilized catalase formulation may be lower, since its protein content is only specified to be ≥ 60%. Even so, this suggests that the catalase concentration required to consume all of the hydrogen peroxide produced by GOx should be fairly low in comparison to the concentration of GOx in the reactor, which would help to reduce costs. But, as the affinity of GOx towards hydrogen peroxide has been found to be similar to its affinity towards dissolved oxygen (DO), it may already become severely inhibited at hydrogen peroxide concentrations as low as 0.51 mM. In contrast, the affinity constant of bovine liver catalase towards hydrogen peroxide has been found to be 35 mM, indicating that its reaction rate would be significantly reduced at hydrogen peroxide

concentrations low enough to avoid inhibition of GOx.[97] This means that, opting for a catalase concentration such that $U_{GOx} = U_{CAT}$, according to the 1:1 stoichiometry of the reaction, would likely require significant hydrogen peroxide accumulation to occur before the catalase reaction rate could balance that of GOx. Instead, to ensure that hydrogen peroxide concentrations during experiments could be minimized as far as possible, a large excess of catalase was employed ($U_{CAT} > 100U_{GOx}$), by supplying each reaction with equal concentrations of catalase and GOx.

The reactor was sparged at 1 vvm (volume gas per volume reaction liquid per minute) with gas (composed of varying ratios of nitrogen and oxygen). To ensure well-mixed conditions, the reactor contents were mechanically stirred at 1000 rpm. Off-gas leaving the reactor was passed through a condenser to avoid any potential volume-loss due to stripping. The temperature and pH of the reactor contents were controlled at 25°C and pH 7, to match the conditions at which kinetic parameters for GOx were available. The reactor was operated as a pH-stat, whereby a proportional-integral (PI) controller regulated the addition of 5 M NaOH to the media to maintain the desired pH, based on measurements from a pH probe in the reactor. Reaction media often contain surface active agents which adsorb to hydrophobic gas-liquid interfaces. In a gas-sparged system, these surfactants stabilize the bubbles, preventing them from coalescing. As such, when the bubbles reach the headspace of the reactor, they form a stable foam instead of bursting. During the experiments, foam formation in the reactor was reduced by manual dropwise addition of Antifoam 204; a mixture of organic non-silicone polypropylene-based polyether dispersions that adsorb to and spread across gas-liquid interfaces to destabilize them. This was done to avoid overflow of the reactor as well as prevent the foam from stripping the reaction volume of enzymes or reagents.

O_2 saturation (%) in the reactor was monitored and logged using robust optical oxygen probes (Pyroscience AT GmbH, Germany). Probes were calibrated by saturating the reaction media, prior to initiation of the reaction by addition of the enzymes, with nitrogen to achieve 0% O_2 saturation and separately, pure oxygen to achieve 100% O_2 saturation. Percentage O_2 saturation was converted to DO concentration (mM) using the Henry's Law constant of oxygen dissolved in pure water (1.3×10^{-5} $mmol.L^{-1}.Pa^{-1}$).[40] During operation, samples (950 μL) were periodically taken from the reactor, using 50 μL of 5 M H_2SO_4 to quench the reactions. These samples were then analyzed by HPLC in an Aminex HPX-87H column (Bio-Rad Laboratories, Inc., USA), at 20°C with a mobile phase flow rate of 0.6 $mL.min^{-1}$ of 5 mM H_2SO_4. Refractive Index (RI) and 205 nm Ultraviolet (UV) spectra were used to determine the glucose and gluconic acid concentrations, respectively. Figures 3.2 and 3.3 show

the HPLC calibration curves for glucose and gluconic acid, respectively. Both compounds exhibit similar refractive index (RI) behavior, but only gluconic acid shows significant UV absorbance at 205 nm. Therefore, to determine the concentration of glucose, the concentration of gluconic acid is first calculated using the corresponding UV calibration curve. This concentration is then converted into an equivalent area using the RI calibration curve of gluconic acid, which is then subtracted from the total area measured on the RI channel. The remaining area is attributed to glucose and converted to units of concentration using the RI calibration curve of glucose.

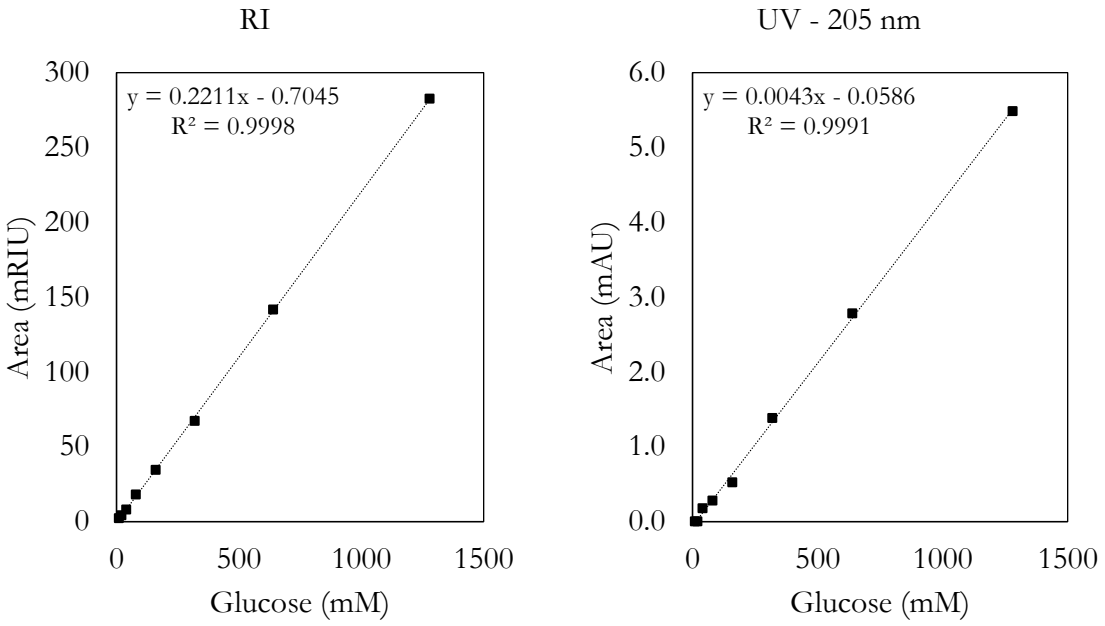

Figure 3.2. Calibration curves for glucose in refractive index (RI) and 205 nm UV channels

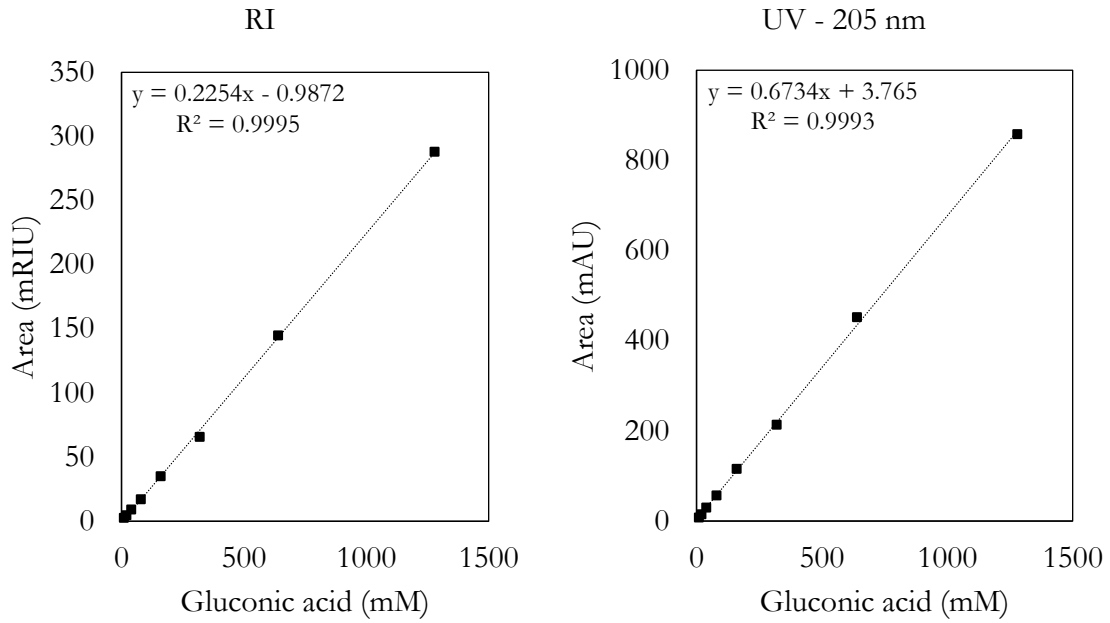

Figure 3.3. Calibration curves for gluconic acid in refractive index (RI) and 205 nm UV channels

Each reaction was monitored for 6 hours (>7 mean residence times), to ensure that steady-state operation could be achieved across all operating conditions. Figure 3.4 illustrates how two identical CSTRs were connected in series, as discussed in Chapter 5. In this configuration, only the first reactor contained glucose prior to initiation of the reaction by addition of enzymes to both reactors.

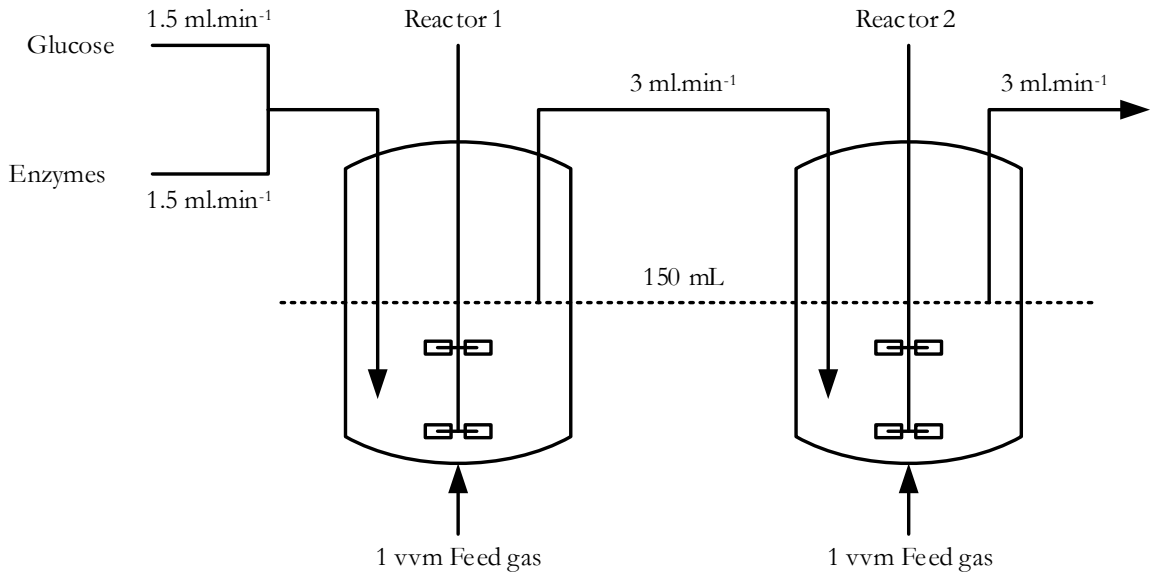

Figure 3.4. Experimental setup comprised of two CSTRs connected in series via a peristaltic pump.

3.3 GOx stability

For a continuous biocatalytic process, it is important to ensure that the enzymes are sufficiently stable to endure prolonged exposure to the selected operating conditions. This is especially important for systems where a fixed amount of enzyme is retained within the reactor. However, in this work, reactors were continuously supplied with a fresh feed of both enzymes during experiments and so it is only necessary to ensure that they remain stable in the feed solution for the duration of the experiment and in the reactor for the residence time. However, as discussed in Chapter 2, the residence time in a CSTR is distributed according to an exponential decay function. This means that a molecule of enzyme entering the reactor may immediately leave as part of the effluent, since the system is well-mixed, but it could also theoretically remain within the reactor for the entire duration of the experiment. Thus, while the enzyme might be stable for the mean residence time, the overall activity may still drop over the course of the experiment.

The stability of an enzyme can be assessed by periodically measuring its activity over time, using an activity assay. Since catalase was supplied to the reactors in such large excess, a drop in the overall catalase activity, unless severe, would likely not impact the results significantly. Therefore, only the stability of GOx was measured. GOx activity can be quantified by coupling the reaction to that of horseradish peroxidase, which uses the hydrogen peroxide by-product of GOx to convert 4-aminoantipyrine and sodium 3,5-dichloro-2-hydroxybenzenesulfonic acid into a pink dye.[98] This secondary reaction can be monitored spectrophotometrically at a wavelength of 515 nm. The activity of the enzyme is then calculated from only the initial rate of reaction, before the effect of substrate depletion becomes significant.

To assess whether the GOx could remain stable over the course of a 6-hour experiment, the reactor was operated as described in the previous section, but in the absence of glucose. The reactor initially contained 0.1 $g.L^{-1}$ GOx and was fed with the same concentration at a rate of 3 $mL.min^{-1}$. Triplicate measurements of the GOx activity were performed on an hourly basis for 6 hours. Activity measurements were also performed on the quiescent enzyme feedstock for comparison. These results are presented in Chapter 4.

3.4 k_La determination

The well-described dynamic gassing-in method[99] was used to estimate gas-liquid mass transfer coefficient, k_La, in the reactors. All k_La values were determined at 25°C, 1000 rpm and 1 vvm feed gas.

The feed gas was switched from nitrogen to pure oxygen to produce a dynamic response in DO concentration that was measured by the oxygen probes. Pure oxygen was used instead of air to reduce the effect of gas-liquid oxygen transfer on the oxygen partial pressure within the bubbles.[100] The oxygen transfer rate (OTR) in the reactor can be calculated according to Equation 3.1, where C_O^* is the partial pressure-dependent solubility of oxygen in water (i.e. at equilibrium: 0.26 mM for air or 1.22 mM for pure oxygen at 1 atm, 25°C). Solution of Equation 3.1 yields Equation 3.2. When plotted using the data of the dynamic response, the k_La is equal to the gradient of the linear region.

$$\mathrm{OTR} = \frac{dC_O}{dt} = k_L a(C_O^* - C_O) \tag{3.1}$$

$$\ln\left(\frac{C_O^* - C_{O,t=0}}{C_O^* - C_O}\right) = k_L a \cdot t \tag{3.2}$$

Chapter 4

Glucose oxidation in a CSTR

This chapter forms the basis of a recently published journal article: Lindeque, R. M.; Woodley, J. M., The Effect of Dissolved Oxygen on Kinetics during Continuous Biocatalytic Oxidations. *Org. Process Res. Dev.* 2020, 24(10), 2055-2063.

4.1 Introduction

In Chapter 2, it was suggested that, while plug-flow operation is attractive for continuous processing, better mixing may be required to carry out multiphase reactions. As such, CSTRs were recommended for biocatalytic oxidations, which utilize gaseous molecular oxygen as a substrate. However, the disadvantages of these reactors were also outlined and so a number of attempts have been made to bypass gas-liquid mass transfer entirely to avoid their use.

There are three alternatives for supplying molecular oxygen to a continuous biocatalytic oxidation. The first is to feed the reaction with a liquid stream containing dissolved oxygen (DO). The solubility of oxygen increases proportionally with pressure. Therefore, a higher DO concentration can be fed to a process by operating at elevated pressures. Using this principle, a six-fold improvement in the reaction rate of glucose oxidase was achieved by operating a tubular microreactor at 34 bar, which raised the oxygen solubility to 43 mM.[101] While this does allow higher reaction rates at the start of a tubular reactor, the maximum product titer that can be achieved at the reactor outlet is still limited due to the stoichiometry of oxidase-catalyzed reactions (1 mol substrate and 1 mol O_2 gives 1 mol product). Moreover, this technique greatly increases the capital and operating costs of an industrial scale process, as well as introduces a significant safety risk.

The second possibility is to generate the DO required for the oxidation reaction *in situ*. As discussed previously, one way of doing this is through the use of catalase[102], which can convert hydrogen peroxide into oxygen and water. However, as discussed in Chapter 1, the stoichiometry of this reaction is rather unfavorable (1 mol H_2O_2 gives 0.5 mol O_2). Thus, for catalase to be the sole source of dissolved oxygen, hydrogen peroxide must actually be supplied in excess to the reaction. This approach was recently used to increase the productivity of galactose oxidase 5-fold in a tubular

microreactor.[103] Nevertheless, hydrogen peroxide can, in some cases, modify the peptide core of an enzyme as well as oxidize some cofactors and prosthetic groups, which may negatively impact enzyme activity or stability.[42, 104] For instance, variants of glucose oxidase[43, 105], laccase[106], bilirubin oxidase[107], D-amino acid oxidase[108] and glycolate oxidase[109], as well as catalase itself[110], to name a few[111], have all been found to be inhibited and/or inactivated by millimolar concentrations of hydrogen peroxide. Another consideration is that the high reactivity and exothermic decomposition of hydrogen peroxide can raise the explosion risk of a chemical process[112], especially when used in combination with certain solvents, acids or bases[113]. This incurs additional costs to ensure safe handling at a larger scale. While this may not be a problem for most biocatalytic processes, which operate under very mild conditions (aqueous, low temperature, low pressure)[114], the growing use of protein engineering or immobilization to improve enzyme tolerance towards elevated temperatures[115] and/or volatile organic solvents[64, 83, 116] could make reactions using more exotic conditions less stable in the presence of hydrogen peroxide. It is precisely for these reasons that oxidases are regularly coupled with catalase primarily to avoid any potential deleterious effects of hydrogen peroxide on the enzyme. The production of dissolved oxygen by catalase just happens to be a secondary benefit when used in tandem with an oxidase.

The third possibility is to simply supply the liquid reaction phase with a gas containing oxygen (air being the most desirable goal), which can then transfer into the liquid phase, facilitated by mechanical mixing. Here, the solubility of oxygen can still be increased by raising its partial pressure in the feed gas or the overall pressure of the system. Due to its simplicity, this approach is particularly attractive for rapid implementation of biocatalytic oxidations in industry, especially since gas-liquid mass transfer typically improves with scale due to longer gas hold-ups.[79] Therefore, the focus of this chapter is to broaden the understanding of oxygen dependence during the continuous biocatalytic oxidation of glucose in a well-mixed stirred tank reactor, where oxygen is supplied to the reaction not only via gas-liquid mass transfer, but also as a by-product of hydrogen peroxide scavenging. This already helps to overcome potential mass transfer limitations by reducing the overall stoichiometry of the system (0.5 mol $O_2 \rightarrow$ 1 mol product), doubling the amount of product that can theoretically be achieved at a given gas-liquid oxygen transfer rate. In particular, the influence of oxygen dependence on the effectiveness with which the enzyme can be used will be examined.

4.2 Results and Discussion

The stability of GOx was measured as described in Chapter 3. Figure 4.1 shows that no significant loss of GOx activity was observed over 6 hours of continuous operation with air as the feed gas. Having shown the enzyme to be sufficiently stable, an initial baseline oxidation reaction was carried out, as outlined in Chapter 3, with air as the feed gas and 0.1 $g.L^{-1}$ GOx and catalase. The resulting concentration profiles of glucose, gluconic acid and DO, over the course of the experiment, are shown in Figure 4.2. High initial and feed concentrations of glucose (~1 M), relative to the K_{MG} of GOx, were used to ensure that oxygen availability would be the dominant rate-limiting factor during the experiment, resulting in a glucose conversion of only 12%.

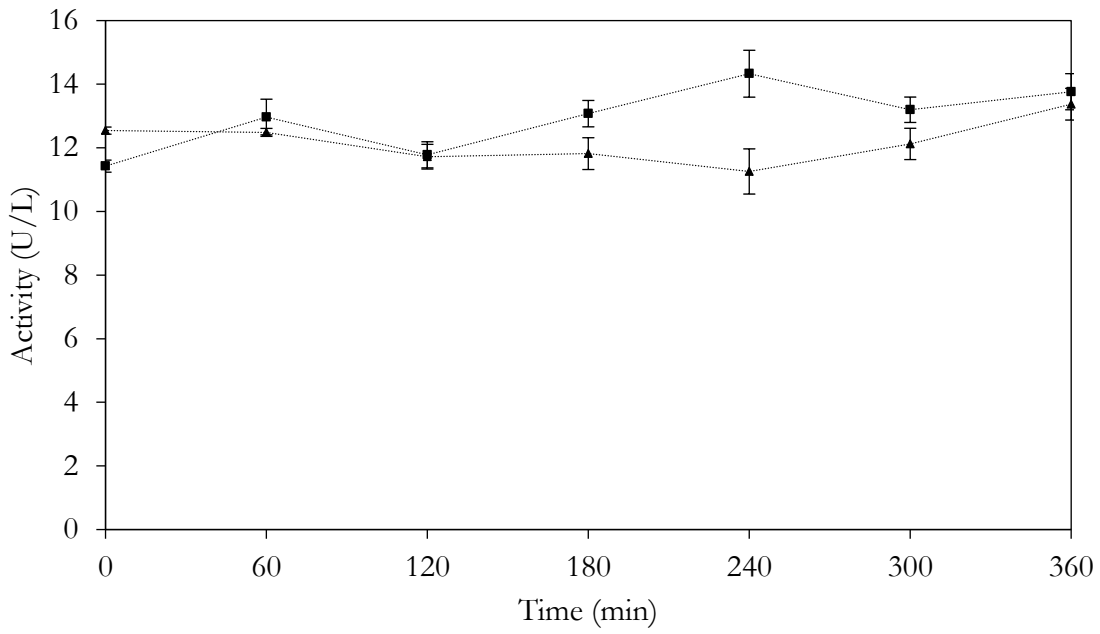

Figure 4.1. Activity of GOx in quiescent solution (■) and CSTR operated at 25°C, 1000 rpm and 1 vvm air (▲).

The solubility of oxygen in water is generally very low. For instance, when supplied as air (21% O_2) its solubility is only 0.26 mM at ambient conditions (25°C, 1 atm).[37a] This greatly limits the driving force for gas-liquid mass transfer of oxygen, regardless of the specific gas-liquid surface area. Additionally, the affinity constants of many oxidases towards oxygen (K_{MO}) are generally high relative to oxygen aqueous solubility at atmospheric pressure, based on data available in the BRENDA database.[41, 117]

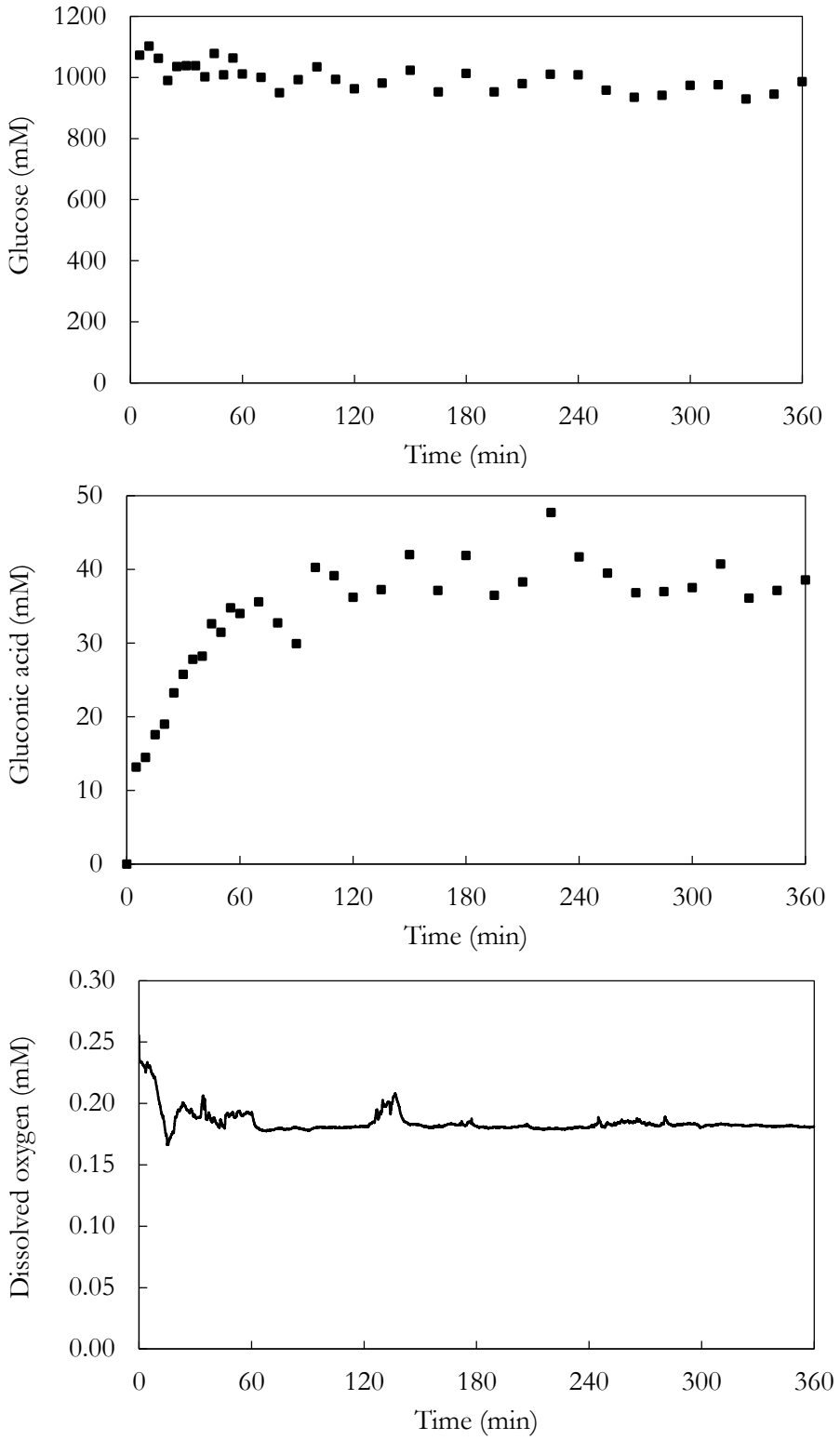

Figure 4.2. Glucose, gluconic acid and dissolved oxygen concentration profiles of baseline experiment with 0.1 $g.L^{-1}$ glucose oxidase and catalase, using air (21% O_2) as feed gas.

For instance, the steady-state DO concentration measured in the baseline experiment (0.18 mM) is almost 3-fold lower than the measured K_{MO} of GOx (0.51 mM[39]). Therefore, the GOx can only operate at 26% of its maximum rate ($V_{max} = k_{cat}.C_{GOx}$), which is an ineffective use of the catalyst. As the system is likely oxygen-limited, the rate could be improved by increasing the aqueous solubility of oxygen, allowing higher dissolved concentrations at steady state. This can be accomplished by increasing the oxygen partial pressure, either through pressurizing the entire system or by supplying oxygen-enriched air (>21% O_2). However, according to the rate law of GOx (Equation 4.1), the overall rate of reaction, which is stoichiometrically equivalent to the oxygen consumption rate (OCR), is also directly proportional to the enzyme concentration. Therefore, it might appear that the most straightforward means of improving productivity would be to simply increase the concentration of GOx in the reactor. But, as illustrated in Figure 4.3, this may not yield the expected return at low DO concentrations. In order to test this, additional experiments were carried out with higher concentrations of GOx and catalase (1 $g.L^{-1}$) as well as with feed gas mixtures containing more oxygen (60, 80 and 100%). The average gluconic acid concentration over the final hour of each experiment was multiplied with the dilution rate (1.2 h^{-1}) to obtain the OCRs shown in Figure 4.4.

$$v_{GOx} = OCR = \frac{k_{cat,GOx} C_{GOx} C_G C_O}{K_{MG} C_O + K_{MO} C_G + C_G C_O} \tag{4.1}$$

When supplied with oxygen-rich feed gases, the OCRs during experiments with 1 $g.L^{-1}$ GOx were significantly higher than any experiment at the reduced enzyme concentration. However, this was not the case when air was used as the feed gas. Compared to the baseline experiment, increasing the GOx concentration by 10-fold only gave a 1.4-fold increase in OCR. In contrast, a 3-fold increase in the oxygen content of the feed gas nearly doubled the OCR, despite the presence of less GOx. This confirms that the system is more sensitive to changes in DO concentration, making it the dominant rate-limiting factor. Increasing the enzyme concentration alone resulted in a significant drop in the steady-state DO concentration within the reactor, to approximately 0.02 mM (23-fold lower than the K_{MO}). Meanwhile, switching the feed gas from air to 60% oxygen allowed the DO concentration in the reactor to stabilize at 0.61 mM (1.2-fold higher than the K_{MO}). Therefore, while it is theoretically possible to improve reaction rates by simply adding more catalyst, it generally reduces how effectively

the catalyst is used. This trade-off can be seen through a comparison of the specific steady-state OCRs ($mmol.g_{GOx}^{-1}.h^{-1}$) of each experiment, as shown in Figure 4.5.

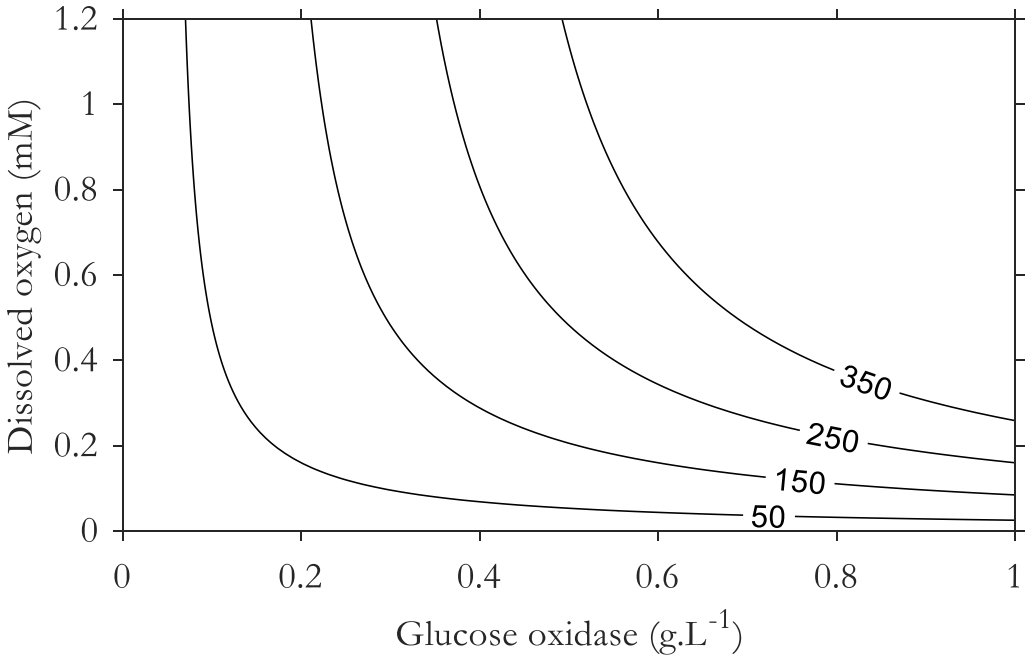

Figure 4.3. Dependence of glucose oxidase reaction rate on concentrations of dissolved oxygen and GOx, based on ping-pong bi-bi rate law and at atmospheric pressure. Each contour represents a constant OCR ($mmol.L^{-1}.h^{-1}$).

In general, the use of less GOx resulted in more DO at steady state, thus making more effective use of the GOx since it was able to operate closer to its maximum rate. This reduces the amount of enzyme required to achieve a desired productivity, which is highly desirable at industrial scale. Therefore, increasing the DO concentration is both a more efficient and economical means of improving reaction performance, as it makes better use of a costly catalyst. Even so, the enzyme is still being used somewhat ineffectively since the degree to which it is saturated with oxygen is less than that of its saturation with glucose ($C_O/K_{MO} << C_G/K_{MG}$). Additionally, the use of oxygen-enriched air in an industrial process presents a safety risk that would necessitate additional costs for safe handling procedures.

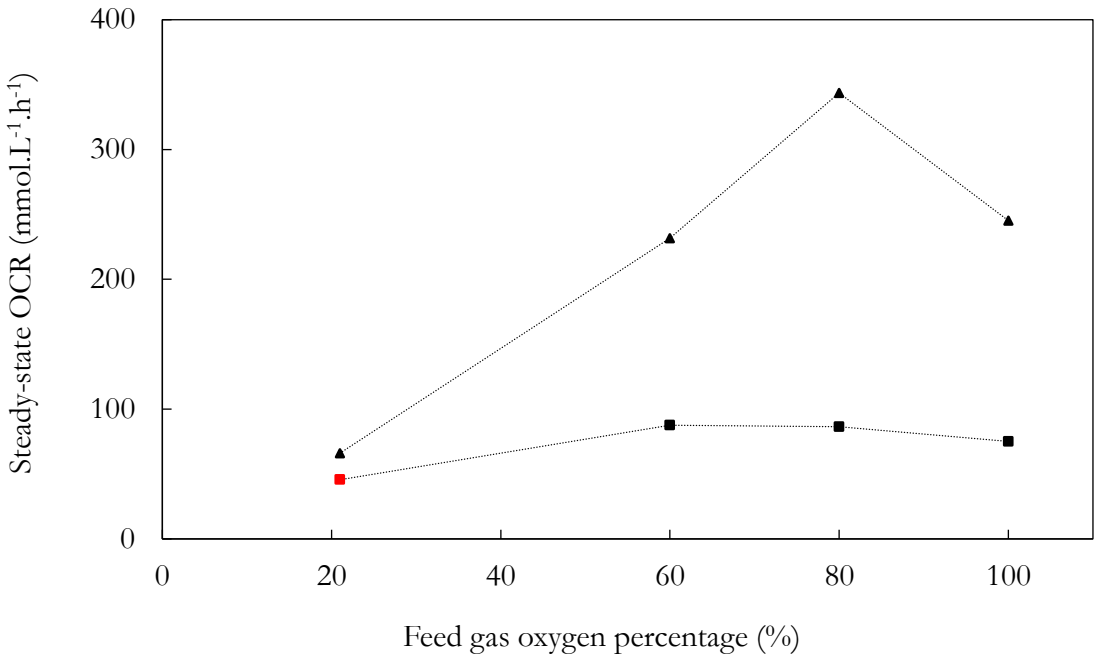

Figure 4.4. Steady-state OCRs of experiments with various feed gas oxygen contents and GOx concentrations of 0.1 $g.L^{-1}$ (■) and 1 $g.L^{-1}$ (▲). Baseline experiment marked in red.

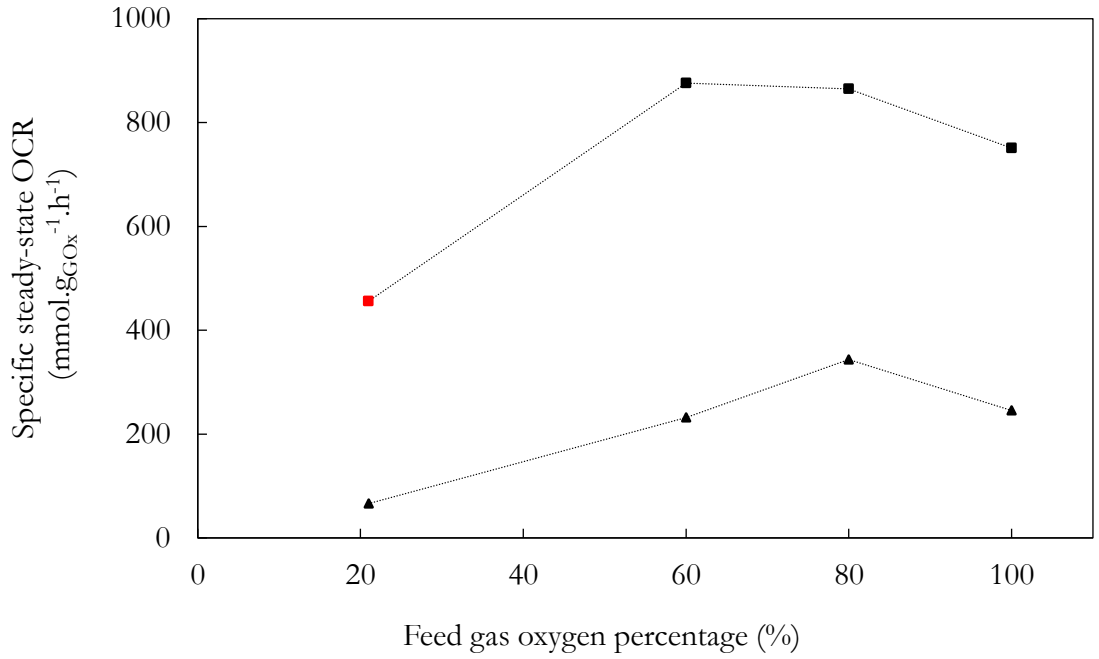

Figure 4.5. Specific steady-state OCRs of experiments with various feed gas oxygen contents and GOx concentrations of 0.1 $g.L^{-1}$ (■) and 1 $g.L^{-1}$ (▲). Baseline experiment marked in red.

At feed gas oxygen contents above 60%, the OCR begins to drop at the lower enzyme concentration. Likewise, a drop occurs at the higher enzyme concentration above a feed gas oxygen content of 80%. Similar trends have previously been observed in experiments with cyclohexanone monooxygenase.[118] Since the effect was detected sooner at lower enzyme concentrations, it points towards enzyme deactivation. As there was a large difference in the steady-state DO concentrations of the experiments using pure oxygen as feed gas (1.11 mM at 0.1 $g.L^{-1}$ GOx and 0.10 mM at 1 $g.L^{-1}$ GOx), the deactivation does not appear to result from oxygen in the liquid phase. While a number of enzymes have been found to be deactivated simply by direct exposure to any hydrophobic gas-liquid interfaces[119], Figure 4.1 shows that the GOx remained stable despite prolonged exposure to air-liquid interfaces. Therefore, it would seem that GOx may be deactivated by direct contact with oxygen at the gas-liquid interface, but that this effect only becomes significant at high oxygen contents. This is not unprecedented, as the presence of oxygen in the gas phase has previously been found to oxidize amino acids on the surfaces of hydrogenases[120] and D-amino acid oxidase[108c]. Unfortunately, the possibility of deactivation at high oxygen contents limits the degree to which increased oxygen partial pressure can be effectively used to improve performance. Furthermore, it is unknown whether pressurizing the system to achieve a higher oxygen partial pressure would exacerbate the deactivation. The addition of surfactants to the reaction mixture may reduce this effect by preferentially binding with the gas-liquid interface to avoid direct contact with the enzyme.[119] Likewise, various methods of immobilization have been described to avoid enzyme deactivation at gas-liquid interfaces.[121] In cases where enzymes are extremely susceptible to this deactivation, oxygen may have to be supplied to the liquid phase through a partially permeable membrane. This is the principle of the tube-in-tube reactor, described in Chapter 2.

The mass transfer coefficient (k_La) of the reactor was determined to be 80 h^{-1} in distilled water at ambient conditions, according to the standard gassing-in method[100a] described in Chapter 3. Using the average DO concentration over the final hour of each experiment, the corresponding steady-state OTRs in the reactor were calculated, according to Equation 4.2, and are shown in Table 4.1. In the absence of catalase, steady state would be achieved when the rate at which oxygen is consumed is equal to the rate at which it is transferred from the gas to the liquid phase (OCR = OTR).[122] However, since catalase produces dissolved oxygen, with a theoretical maximum rate equal to half that of the OCR, gas-liquid oxygen transfer only accounts for a portion of the oxygen consumed, the rest of which must be produced by catalase (Equation 4.3). Table 4.1 also shows the calculated oxygen

production rate (OPRs) of each experiment, as well as its contribution towards the measured OCR (i.e. OPR/OCR).

$$\mathrm{OTR} = k_L a(C_O^* - C_O) \tag{4.2}$$

$$\mathrm{OPR} = \mathrm{OCR} - \mathrm{OTR} \tag{4.3}$$

Table 4.1. Dissolved oxygen concentrations and consumption rates measured at steady state allow calculation of corresponding oxygen transfer and production rates.

GOx ($g.L^{-1}$)	Feed gas (% O_2)	DO (mM)	OTR ($mmol.L^{-1}.h^{-1}$)	OCR ($mmol.L^{-1}.h^{-1}$)	OPR ($mmol.L^{-1}.h^{-1}$)	OPR/OCR
0.1	21	0.18	6	46	40	0.87
	60	0.61	10	88	78	0.89
	80	0.89	6	87	81	0.93
	100	1.11	8	75	67	0.89
1	21	0.02	19	66	47	0.71
	60	0.10	50	232	182	0.78
	80	0.17	64	344	280	0.81
	100	0.10	89	245	156	0.64

The estimated OPR/OCR ratios of all the experiments exceed their maximum theoretical value, based on the overall stoichiometry of the coupled enzyme reactions (0.5 mol O_2 produced per mol O_2 consumed). Since this is not possible, it likely means that the OTRs were in fact underestimated and that the actual k_La during these experiments must have been higher than that measured in distilled water. For instance, if it is assumed that catalase operates such that the OPR is always at its theoretical maximum, average k_La values as high as 394 and 163 h^{-1} for GOx concentrations of 0.1 and 1 $g.L^{-1}$, respectively, would be required to achieve sufficient OTRs to account for the measured OCRs. This also suggests that enzyme concentration may have a significant impact on k_La, in which case other components in the reaction media (glucose, gluconic acid, buffer) may also have an effect. The amphipathic nature of enzymes causes them to preferentially adsorb to the hydrophobic gas-liquid

interface of a bubble.[123] This often leads to foaming in systems that are agitated and aerated, an effect which is exacerbated at higher enzyme concentrations.

When sparged in a bubble column, catalase solutions were found to produce a stable foam. However, GOx solutions did not, likely due to antifoaming additives in the industrial formulation. As described in Chapter 3, an antifoaming agent was manually added to the reactor when overflow, due to foaming, was observed to be imminent. Although the amount added to the reactor was kept to an absolute minimum, antifoaming agents are still known to significantly reduce k_La[124]. This can be seen in Figure 4.6, which compares the DO concentration profiles for both experiments using 80% oxygen as feed gas. The large degree of foaming at higher catalase concentrations necessitated periodic dropwise addition of antifoam, which was immediately followed by a significant, albeit temporary, drop in the DO concentration.

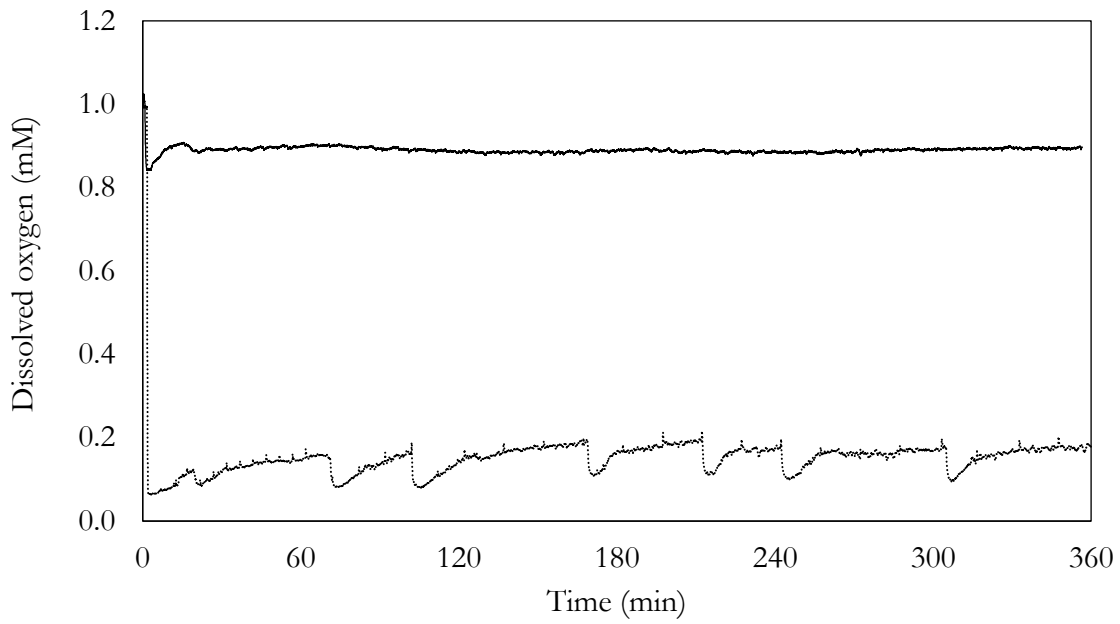

Figure 4.6. Dissolved oxygen concentration profiles of experiments using 80% O_2 as feed gas and GOx concentrations of 0.1 g/L (solid line) and 1 g/L (dotted line). Dropwise addition of antifoam to the latter to avoid reactor overflow caused significant drops in the DO concentration.

The gassing-in method was used to determine k_La values in mixtures containing buffer, GOx, catalase and antifoam to compare against that measured in distilled water, the results of which are shown in Table 4.2. The maximum DO concentrations measured during these experiments were also

recorded. Since the DO probe was only calibrated in distilled water, these concentrations indicate that the mixture composition had an insignificant effect on the solubility of oxygen. The k_La in 100 mM potassium phosphate (KPi) buffer was found to be nearly double that of distilled water. This likely resulted from a reduction in surface tension, as the bubbles were observably smaller in size[125]. Addition of a low concentration (0.1 $g.L^{-1}$) of GOx to the buffer further increased the k_La by 12%, while the same concentration of catalase added to the buffer raised the k_La by 33%. This shows that the effect of enzymes on k_La may differ depending on their structure or formulation. When both enzymes were added to the buffer, each at a concentration of 0.1 $g.L^{-1}$, the k_La was measured to be double that of buffer alone. This indicates that total enzyme concentration has a large, nonlinear effect on mass transfer of oxygen into the liquid, which likely stems from increased enzyme adsorption to the bubble interfaces, preventing them from coalescing to form larger bubbles. Therefore, at high enzyme concentrations, interfacial areas for gas-liquid mass transfer are expected to be higher. When a single drop of antifoam was added to this mixture the k_La was reduced by 39% to a value even lower than that of pure buffer, since the antifoam destabilizes gas-liquid interfaces and improves coalescence. Unfortunately, this suggests that the gassing-in method cannot be used to test the effect of higher enzyme concentrations (1-2 $g.L^{-1}$) on k_La, due to excessive and uncontrollable foaming. Furthermore, since the method relies on measuring DO concentrations, the k_La can only be determined in the absence of any oxygen-dependent reactions. The catalytic action of GOx and catalase, as well as the presence of glucose and gluconic acid may also affect the k_La. This is further explored in Chapter 6.

Table 4.2. k_La and maximum DO concentrations in mixtures of different composition

Mixture components						
Water	KPi buffer [100 mM]	GOx [0.1 $g.L^{-1}$]	Catalase [0.1 $g.L^{-1}$]	Antifoam [0.055 $g.L^{-1}$]	k_La (h^{-1})	Max DO (mM)
X					80	1.21
	X				159	1.23
	X	X			178	1.23
	X		X		212	1.21
	X	X	X		320	1.21
	X	X	X	X	126	1.21

4.3 Conclusions

Retrofitting existing batch stirred tank reactors to operate continuously not only in the gas phase, but the liquid phase as well, would potentially allow faster industrial implementation of gas-dependent biocatalytic reactions than switching to tubular reactor configurations. However, the poor water-solubility of oxygen presents an obstacle to achieving adequate reaction rates, especially at atmospheric pressure. While some oxidases have such high affinities towards dissolved oxygen that they are practically oxygen-independent, like choline oxidase (K_{MO} = 2.6 μM)[126], the oxygen affinity of GOx is comparatively low (K_{MO} = 0.51 μM). This limits the reaction rate that can be achieved with air as the feed gas and prevents the enzyme from being used effectively ($v << V_{max}$). While the reaction rate could be improved by increasing the enzyme concentration, this further reduces DO concentrations, thus making even less effective use of the enzyme.

Raising the oxygen partial pressure of the gas in the reactor, to increase the water-solubility of oxygen, is a more effective means of improving reaction performance. Nevertheless, the stability of GOx appears to be reduced when exposed to feed gases comprised of more than 60-80% oxygen. At atmospheric pressure, this limits the solubility of oxygen to just 0.73 mM, which, even if the OTR were high enough to keep the reaction media fully saturated with oxygen, would still not enable GOx to operate close to its maximum rate. Pressurization of the reactor could be used to further raise the oxygen partial pressure, although how this would affect the deactivation of the enzyme at the gas-liquid interface is unknown. As such, a better solution would be to employ protein engineering to improve the affinity of GOx towards dissolved oxygen. In fact, directed evolution has already successfully been used to lower the K_{MO} of D-amino acid oxidase by 10-fold.[127]

The volumetric mass transfer coefficient in a CSTR was found to be significantly affected by media composition, warranting further investigation in Chapter 6.

Chapter 5

Glucose oxidation in dual CSTRs

This chapter is intended for later publication.

5.1 Introduction

In Chapter 4, it was found that the rate of biocatalytic glucose oxidation in a CSTR was predominantly limited by the dissolved oxygen (DO) concentration that could be achieved in the system. Increasing the partial pressure of oxygen in the feed gas was found to result in higher rates but, at atmospheric pressure, the gains in oxygen solubility are simply too small to overcome this limitation, due to the comparatively low affinity of glucose oxidase towards oxygen. Moreover, the results suggest that the enzyme may become more susceptible to deactivation if directly exposed to gases with high oxygen contents. Of course, reaction rates can also be increased through higher enzyme concentrations, but this creates a trade-off between reaction performance and effective use of the enzyme, which may drastically increase the cost contribution of the enzyme to the process. One means of combatting this is to increase the biocatalyst yield ($g_{product}.g_{enzyme}^{-1}$). This is normally done by retaining the enzyme within the reactor by immobilization to a heterogenous support material, the pros and cons of which were outlined in Chapter 2. If a soluble catalyst is preferred, membranes can be used to retain the enzyme within the reactor, but these suffer from drawbacks like fouling and concentration polarization. Furthermore, if stability is a concern, as the previous chapter suggested could be the case, retention of a fixed amount of enzyme may be a net negative for prolonged operation. In such cases, the biocatalyst yield can instead be increased by feeding the enzyme leaving the reactor into an additional reactor, where it can continue to produce. In theory, if enough CSTRs were arranged in series their behavior would even begin to resemble a plug-flow reactor, which was found to be a highly desirable reactor configuration for continuous operation in Chapter 2. In this chapter, biocatalytic glucose oxidation in a series of identical CSTRs is modelled to assess the practicality of this configuration.

5.2 Single vs. Multiple CSTRs

The coupled GOx-catalase system can be modeled as a system of ordinary differential equations (ODEs), Equations 5.1 to 5.6, which represent the mole balances of glucose, dissolved oxygen, gluconic acid and hydrogen peroxide in the reactor, respectively.

$$\frac{dC_G}{dt} = \frac{Q}{V}\left(C_{G,F} - C_G\right) - v_{GOx} \tag{5.1}$$

$$\frac{dC_O}{dt} = \frac{Q}{V}\left(C_{O,F} - C_O\right) - v_{GOx} + \frac{1}{2}v_{Cat} + k_L a(C_O^* - C_O) \tag{5.2}$$

$$\frac{dC_{GA}}{dt} = \frac{Q}{V}\left(C_{GA,F} - C_{GA}\right) + v_{GOx} \tag{5.3}$$

$$\frac{dC_{HP}}{dt} = \frac{Q}{V}\left(C_{HP,F} - C_{HP}\right) + v_{GOx} - v_{Cat} \tag{5.4}$$

$$v_{GOx} = \frac{k_{cat,GOx}C_{GOx}C_G C_O}{K_{MG}C_O + K_{MO}C_G\left(1 + \frac{C_{HP}}{K_I}\right) + C_G C_O} \tag{5.5}$$

$$v_{CAT} = \frac{k_{cat,CAT}C_{CAT}C_{HP}}{K_{MHP} + C_{HP}} \tag{5.6}$$

High substrate conversions are attractive for both the production of simple commodity chemicals, where low profit margins demand efficient substrate use, and complex fine chemicals, where leftover substrates from one reaction in a multistep sequence may inhibit those downstream. High conversions also help to simplify downstream purification of the final product[24a]. But, while the well-mixed nature of CSTRs allows for increased mass transfer rates, it also ensures that the product stream leaving the reactor will always contain some substrate, since the contents of the reactor are homogenous.[128] The conversion in the reactor and, subsequently, the concentration of substrate in the product stream are determined by the amount of catalyst. However, since the rate of a biocatalytic reaction is heavily

dependent on substrate concentration, achieving higher conversions requires large amounts of enzyme to counter the decrease in reaction rate due to substrate depletion. Equations 5.1 to 5.6 were solved in MATLAB for a variety of feed gas compositions (% O_2) and operating pressures, with a feed glucose concentration of 1 M. Figure 5.1 shows the resulting relationships between GOx concentration and steady-state glucose conversion. Also shown are the results when it is assumed that oxygen can be made available in such high excess ($C_O >> K_{MO}$) that the reaction is effectively oxygen-independent.

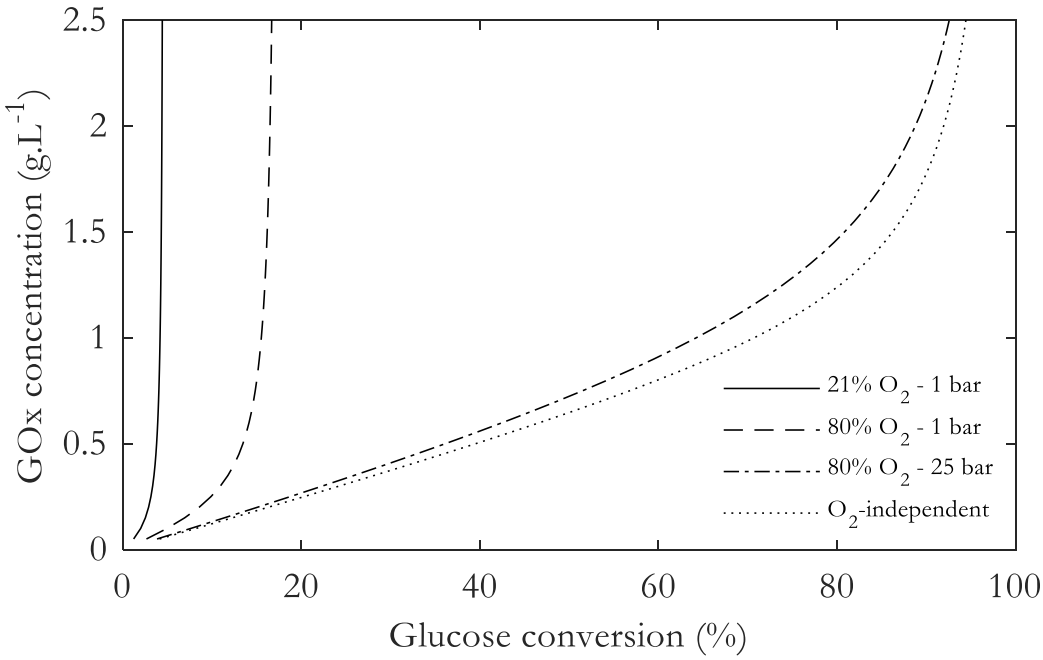

Figure 5.1. Glucose oxidase concentration required to achieve desired conversion of a 1 M glucose feed stream in a single CSTR, with different operating pressures and gas feed compositions.

Since the solubility of oxygen in water is much lower than that of glucose, relative to the corresponding affinity constants of GOx towards each, oxygen is more often the dominant rate-limiting substrate. For this reason, any increase in reaction rate due to an increase in enzyme concentration is quickly outweighed by the concurrent effect of reducing the DO concentration. This is exacerbated by the fact that the rate of gas-liquid oxygen transfer is typically slow in comparison to the reaction (k_La was assumed to be 100 h^{-1} in the model). As a result, there exists an upper limit to the glucose conversion that can be achieved in a single CSTR by raising enzyme concentration, proportional to the oxygen partial pressure in the feed gas. Furthermore, high enzyme concentrations make ineffective use of the catalyst ($v_{GOx} << k_{cat}.C_{GOx}$), as illustrated in Figure 5.2, inflating operating costs.

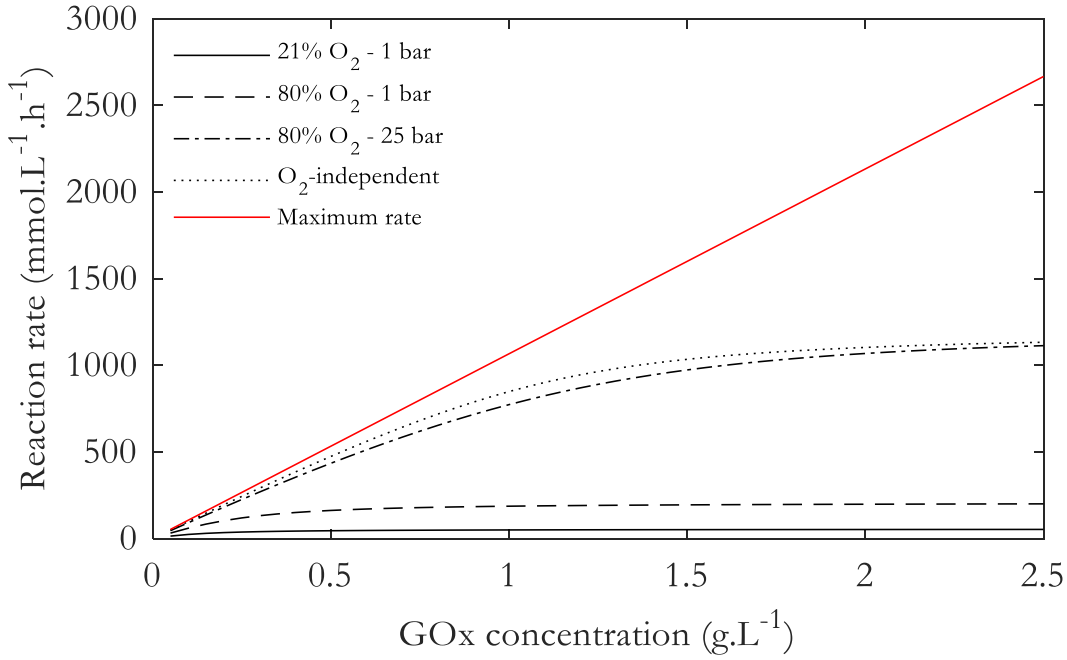

Figure 5.2. Reaction rate in single CSTR versus maximum rate as GOx concentration increases. Higher GOx concentrations result in less effective use due to substrate depletion.

In theory, a maximum conversion of approximately 94% could be achieved, provided the reaction can be completely saturated with dissolved oxygen. However, as Figure 5.1 shows, a pressure increase of more than 25-fold would be required to sufficiently raise the oxygen solubility to reach this upper limit, which significantly raises the safety risk of the process and necessitates additional capital investment. Regardless, even with a high GOx concentration, complete conversion could not be achieved, as the reaction inevitably becomes limited by low glucose concentrations. Therefore, if near-complete conversion is desired, it would be inefficient to operate an oxygen-dependent biocatalytic reaction in a single CSTR.

This problem can potentially be overcome by instead operating multiple CSTRs in series, at least until the enzyme becomes completely inactivated. Figure 5.3 shows how the overall glucose conversion increases across a series of identical CSTRs, under different operating conditions. Although the enzyme can be used more effectively at a relatively low enzyme concentration (0.1 $g.L^{-1}$), achieving near-complete conversion would require an impractical number of reactors (>10), even if the reaction were fully saturated with oxygen. By increasing the enzyme concentration 10-fold, the number of reactors required to reach near-complete conversion can be reduced to 8 at atmospheric pressure and further down to 3 at significantly higher pressures. However, in all cases, the degree to which the

conversion is improved with the addition of subsequent reactors begins to rapidly diminish after the second reactor in the series. For this reason, it would appear to be most practical to simply optimize a dual-reactor configuration to achieve the highest conversion with the least amount of enzyme possible, since it reaps the most benefit from connecting CSTRs in series without making the system overly complicated or costly to operate. Therefore, further experiments were carried out in a series of two identical CSTRs, as described in Chapter 3.

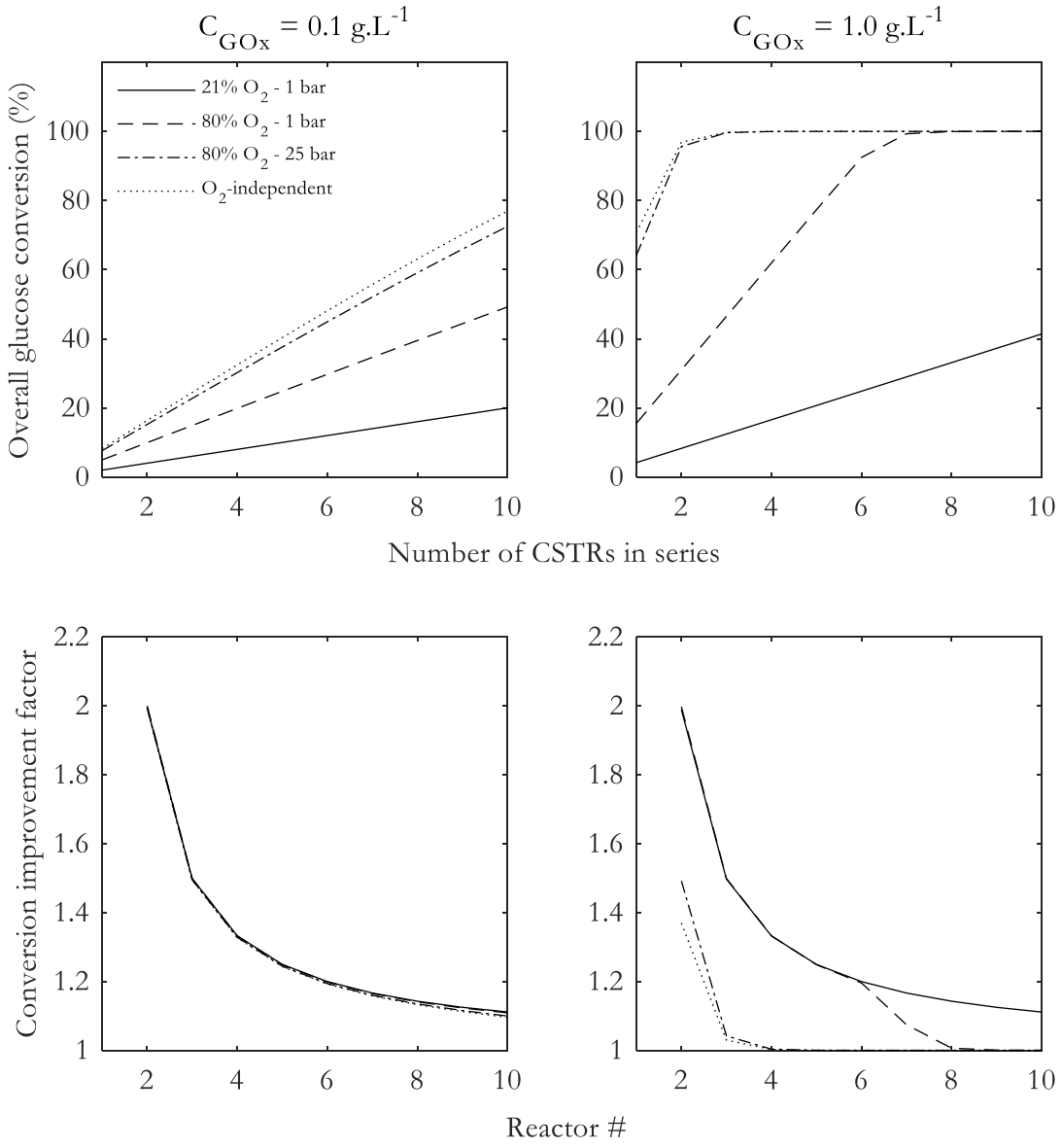

Figure 5.3. Overall glucose conversion across a series of identical CSTRs and factor by which overall conversion improves with addition of each reactor in the series.

5.3 Results and discussion

Figure 5.4 shows the results of carrying out the glucose oxidation reaction in a series of two identical CSTRs, with 1 $g.L^{-1}$ of each enzyme and 80% oxygen as the feed gas. In Chapter 4, these conditions were found to result in the highest productivity in a single CSTR, which translates to a biocatalyst yield of 56 $g_{GA}.g_{GOx}^{-1}$. The results show that the glucose concentrations, particularly those of the second reactor, were subject to some variability between experiments. This is likely due to small differences in the calibrated flow rates into and out of the first reactor. Nevertheless, since the system is predominantly oxygen-limited, these differences produced little variation in the gluconic acid concentrations. The most variability between experiments was observed in the DO concentrations in the second reactor, which is an unfortunate consequence of controlling the foam formation with an antifoaming agent, as described in Chapter 4, as well as the sensitivity of the oxygen probes. These effects were less pronounced in the first reactor, where DO concentrations were significantly lower.

Interestingly, the overall glucose conversion was increased by a factor of 3.2 after the second reactor, which is significantly higher than the model predicts it would in Figure 5.3. This likely stems from the fact that the two CSTRs are not in fact identical, as was assumed in the model, in that their media compositions differ. In Chapter 4, this was found to have a large effect on the k_La. Specifically, the results suggest that the k_La in the second reactor was higher than that in the first, indicating that k_La may be positively affected by gluconic acid and/or negatively affected by glucose. It is unlikely that dissolved oxygen accumulation occured in the second reactor, and not the first, because the reaction became glucose-limited. Figure 5.1 shows that, even if the reaction were oxygen-independent, glucose limitation would only begin to limit reaction rates above a conversion of roughly 70%, corresponding to a glucose concentration of 300 mM. Therefore, a higher k_La in the second reactor would appear to have been the cause of the higher dissolved oxygen concentration. This warrants further investigation into the dependence of k_La on media composition, which is the focus of Chapter 6. Another interesting aspect of the increase in dissolved oxygen concentration along the series is that it suggests the enzyme is used more effectively in the second reactor than in the first. This is confirmed by the OCRs of reactors 1 and 2 being 236 and 343 $mmol.L^{-1}.h^{-1}$, respectively, based on the amount of gluconic acid produced within each reactor. This is contrary to what would be expected in a series of CSTRs when operating with a single-substrate enzyme. In such cases, the concentration of the rate-limiting substrate decreases in each subsequent reactor and so, while the conversion still increases along the series, the enzyme is used less effectively. Moreover, the biocatalyst yield from the two-

reactor system was calculated to be 95 $g_{GA}.g_{GOx}^{-1}$, 1.7-fold higher than experiments performed in a single reactor. Both of these improvements help to reduce the overall cost contribution of the enzyme.

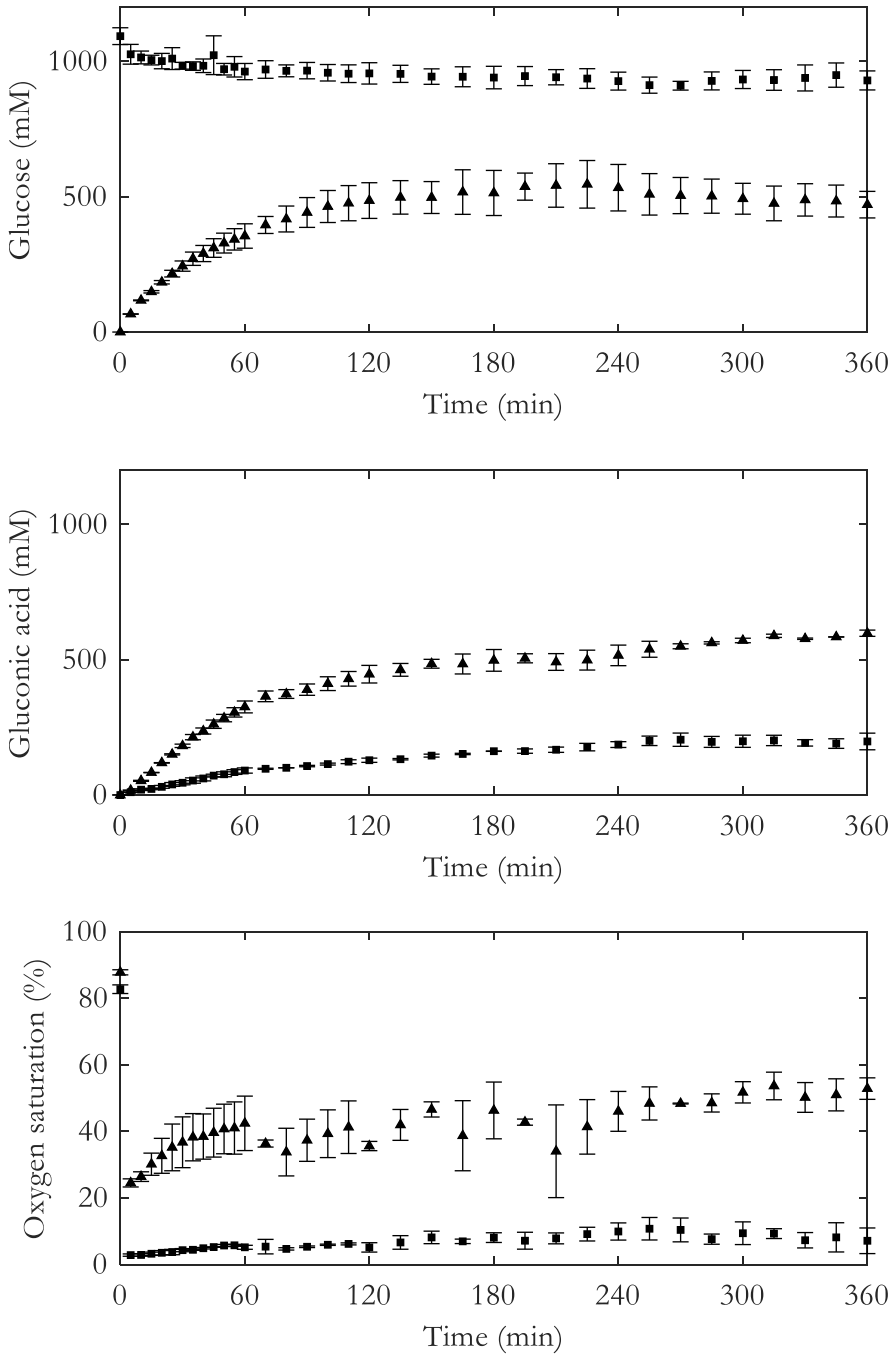

Figure 5.4. Glucose and gluconic acid concentration, as well as oxygen saturation, profiles in Reactor 1 (■) and Reactor 2 (▲), with 1 $g.L^{-1}$ glucose oxidase and catalase, as well as 80% O_2 as feed gas. Error bars represent standard error of the mean.

5.4 Conclusions

The maximum conversion that can be achieved in a CSTR is always limited by substrate depletion if the reaction rate is dependent on substrate concentration. For biocatalytic glucose oxidation, the low water-solubility of oxygen relative to the K_{MO} of GOx drastically limits the conversion that is possible in a single CSTR without significant pressurization. An alternative means of improving conversion is to connect multiple CSTRs in series. Given enough reactors, it would even be possible to approximate plug-flow behavior. However, a basic model of the system shows that, while shifting from one to two CSTRs can double overall conversion, the gains from subsequent reactors quickly diminish. Thus, to simplify the system and reduce capital investment, it may be more practical to simply operate two CSTRs in series. In fact, experimental results showed that the overall conversion was actually tripled by addition of a second reactor, where the reaction was less oxygen-limited. Improved conversion and more effective use of the enzyme also help to reduce its overall cost contribution.

Chapter 6

Mass transfer coefficient

This chapter is intended for later publication.

6.1 Introduction

Since biocatalytic oxidations utilize molecular oxygen as a substrate, their reaction rates are frequently tied to the rate at which oxygen can be transferred from a gas phase into an aqueous reaction medium, especially since they tend to be orders of magnitude faster than aerobic fermentations, simply by virtue of allowing higher enzyme loadings. Consequently, in Chapter 2, it was recommended that these reactions be carried out in well-mixed stirred tank reactors that are sparged with an oxygen-rich gas. The oxygen transfer rate (OTR) in the reactor is comprised of two parts (Equation 6.1); namely the volumetric gas-liquid mass transfer coefficient (k_La) and the difference between the saturation oxygen concentration (C_O^*) at the bubble surface and that of the bulk liquid (C_O), referred to as the driving force. The saturation concentration of oxygen at any partial pressure can be accurately calculated using Henry's law, while the dissolved oxygen (DO) concentration in the bulk liquid can be measured with a range of electrochemical or optical probes. However, since k_La cannot be measured directly and is complex to calculate from first principles, due to its dependence on a broad range of physiochemical reactor and reaction properties, it normally has to be estimated from experimental data. Thus, maximizing the accuracy of the estimation is crucial, since k_La significantly impacts the design, scale-up and operation of an oxygen-dependent process.[129] In Chapter 4, it was found that k_La appears to be highly dependent on media composition. As such, the focus of this chapter is to further investigate the effects of individual media components on k_La and assess whether these effects can be used to accurately predict k_La. The gassing-in method, detailed in Chapter 3, was used to determine all k_La values.

$$\mathrm{OTR} = \frac{dC_O}{dt} = k_La(C_O{}^* - C_O) \tag{6.1}$$

6.2 Results and discussion

The k_La represents the hydrodynamic conditions in a reactor, which are influenced by its geometry as well as its operating conditions.[130] A number of empirical correlations to predict k_La in stirred tank reactors have been proposed[129a, 129c, 131], of which the following form is most frequently used

$$k_La = \alpha \cdot {v_s}^{\beta} \left(\frac{P_G}{V}\right)^{\gamma} \tag{6.2}$$

where v_s is the superficial gas velocity and P_G/V is the volumetric gassed power input. Values for the constants α, β and γ have been determined for a number of systems in recent literature[100b, 129a, 130, 132]. The superficial gas velocity of bubbles rising through a medium of known density and viscosity can be estimated if the Sauter mean diameter of the bubbles is known.[133] Alternatively, if the bubble size distribution has not been characterized, the superficial gas velocity can be roughly estimated using the cross-sectional area of the reactor or sparger and the volumetric gas flowrate.[99b] The gassed power input is far more complex to estimate. For instance, it is influenced by the number[130], diameter and rotational speed of the impellers in the reactor, all of which are independent of the media composition.[134] However, it is also influenced by the density and viscosity of the liquid phase in so far as they influence the Reynold's number.[134] In fact, for non-Newtonian fluids, the correlation is modified to include an additional inverse proportionality to viscosity (μ) as follows

$$k_La = \alpha \cdot {v_s}^{\beta} \left(\frac{P_G}{V}\right)^{\gamma} \mu^{\delta} \tag{6.3}$$

where δ is normally between -0.41 and -1.[99b, 132] Thus, the estimated value of k_La is partly dependent on the composition and subsequent properties of the liquid phase. However, since reaction media are typically composed of multiple reagents, including the product itself, estimation of k_La may be costly to evaluate experimentally, particularly at larger scales. Consequently, for practical purposes, k_La is often studied in model fluids that simply approximate the density and viscosity of the final reaction media, but this often produces underestimated values.[99b, 130, 132] For instance, biocatalytic reactions

occur predominantly in aqueous media and, unlike fermentations, have relatively simple reaction mixtures. Therefore, water may seem like the logical choice of model fluid for k_La estimation. However, in Chapter 4 it was shown that k_La values determined in water lead to underestimated performance predictions for glucose oxidation in a CSTR. When measured in a mixture more closely resembling the reaction media (0.1 M potassium phosphate buffer, 0.1 $g.L^{-1}$ GOx and catalase), the k_La was found to be 4-fold higher. This demonstrates the large impact that even small differences in media composition can have on k_La estimation, which is especially problematic during start-up or batch operation.[130]

In these reactions, the media was comprised of five major components, namely glucose oxidase, catalase, potassium phosphate buffer, glucose and gluconic acid. Since sodium hydroxide addition was used to control pH during the CSTR reactions in Chapters 4 and 5, the effect of sodium gluconate could also be of interest. The mass transfer coefficient was measured in varying concentrations of each of these components. The effects of potassium phosphate buffer, glucose, gluconic acid and sodium gluconate are compared in Figure 6.1 and the effects of GOx and catalase are compared in Figure 6.2. Of the 6 components tested, all but glucose increased the k_La, relative to that measured in distilled water, confirming what was found in Chapter 4. Table 6.1 shows the average pH values that were measured in the solutions of each component. It appears that pH is not responsible for the differences in k_La, since buffer and gluconic acid have similar effects. Alternatively, changes in surface tension at the gas-liquid interface, due to the presence of each component, could influence bubble sizes.[135] Lower surface tensions result in the formation of smaller bubbles with more uniform spherical shapes that increase gas hold-up and interfacial area for mass transfer.[136]

Table 6.1. Average pH measured across tested concentration range of each media component

Media component	Average pH
Potassium phosphate buffer	7.0 ± 0.2
Glucose	6.1 ± 0.4
Gluconic acid	2.4 ± 0.3
Sodium gluconate	7.1 ± 0.1
Glucose oxidase	6.2 ± 0.2
Catalase	6.1 ± 0.4

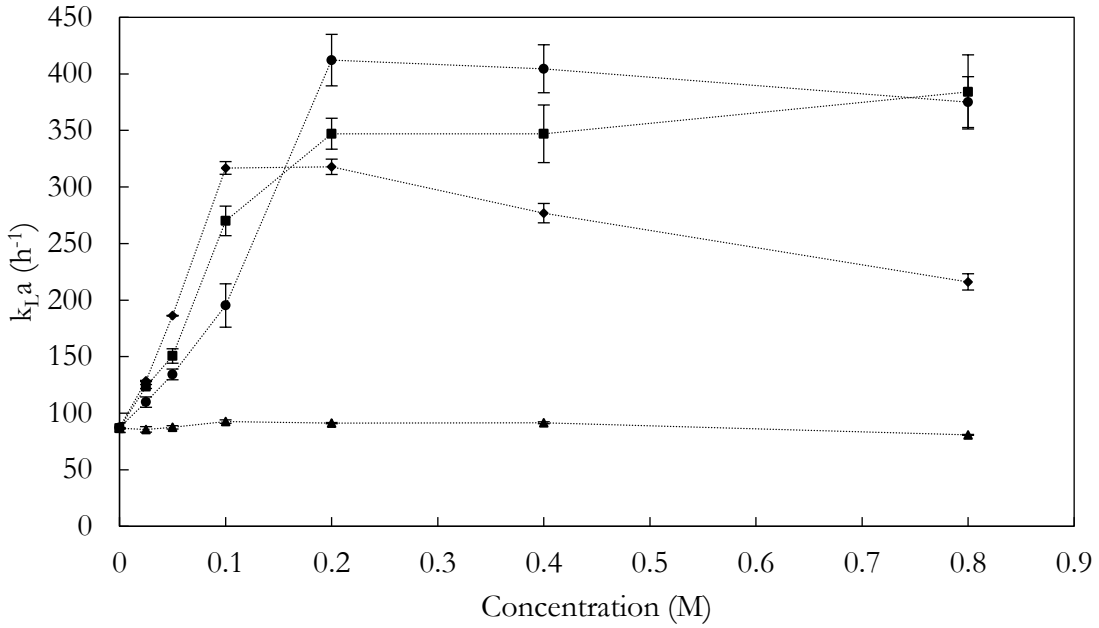

Figure 6.1. k_La measured in buffer (■), glucose (▲), gluconic acid (●) and sodium gluconate (♦) solutions using gassing-in method with pure oxygen as feed gas. Error bars represent standard error of the mean.

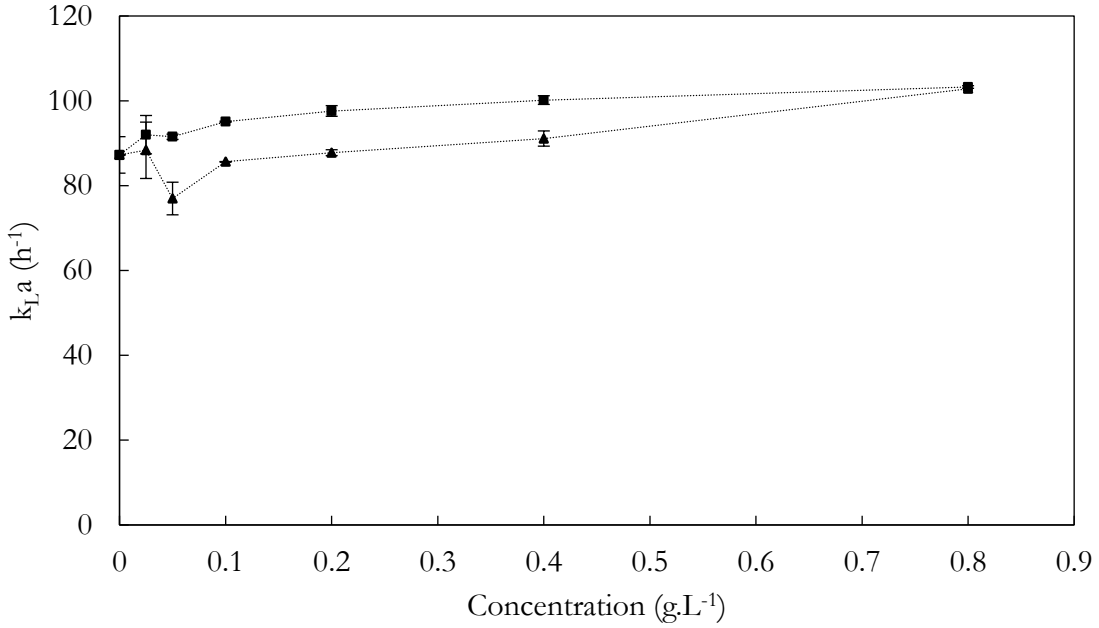

Figure 6.2. k_La measured in glucose oxidase (■) and catalase (▲) solutions using gassing-in method with pure oxygen as feed gas. Error bars represent standard error of the mean.

Cations and anions have been found to affect surface tension differently depending on how they interact with the gas-liquid interface. Structure-making ions can better organize the water dipoles in the bulk water than at the interface, causing them to leave the interface and increase surface tension.[135a] Conversely, structure-breaking ions reduce surface tension by adsorbing to the interface, because the hydrogen bonding network of the bulk water is able to better organize without these ions.[135a] In general, most small ions, like Na^+ or K^+, predominantly desorb from the interface and so increase surface tension.[137] This might explain the reduced effect of sodium gluconate on the k_La, relative to that of gluconic acid. In contrast, large singly-charged hydrophobic anions adsorb to the interface, reducing surface tension in accordance with their size.[137a, 138] For example, it has been found that, while sodium acetate (82.03 $g.mol^{-1}$) has a net positive effect on surface tension, the effect of sodium propanoate (96.07 $g.mol^{-1}$) is negative and that of sodium butanoate (110.09 $g.mol^{-1}$) even more so, due to the increasing size of the anions.[137a] However, while gluconate is a larger anion than butanoate, it contains many hydroxyl groups that enable the formation of hydrogen bonds in water. Therefore, whether it would exhibit a similar negative effect on surface tension remains unknown. At concentrations above 0.2 M, the effects of sodium gluconate and gluconic acid appear to decrease at a similar rate. If gluconate ions do in fact adsorb to the gas-liquid interface, this may suggest that excess adsorbance can begin to impede oxygen mass transfer into the bulk liquid.

The presence of each enzyme caused a slight increase in estimated k_La. Enzymes are large macromolecules that often contain hydrophobic residues, which causes them to adsorb to hydrophobic surfaces, such as gas-liquid interfaces. Adsorption of proteins at these interfaces also reduces their surface tension, resulting in smaller gas bubbles with larger surface-to-volume ratios.[139] However, due to steric hindrances, the extent of protein adsorption is likely far less than that of ion adsorption, which may explain the limited effect of the enzymes on k_La. For instance, the plateau in estimated k_La above GOx concentrations of 0.4 $g.L^{-1}$ could suggest that the bubble surfaces became saturated with the enzyme. Unlike GOx, the addition of catalase resulted in significant foam formation as concentrations were increased, which may have reduced the catalase concentration in solution and thus its impact on k_La. In Chapter 4, the use of an antifoaming agent, even in small amounts, was found to significantly reduce k_La, and so the foam formation was unavoidable. Nonetheless, these results demonstrate that the k_La during a biocatalytic oxidation may be partly dependent on the structures and formulations of the enzymes involved. Interestingly, in Chapter 4, it was found that,

when combined with buffer, catalase had a larger positive impact on k_La than GOx. This suggests that the effects of individual media components may synergize with or antagonize one another.

Nevertheless, changes in surface tension may not be the only factor that influences the k_La. For instance, each of the component salts of the buffer (potassium di-hydrogen phosphate and di-potassium hydrogen phosphate) have been shown to individually increase surface tension.[137a] Accordingly, the presence of buffer would be expected to reduce interfacial area and, consequently, lower the estimated value of k_La, contrary to the data in Figure 6.1. It is possible that, since both potassium and phosphate ions preferentially desorb from the gas liquid interface[137a], the thickness of the bubble surface layer may be reduced and its circulation less inhibited.[136a] This would result in a larger liquid-side mass transfer coefficient, k_L, of which the positive effect on k_La may outweigh the negative impact of a reduced interfacial area. This could explain why the effect of buffer does not appear to decrease at concentrations higher than 0.2 M, like that of gluconic acid or sodium gluconate.

So far, only individual effects of media components have been examined in detail. To ascertain the degree to which these effects might interact with one another, a full factorial design of experiments was performed with two factors (buffer and sodium gluconate concentration) and 6 levels each. These results are displayed in Figure 6.3. It can be seen that there is a significant negative interaction between these two factors, culminating with an estimated k_La of only 96 h^{-1} when both components were present at concentrations of 0.8 M. This suggests that the overall ionic strength of the media, regardless of the individual ionic species, might also have an impact on k_La, that becomes dominant at higher ion concentrations. Quadratic polynomials are typically used to approximate response surfaces.[140] In this case, a quadratic polynomial was found to fit the data in Figure 6.3 with an adjusted R^2 value equal to only 0.78. This goodness-of-fit would likely be reduced even further by the introduction of additional media components as variables. For this reason, the prediction of k_La in multicomponent reaction media based only on composition is likely to be extremely inaccurate, as well as time and resource intensive.

The average maximum oxygen saturation measured during all of the experiments in this chapter was 100.6 ± 0.7 %. Since the oxygen probe was always calibrated in distilled water, this strongly suggests that the solubility of oxygen was essentially unaffected by the presence of any media components in the aqueous GOx system. Of course, this may not be the case in systems with organic co-solvents. In contrast, the average measured k_La is 166 ± 97 h^{-1}.

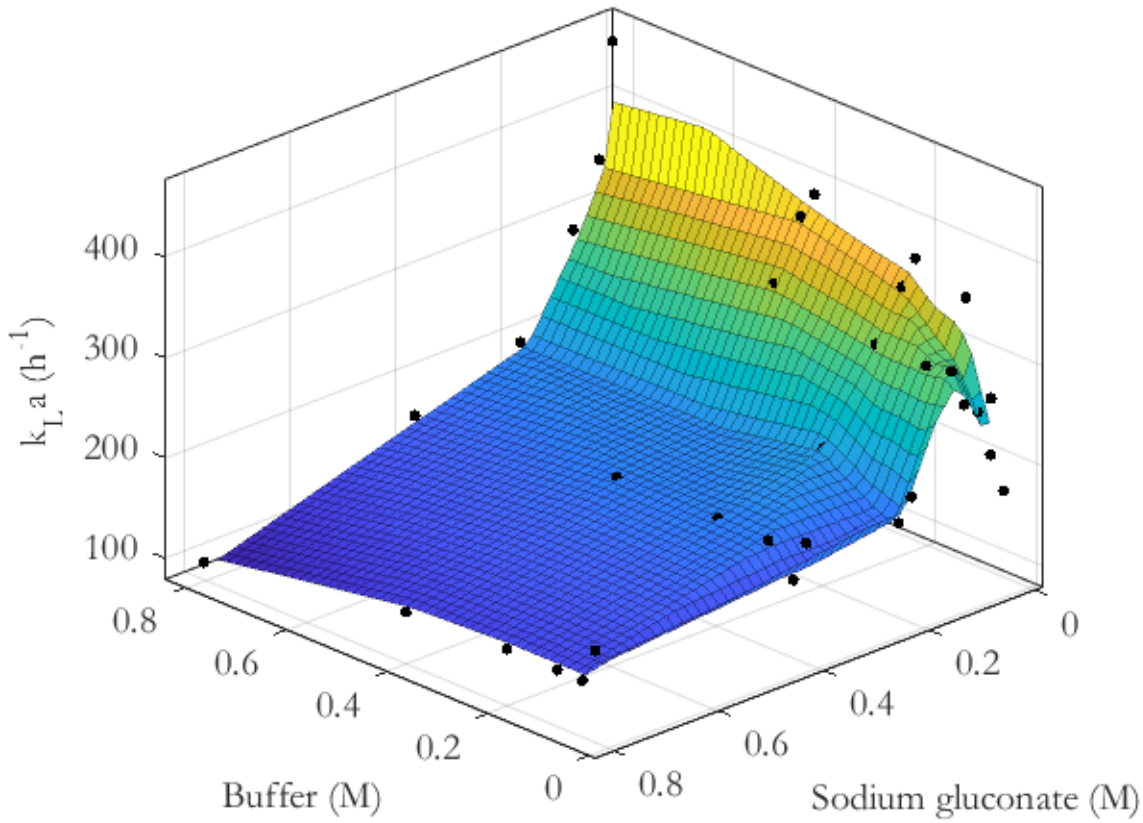

Figure 6.3. k_La measured in buffer/sodium gluconate solutions using gassing-in method and pure oxygen as feed gas, with linear interpolant surface to ease visualization.

k_La Estimation

Since accurate prediction of k_La on the basis of media composition seems to be impractical, it must instead be estimated from experimental data. However, there are a variety of techniques for doing so, often characterized as dynamic or steady-state. Dynamic methods involve making a step change to a physical operating condition to produce a change in DO concentration, which is measured by a DO probe, in the absence of any oxygen producing or consuming reactions. The k_La is then estimated by fitting the transient DO data to an appropriate model for oxygen absorption into the system. The gassing-in method is most commonly used[99, 129b, 131, 141], in which the feed gas is switched from one with a low oxygen concentration (nitrogen or air) to another with a higher oxygen concentration (oxygen or enriched air), while maintaining near constant gas flow rate and agitation to avoid significant changes in gas hold-up and bubble size distribution. Alternatively, a step change in the total pressure of the system can be used to produce a response in the dissolved oxygen concentration, since the

solubility of oxygen is proportional to its partial pressure within the feed gas. This is referred to as the dynamic pressure method[100a]. The downside of this method is that not all laboratory setups are equipped to operate under pressure or vacuum. Nevertheless, it has the advantage that a change in overall pressure has a rapid and simultaneous effect on the oxygen partial pressure within all of the gas bubbles in the liquid.[100a] This is especially important in larger reactors where the residence time of gas bubbles can be long relative to the time scale of mass transfer (k_La^{-1}). In such cases, a step change in the oxygen concentration of the feed gas does not instantaneously affect the entire reactor, creating time delays which distort the estimated k_La unless accounted for in the model.[132] Even so, pressure variations also affect bubble size and, subsequently, gas hold-up.[100b] Moreover, the sensitivity of the DO probe dictates the degree to which the pressure needs to be increased or decreased to produce a significant response. Larger pressure changes produce larger differences in driving force, which are easier to accurately measure.[100b]

Since dynamic methods utilize DO data measured by a probe, any dynamic behavior of the probe can itself influence the accuracy of estimation unless accounted for in the oxygen absorption model.[100a, 132, 142] For instance, probes rarely respond instantaneously to a change in DO concentration. The response time, τ_R, of a probe can be estimated by measuring its response to a step change in oxygen concentration e.g. by moving the probe from air into water saturated with pure oxygen, as shown in Figure 6.4. If the probe exhibits first order dynamics to a step change, the response time is defined as the time required for the probe to measure 63% of the difference between the initial and final saturation values.[99a, 141a, 143] Therefore, following a step change, the measured DO concentration will only reach 99% of the new saturation value after a period of five response times. This means that the probe dynamics can only be ignored entirely if $5\tau_R$ is less than k_La^{-1}.[136a] The DO probe used in Chapter 4 was found to have a response time of 6 s. Figure 6.5 shows that this response time would only become negligible when measuring k_La values less than 120 h^{-1}, which is relatively low for the reactors used in Chapters 4 and 5. As such, the probe response time cannot be ignored and must be accounted for to ensure accurate k_La estimation.

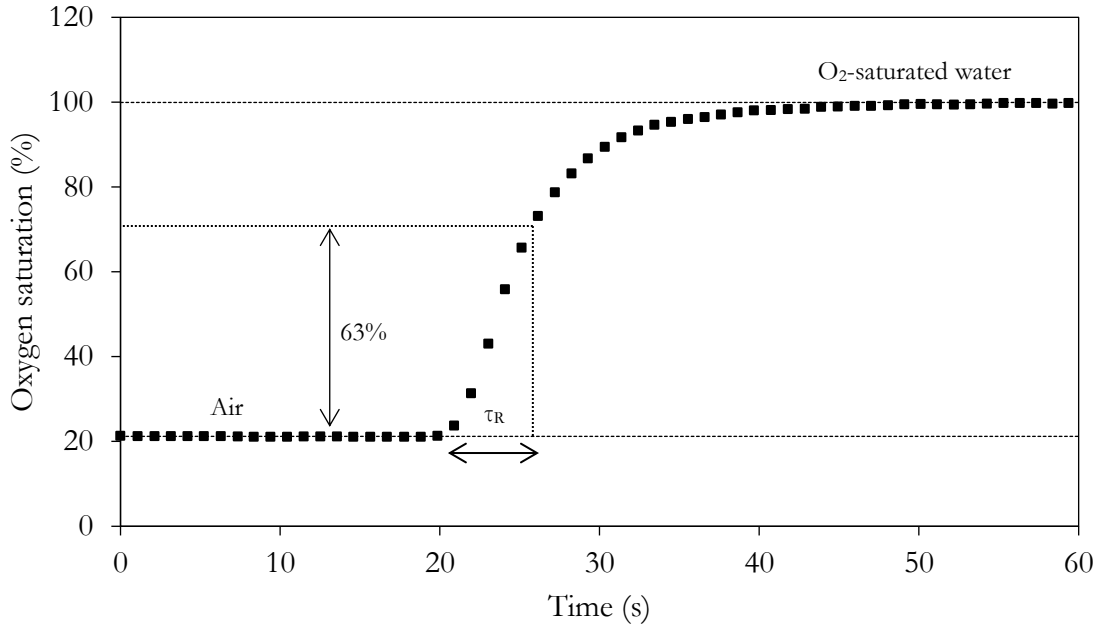

Figure 6.4. Calculation of response time after DO probe is moved from air to oxygen saturated water to produce a step change in dissolved oxygen concentration.

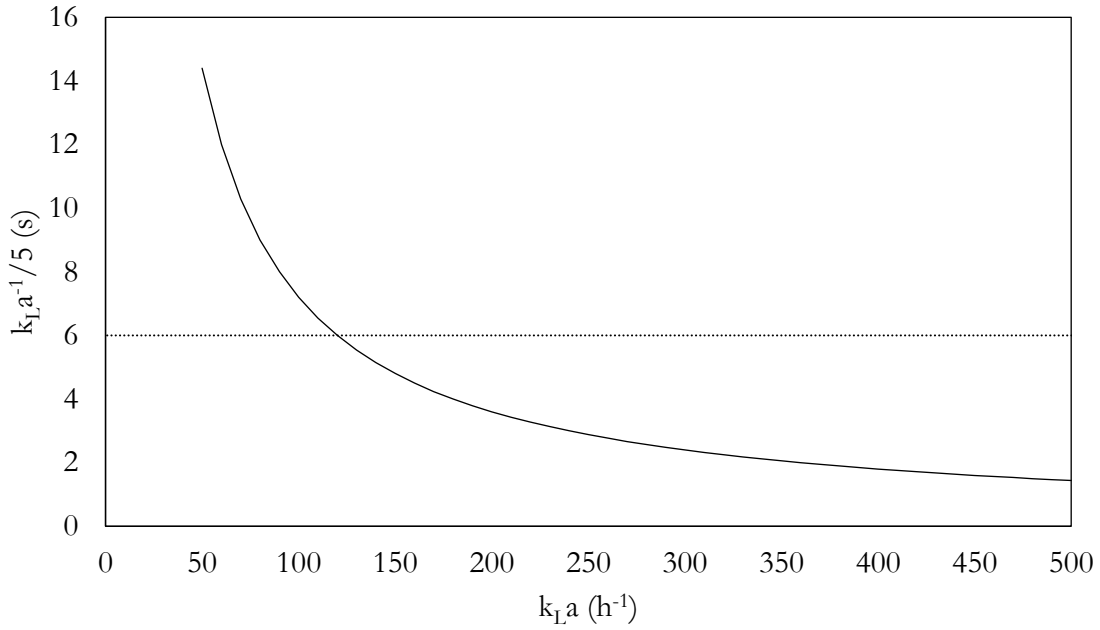

Figure 6.5. k_La versus response time required to ignore probe dynamics. Dotted line represents the response time of the DO probe used in Chapter 4.

The probe dynamics can be modelled as follows

$$\frac{dC_O^m}{dt} = \frac{(C_O - C_O^m)}{\tau_R} \tag{6.4}$$

where $C_{O,m}$ represents the DO concentration measured by the probe.[99a] By simultaneously solving Equations 6.1 and 6.4 with measured transient DO data, the actual DO response to a step change in oxygen concentration can be modelled and used to estimate a more accurate value of k_La, as shown in Figure 6.6. Accounting for the probe response time increased the estimated values of k_La by 6% in distilled water and 12% in 0.8 M potassium phosphate buffer.

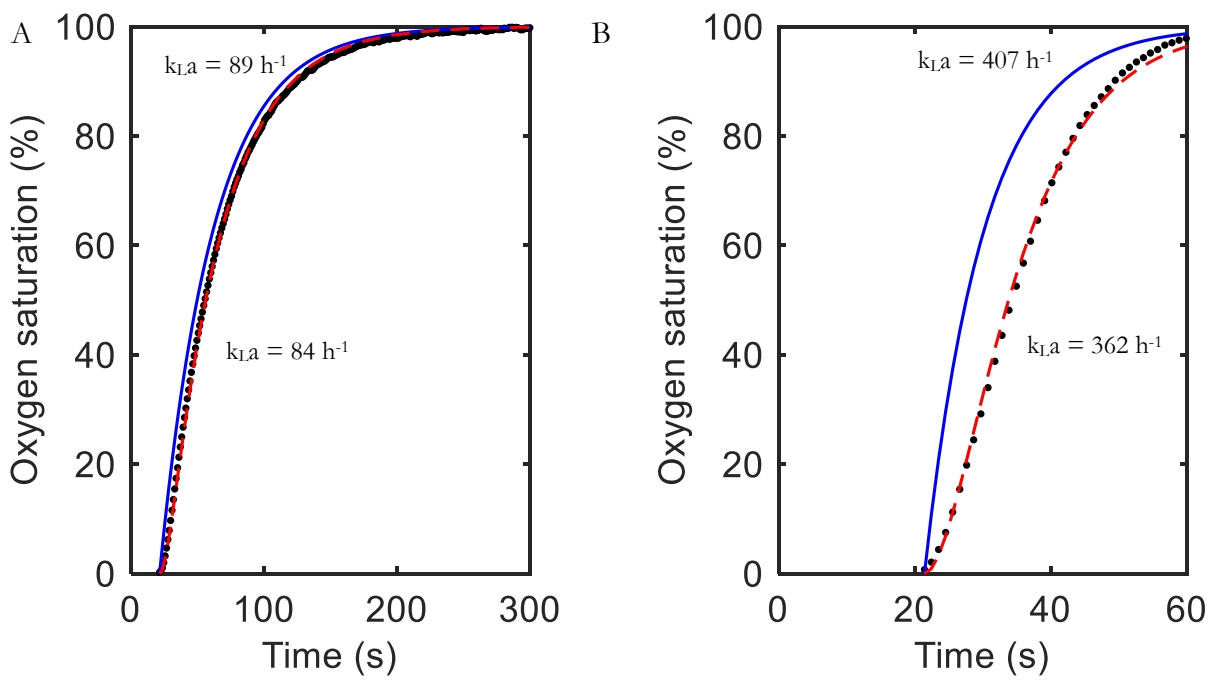

Figure 6.6. Probe dynamic response (dashed line) fitted to measured DO data to model adjusted DO dynamic response (solid line) for k_La estimation in A) distilled water and B) 0.8 M potassium phosphate buffer (pH 7).

Steady-state techniques for estimating k_La involve monitoring the flowrates and compositions of gas and liquid streams into and out of a reaction that consumes or produces oxygen, from which

component mass balances across the system can be used to calculate k_La.[130] This enables the use of more accurate analytical techniques if DO probes with sufficiently low response times are not available. Model reactions that are commonly used include sulfite oxidation, hydrazine oxidation and hydrogen peroxide decomposition.[99c, 100a] However, as it has now been established that k_La is greatly influenced by media composition, the use of a model reaction as an approximation of a system of interest would be ill-advised. Furthermore, the rate of the reaction may influence estimation of the k_La. For instance, if the rate is high, the reaction may enhance the liquid side mass transfer coefficient of oxygen, k_L, at the gas-liquid interface.[99c, 100a, 144] Conversely, if the rate is low, the bulk liquid may not be entirely depleted of dissolved oxygen, complicating estimation of the driving force.[99c, 100a]

All of the techniques discussed so far have limitations. Thus, it seems like the only way to reliably estimate the k_La for a specific reactor/reaction combination during operation might be to perform an experiment at the desired operating conditions, gather both dynamic and steady-state data for as many of the reagents as possible and then fit a model of the system to the resulting concentration profiles. This is the focus of Chapter 7.

6.3 Conclusions

In this chapter, it was found that media composition has a significant effect on the gas-liquid mass transfer coefficient. While some of this may result from slight changes to the density and viscosity of the media, which can affect the specific gassed power input of a CSTR, it is likely that these influences are also somewhat based on how each media component interacts with the gas-liquid interface. These interactions may affect interfacial area, by changing the surface tension of the media, or the liquid-side mass transfer coefficient, by altering the thickness and recirculation of the surface layer surrounding the gas bubbles. Further research is required to elucidate the underlying mechanisms. In the GOx system, all major media components, were found to have a positive effect on k_La, except for glucose, which had no effect. However, it was also found that these individual effects may negatively interact with each other. This makes it very difficult to accurately express k_La as a function of media composition for prediction purposes. Thus, the alternative is to continue to estimate k_La from experimental data. However, to account for the specifics of a particular reactor/reaction system, it is proposed that a model be fit to experimental data collected during a reaction in the reactor of interest. This will be the topic of the next chapter.

Chapter 7

Estimation of process parameters

This chapter is intended for later publication.

7.1 Introduction

As computer processing power and our understanding of the mechanisms behind complex physical and chemical phenomena continue to improve, so does our ability to digitally simulate such phenomena, which presents a means of designing and optimizing production processes in less time and with fewer resources. For this reason, the design of a physical process should always be done in parallel with that of its digital counterpart. The degree to which the physical and digital realms are integrated gradually increases as the process moves closer to commercial operation. During the early stages of process design, a digital representation that operates independently of the physical system, known as a digital model, is typically constructed to simulate its behavior.[145] To construct the digital model and validate its accuracy, data collected from experiments are manually supplied as model inputs. Following that, the model can be used without additional data input to optimize the performance of the system or design future experiments. As the design of the process continues into later stages, the digital model can be partially integrated with the physical process through automatic input of measured data into the model. In this way, the digital model becomes a digital shadow, operating in parallel with, and dependent on, the physical process, but without affecting it.[146] Based on the automated input of data measured from the physical process during operation, the digital shadow is able to forecast changes to the process which can then be compared to actual observed changes in order to validate its predictive capabilities. If the digital shadow is found to predict the future behavior of the physical process with sufficient accuracy, it may be used as a digital twin, whereby the simulated data it generates is automatically used to enact changes to the physical process to control against deviations from optimal operation.[147] In such cases, the physical and digital realms are completely integrated, in that changes in the physical system affect the digital simulation, which in turn affects the physical system. Nevertheless, the foundation of this relies on the development of the initial digital model, the accuracy of which hinges on our mechanistic understanding of the physical system. Fortunately, this means that a digital model may also act as a powerful diagnostic tool to

highlight gaps in our understanding of a process. In this chapter, the model for biocatalytic glucose oxidation in a dual-CSTR configuration, introduced in Chapter 5, will be further developed to expand its application towards estimation of critical process parameters, such as k_La.

7.2 Model description

The major challenges of accurately modelling the glucose oxidase reaction are twofold. First, the rate law describing GOx kinetics (Equation 7.1) is more complex than the standard Michaelis-Menten kinetics of single substrate enzymes. As a result, the rate constant (k_{cat}) and substrate affinity constants for each substrate (K_{Mi}) are difficult to determine experimentally due to the wide range of dissolved oxygen (DO) concentrations, both above and below the K_{MO}, which would need to be tested during characterization. For example, achieving low DO concentrations requires accurate mass flow control at very low flow rates, while achieving high enough concentrations to saturate the enzyme generally requires pressurization. For this reason, GOx has previously been characterized in a tube-in-tube reactor, which facilitates rapid oxygen mass transfer through a semi-permeable membrane and pressurization up to 10 bar.[39] The kinetics of GOx are further complicated by the occurrence of competitive product inhibition. Although glucono-1,5-lactone is quickly hydrolyzed to gluconic acid, which is structurally distinct from glucose, hydrogen peroxide may reversibly bind to the reduced form of the enzyme, instead of oxygen, increasing the apparent K_{MO} of the enzyme. The inhibition constant, K_I, has been found to be approximately equal to the K_{MO}.[43] Additionally, many enzymes are known to be inactivated by hydrogen peroxide.[42] Therefore, for continuous operation using GOx, the by-product must be continuously scavenged. This can be done by coupling GOx with catalase, which consumes hydrogen peroxide to produce oxygen and water. The rate law describing the kinetics of catalase (Equation 7.2) is much simpler than that of GOx, but the rate constant and affinity constant of catalase can be difficult to characterize due to its high reaction rates and deactivation at relatively low concentrations of hydrogen peroxide (> 70 mM)[148]. The addition of catalase to the reaction not only removes hydrogen peroxide but also produces some dissolved oxygen (0.5 mol per mol H_2O_2 scavenged) that can subsequently be consumed by GOx. However, due to the stoichiometry of the reaction, the coupled enzyme system is not self-sufficient. Therefore, oxygen must still be supplied to the enzyme, typically through bubbling of air or oxygen into the reaction media. Herein lies the second challenge to modelling the system. Oxygen is supplied to the oxidation reaction by two means: transfer into the liquid phase from the gas phase (Equation 7.3), governed by the mass transfer coefficient (k_La) and saturation concentration of oxygen (C_O^*), and the production of dissolved oxygen by catalase.

$$v_{GOx} = \frac{k_{cat,GOx} C_{GOx} C_G C_O}{C_G C_O + K_{MO} C_G \left(1 + \frac{C_{HP}}{K_I}\right) + K_{MG} C_O} \tag{7.1}$$

$$v_{CAT} = \frac{k_{cat,CAT} C_{CAT} C_{HP}}{K_{MHP} + C_{HP}} \tag{7.2}$$

$$OTR = k_L a (C_O^* - C_O) \tag{7.3}$$

The mole balances in a CSTR can be modelled by a set of algebraic equations that, when solved, yield the steady-state concentrations of each reaction species. However, modelling the mole balances as a system of ODEs, as done in Chapter 5, allows the inclusion of dynamic behavior at start-up. The model is comprised of the mole balances for glucose, oxygen, gluconic acid and hydrogen peroxide in each reactor, as well as the dynamics of the dissolved oxygen probes presented in Chapter 6 (Equations 7.4 to 7.13). Solution of the system of equations and subsequent sensitivity analyses and parameter estimation by nonlinear least squares regression was implemented in MATLAB, based on code by Sin and Gernaey[149]. The experimental data presented in Chapter 5 was used for parameter estimation. The response times of the DO probes used in Reactors 1 and 2, were calculated to be 6 and 10 s, respectively, according to the method shown in the previous chapter.

$$\frac{dC_{G,R1}}{dt} = \frac{Q}{V_{R1}}\left(C_{G,F} - C_{G,R1}\right) - v_{GOx} \tag{7.4}$$

$$\frac{dC_{O,R1}}{dt} = \frac{Q}{V_{R1}}\left(C_{O,F} - C_{O,R1}\right) - v_{GOx} + \frac{1}{2}v_{CAT} + k_L a\left(C^*_{O,R1} - C_{O,R1}\right) \tag{7.5}$$

$$\frac{dC^m_{O,R1}}{dt} = \frac{\left(C_{O,R1} - C^m_{O,R1}\right)}{\tau_{R,R1}} \tag{7.6}$$

$$\frac{dC_{GA,R1}}{dt} = \frac{Q}{V_{R1}}\left(C_{GA,F} - C_{GA,R1}\right) + v_{GOx} \tag{7.7}$$

$$\frac{dC_{HP,R1}}{dt} = \frac{Q}{V_{R1}}\left(C_{HP,F} - C_{HP,R1}\right) + v_{GOx} - v_{CAT} \tag{7.8}$$

$$\frac{dC_{G,R2}}{dt} = \frac{Q}{V_{R2}}\left(C_{G,R1} - C_{G,R2}\right) - v_{GOx} \tag{7.9}$$

$$\frac{dC_{O,R2}}{dt} = \frac{Q}{V_{R2}}\left(C_{O,R1} - C_{O,R2}\right) - v_{GOx} + \frac{1}{2}v_{CAT} + k_L a\left(C^*_{O,R2} - C_{O,R2}\right) \tag{7.10}$$

$$\frac{dC^m_{O,R2}}{dt} = \frac{\left(C_{O,R2} - C^m_{O,R2}\right)}{\tau_{R,R2}} \tag{7.11}$$

$$\frac{dC_{GA,R2}}{dt} = \frac{Q}{V_{R2}}\left(C_{GA,R1} - C_{GA,R2}\right) + v_{GOx} \tag{7.12}$$

$$\frac{dC_{HP,R2}}{dt} = \frac{Q}{V_{R2}}\left(C_{HP,R1} - C_{HP,R2}\right) + v_{GOx} - v_{CAT} \tag{7.13}$$

7.3 Results and Discussion

To determine whether the experimental data from Chapter 5 can be modelled, the values for 8 model parameters are required, as shown in Table 7.1. Initial values of the kinetic constants of GOx[39] and catalase[97] were obtained from literature, while the initial value of the inhibition constant for GOx was assumed to be equal to that of the K_{MO}[43]. The initial mass transfer coefficients of each reactor were determined using the gassing-in method in distilled water. While the sparging rate, stirring speed and working volume were kept constant in both reactors, the media composition is only constant once steady-state is reached. As such, k_La is expected to change over the course of the reaction. However, in Chapter 6, it was found that expressing k_La as a function of media composition would likely be highly inaccurate. As such, k_La in each reactor was kept constant. The Henry's constant, used to calculate saturation concentrations of oxygen from the partial pressure of oxygen, p_{O2}, in the feed gas (Equation 7.14), was assumed to be equal to the value for pure oxygen dissolved in water ($1.3x10^{-5}$ $mmol.L^{-1}.Pa^{-1}$ according to the NIST database). This assumption is based on the fact that, in Chapter 6, the oxygen probe, calibrated in distilled water, measured the same maximum oxygen saturation regardless of media composition.

$$C_O^* = H \cdot p_{O_2} \tag{7.14}$$

Table 7.1. Initial values of model parameters and estimated values after nonlinear regression

Parameter	Reactor	Initial value	Estimated value	Relative error (%)	Unit
$k_{cat,GOx}$	-	17.78	73.87	1127	$\mu mol.min^{-1}.mg^{-1}$
K_{MO}	-	0.51	2.07	30	mM
K_{MG}	-	75.2	118.0	1810	mM
K_I	-	0.51	0.08	48	mM
$k_{cat,CAT}$	-	32000	5170	3071741	$\mu mol.min^{-1}.mg^{-1}$
K_{MHP}	-	35	34	1444	mM
k_La	1	94	246	19	h^{-1}
	2	96	848	90	

With the initial values of the parameters set, the model output was compared to the experimental glucose (C_G) and gluconic acid (C_{GA}) concentration profiles and measured oxygen saturation (S_O)

profiles, shown in Figure 7.1, along with the predicted concentration profile of hydrogen peroxide (C_{HP}) during the experiments. The modeled C_G, C_{GA} and S_O profiles fit the experimental data very poorly, however, they do exhibit similar trends. This suggests that the model equations should be capable of modeling the data, but that the initial values are likely incorrect. To test this, nonlinear regression was performed with all 8 parameters, the results of which are shown in Figure 7.2. The estimated values for each parameter are shown in Table 7.1.

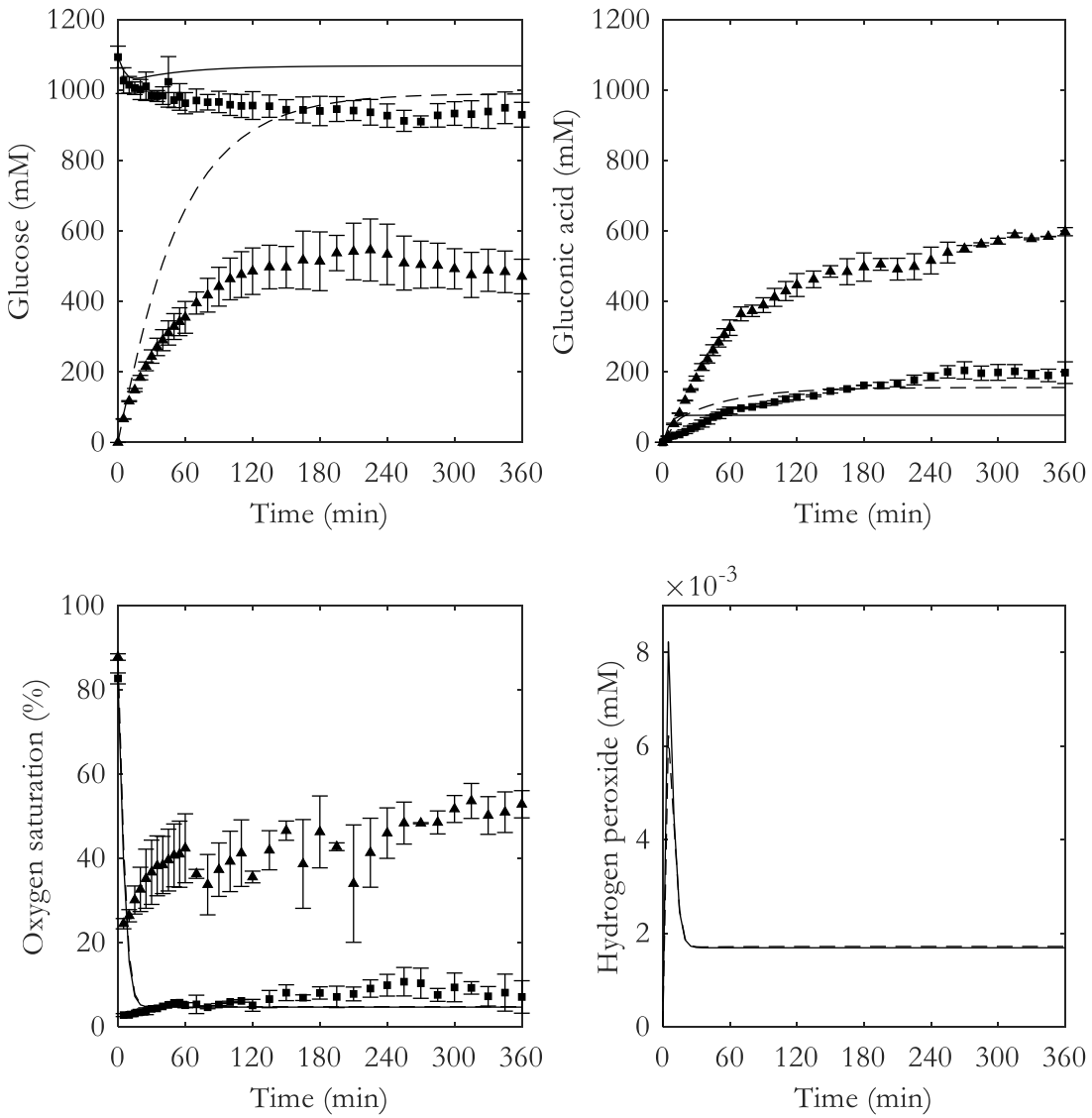

Figure 7.1. Experimental data from Reactor 1 (■) and Reactor 2 (▲) compared to predicted C_G, C_{GA}, S_O and C_{HP} profiles in Reactor 1 (-) and Reactor 2 (--), using initial values for model parameters.

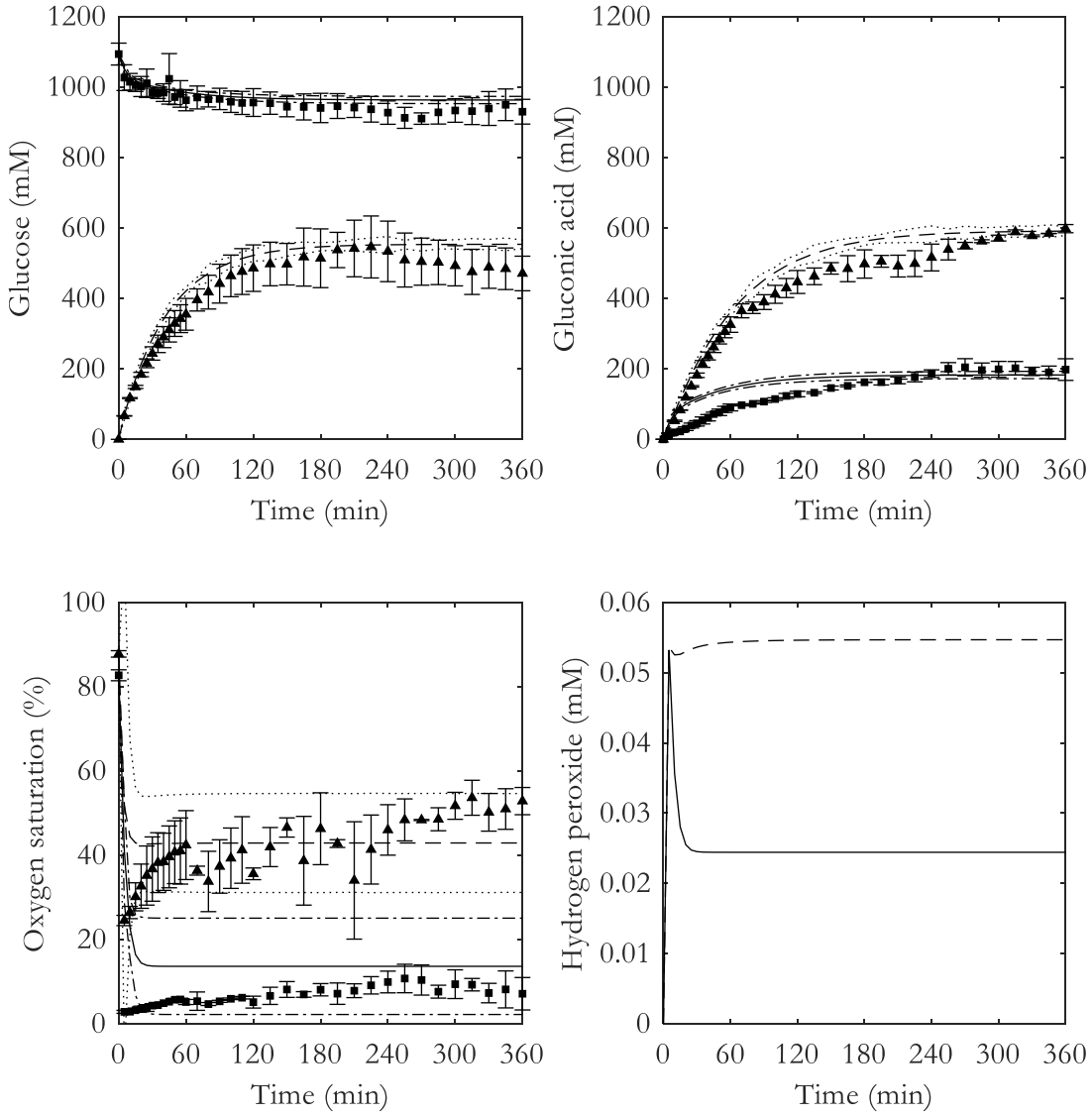

Figure 7.2. Experimental data from Reactor 1 (■) and Reactor 2 (▲) compared to predicted C_G, C_{GA}, S_O and C_{HP} profiles in Reactor 1 (-) and Reactor 2 (--), with 95% confidence intervals for Reactor 1 (dash-dot lines) and Reactor 2 (dotted lines), following nonlinear regression of 8 parameters.

Following parameter estimation by nonlinear regression, the fit of the predicted profiles to the experimental data was significantly improved. However, the gluconic acid concentrations in each reactor are slightly overestimated. This may be a result of making the k_La in each reactor a constant parameter despite dynamic changes in media composition. Alternatively, the pump flow rates may have deviated slightly from their calibrated setpoints over the course of the experiments. Additional

experimental data would likely help to improve the fit, within the margins of experimental error. While the fit of the model to the data has been improved substantially, the estimated values of many of the parameters are highly uncertain, as indicated by large relative errors.[149a] The primary reason for this is that the model is nonlinear and many of the parameters are positively or negatively correlated with one another[145b, 150], as shown by the correlation matrix in Figure 7.3. This means that the model is non-identifiable i.e with the limited data available, it is impossible to estimate all 8 model parameters with certainty. Therefore, to make the model identifiable, the number of estimated parameters must be reduced.[151] To assist in the selection of which parameters to eliminate, the importance of each parameter can be ranked by determining how sensitive each of the 8 state variables (C_G, C_{GA}, S_O and C_{HP} in each reactor) are to slight changes in each of the model parameters. These individual effects were then summed to find the total effect that each parameter has on the model (Figure 7.4).

	$k_{cat,GOx}$	K_{MO}	K_{MG}	K_I	$k_{cat,CAT}$	K_{MHP}	k_La_{R1}	k_La_{R2}
$k_{cat,GOx}$	1.0	1.0	1.0	-0.2	0.2	-0.5	0.1	0.2
K_{MO}	1.0	1.0	1.0	-0.2	0.2	-0.5	0.1	0.2
K_{MG}	1.0	1.0	1.0	-0.2	0.2	-0.5	0.1	0.2
K_I	-0.2	-0.2	-0.2	1.0	-1.0	0.1	0.0	0.0
$k_{cat,CAT}$	0.2	0.2	0.2	-1.0	1.0	-0.1	0.0	0.0
K_{MHP}	-0.5	-0.5	-0.5	0.1	-0.1	1.0	-0.1	-0.1
k_La_{R1}	0.1	0.1	0.1	0.0	0.0	-0.1	1.0	-0.1
k_La_{R2}	0.2	0.2	0.2	0.0	0.0	-0.1	-0.1	1.0

Figure 7.3. Correlation matrix of 12 model parameters after nonlinear regression. Strong positive or negative correlation between parameters is indicated by green or red color respectively.

According to the sensitivity analyses, the most important parameters are the mass transfer coefficients in both reactors, the rate constant of GOx, and its affinity constant towards oxygen. This is expected since the reaction is oxygen limited, especially in Reactor 1. Of lesser importance are the kinetic parameters of catalase, as well as the inhibition constant of GOx, which all have similar impacts on

the model. This is likely due to the fact that catalase was supplied in a large excess to minimize the concentration of hydrogen peroxide. Furthermore, no hydrogen peroxide data was supplied to the model. Lastly, K_{MG} is the least important parameter due to the fact that the glucose concentrations are relatively large throughout the experiments and so the reaction is not glucose-limited. Thus, small changes to the K_{MG} have little impact on the model and so it can be reasonably excluded as a parameter.

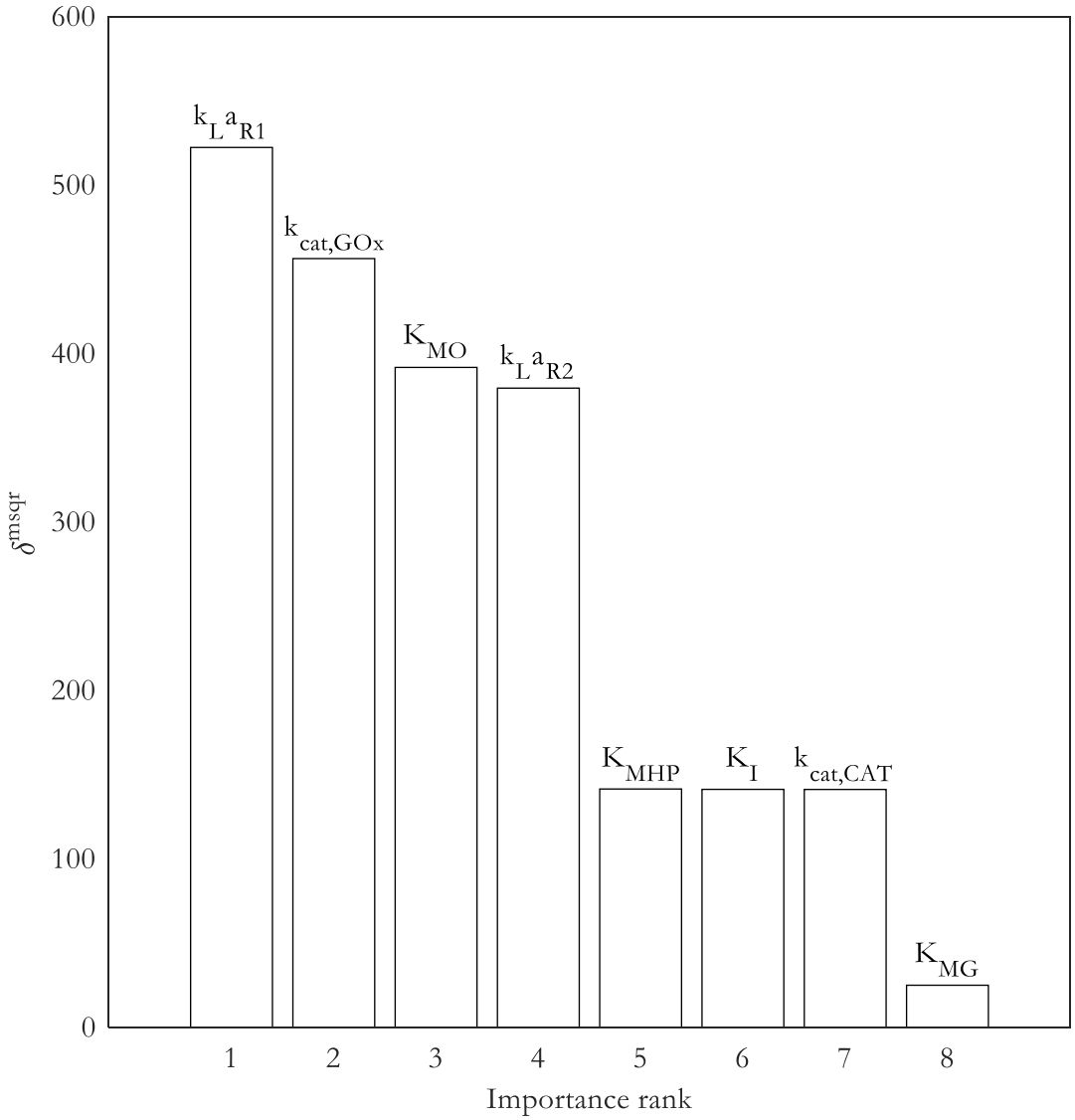

Figure 7.4. Model parameters ranked according to the summed sensitivity of model variables to changes in each parameter (δ^{msqr}).

However, excluding parameters purely based on their importance rank is not guaranteed to make the model more identifiable, as it does not necessarily reduce the degree of correlation between the remaining parameters. The degree of linear dependence between a set of parameters can be quantified by their collinearity/condition index. Generally, a collinearity index of under 30 is recommended for a model to be considered identifiable[152]. With 8 parameters in total, 247 possible combinations of at least two parameters exist, each with their own collinearity index. For instance, the subset containing all 8 parameters has a collinearity index of 30375. Excluding the least important parameter, K_{MG}, only reduces the collinearity index to 29686. Therefore, additional parameters need to be excluded. With the 7 remaining parameters, 120 possible parameter subsets exist, of which 44 have collinearity indices below 30. It is desirable to predict as many parameters as possible and so only the largest of these subsets, shown in Table 7.2, are considered first.

Table 7.2. Subsets of 4 parameters with correlation indices less than 30

Subset	Parameters							Collinearity index
	$k_{cat,GOx}$	K_{MO}	K_I	$k_{cat,CAT}$	K_{MHP}	k_La_{R1}	k_La_{R2}	
1		X			X	X	X	4.92
2		X		X		X	X	4.92
3		X	X			X	X	4.93
4	X				X	X	X	5.43
5	X			X		X	X	5.44
6	X		X			X	X	5.44
7	X	X				X	X	28.55

As indicated by the correlation matrix, the mass transfer coefficients of both reactors are not strongly correlated and so they are present in all of the parameter subsets. In contrast, the correlation between the remaining parameters prevents more than two from being estimated with certainty. Unfortunately, it was found that, despite all having collinearity indices of less than 30, parameter estimation with each of these subsets still resulted in estimated values with large relative errors. As such, a subset of 3 parameters was selected, including the k_La in each reactor and the rate constant of GOx, since it has the largest impact on the model of all the enzyme kinetic parameters. The collinearity index of this subset is 0.68. The results of the parameter estimation with these 3 parameters are displayed in Table 7.3 and Figure 7.5.

Table 7.3. Estimated parameter values following nonlinear regression after identifiability analysis

Parameter	Reactor	Initial value	Estimated value	Relative error (%)	Unit
$k_{cat,GOx}$	-	17.78	20.05	7.1	$\mu mol.min^{-1}.mg^{-1}$
k_La	1	94	239	3.7	h^{-1}
	2	96	833	9.7	

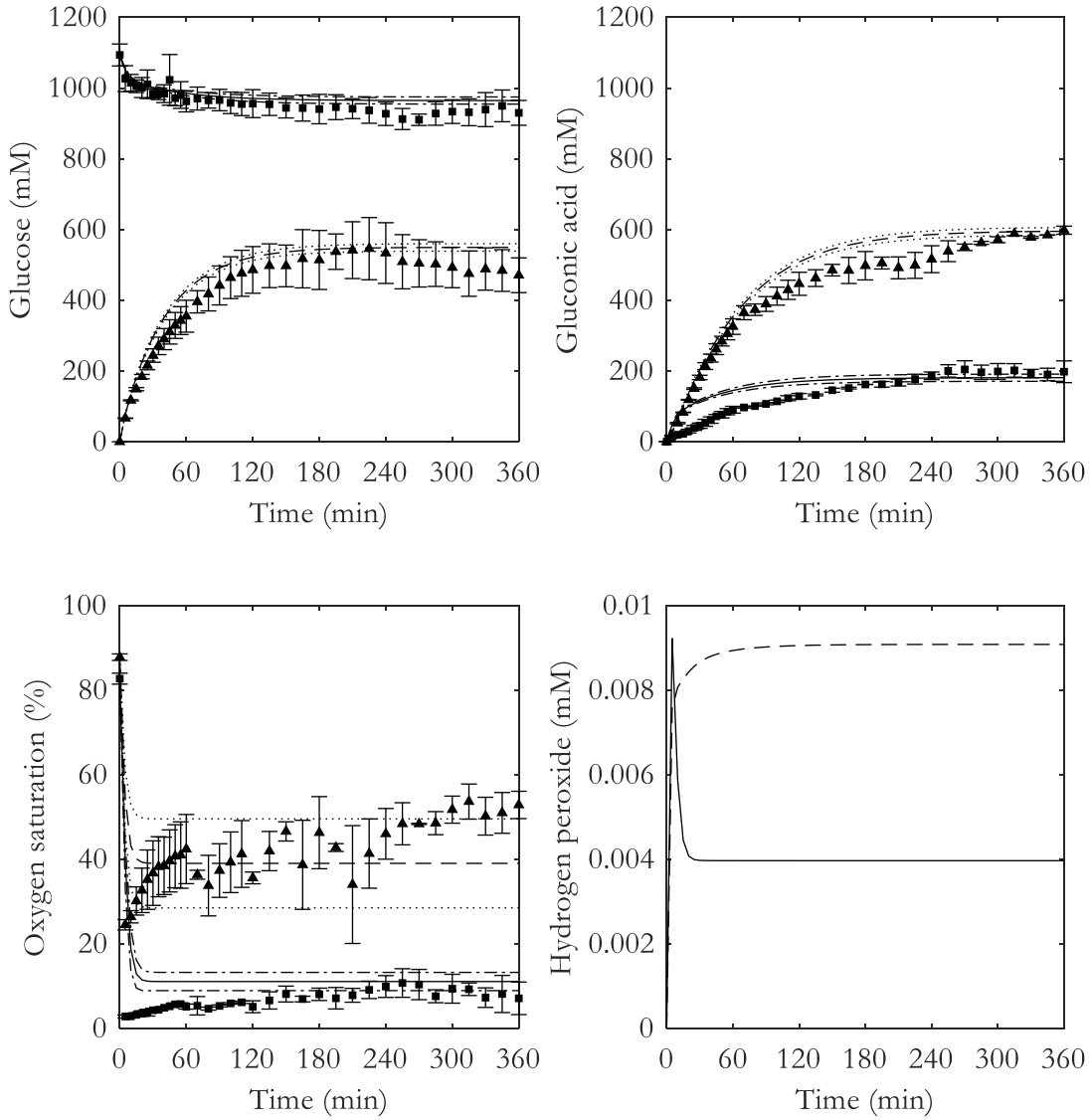

Figure 7.5. Experimental data from Reactor 1 (■) and Reactor 2 (▲) compared to predicted C_G, C_{GA}, S_O and C_{HP} profiles in Reactor 1 (-) and Reactor 2 (--), with 95% confidence intervals for Reactor 1 (dash-dot lines) and Reactor 2 (dotted lines), following nonlinear regression of 3 uncorrelated parameters.

The relative errors of the new estimated values are all less than 10%, which indicates that the 3 selected parameters have been predicted with a degree of certainty. Additionally, the model fit to the data is largely unchanged. Considering the error of prediction, the estimated rate constant of GOx is not significantly different from the literature value. This shows the value of characterizing oxidases in a tube-in-tube reactor, which enables high dissolved oxygen concentrations by allowing pressurization up to 10 bar.

As suggested by the results of Chapter 4, the k_La values in both reactors are substantially higher than those measured in distilled water. Additionally, as predicted in Chapter 5, the k_La in the second reactor is higher than in the first, likely due to the difference in media composition. In fact, it is roughly 2-fold higher than any of the k_La values measured in solutions of each individual media component, presented in Chapter 6. This suggests that the individual positive effects of the enzymes, buffer and product on k_La are combined when they are all present in solution. The strong negative interactions between buffer and sodium gluconate at high concentrations, observed in Chapter 6, were likely avoided as a result of the buffer concentration during the experiments being constant at only 0.1 M. However, the increased k_La values may also be due, in part, to the fast reaction taking place in the liquid film surrounding the gas bubbles, which has been known to enhance the liquid-side mass transfer coefficient, k_L, during a variety of gas-liquid reactions.[153] This theory is supported by the tendency of enzymes to adsorb to gas-liquid interfaces.

Finally, while gluconic acid concentrations of up to roughly 600 mM were produced, the predicted concentrations of hydrogen peroxide never exceeded 0.01 mM, which is significantly lower than the assumed initial value for the inhibition constant of GOx. Therefore, an excess of catalase appears to be an effective, albeit costly, means of avoiding GOx inhibition or inactivation due to the co-product.

Improving performance

Having modelled the system with relative accuracy, it is now possible to assess strategies of improving the performance of the reaction. This can either be done through engineering of the process or the enzyme itself. For instance, the enzyme concentration or operating pressure can be increased to achieve higher reaction rates. Alternatively, the enzyme can be engineered to increase its activity or affinity towards oxygen. The model was used to predict the effect that increasing each of these factors by an order of magnitude would have on the process metrics, described in Chapter 1. The results are shown in Table 7.4. These predictions were made with the previously estimated k_La values, which were

assumed to remain constant. However, in reality, these values are likely to change subject to changes in media composition. Feed gas compositions of 80% O_2 were used for all predictions.

Table 7.4. Predicted reaction performance following improvements to the process or enzyme

Process metric	Unit	Current	Process improvements		Enzyme improvements	
			C_E x 10	P x 10	$k_{cat,GOx}$ x 10	K_{MO} ÷ 10
Conversion	%	66.5	99.4	95.1	99.3	85.3
Product concentration	$g_{GA}.L^{-1}$	149	223	214	223	191
Biocatalyst yield	$g_{GA}.g_{GOx}$	149	22	214	223	191
Productivity	$g_{GA}.L^{-1}.h^{-1}$	90	134	128	134	115

A 10-fold increase in the concentration of both enzymes could allow near-complete conversion to be achieved in just two reactors. The resulting increase in product concentration leaving the system would facilitate downstream processing. However, this would drastically reduce not only the effectiveness with which the GOx is used, but also the biocatalyst yield. Therefore, this strategy is only feasible if the cost contribution of the enzyme is extremely low. If this is not the case, the same gains in conversion, product concentration and productivity could be achieved by an equivalent increase to the activity of the enzyme, without compromising the biocatalyst yield. Nevertheless, the enzyme will still be used ineffectively as long as the DO concentrations are low relative to the K_{MO}. Increasing the pressure of the two reactors to 10 bar could also allow much higher conversions, by raising the solubility of oxygen to 9.6 mM, but this strategy increases both capital and operating costs. Moreover, even higher pressures would be required to reach near-complete conversion. It is also unknown what effect further raising the oxygen partial pressure in the gas phase will have on the stability of the GOx. The alternative is to reduce the K_{MO} of GOx with protein engineering to allow it to operate faster at lower DO concentrations. However, due to the nonlinearity of the GOx kinetics, a 10-fold reduction in K_{MO} does not yield the same improvements as a 10-fold increase in pressure, which is proportional to the driving force for oxygen transfer.

Besides increasing pressure, there are alternative process improvements that can be implemented to increase the oxygen transfer rate, since it is also dependent on k_La. As discussed in previous chapters, increasing the interfacial area available for gas-liquid oxygen mass transfer raises the mass transfer coefficient.[144d, 154] In stirred tank reactors, where the gas phase directly contacts the liquid phase,

interfacial area can be improved by increasing gas flowrate or using spargers with smaller pore sizes to generate bubbles with larger surface-to-volume ratios and hold-ups.[144d] One potential downside to this, however, is that it may exacerbate deactivation of the GOx by increasing the area over which it can come into direct contact with the oxygen-rich feed gas. Sintered frits made from polytetrafluoroethylene (PTFE) or stainless steel (SS) have become particularly attractive in recent years for use as spargers due to their microporous structures. Mass transfer coefficients were estimated in distilled water using spargers with a variety of pore sizes and at different gas flowrates, the results of which are shown in Figure 7.6.

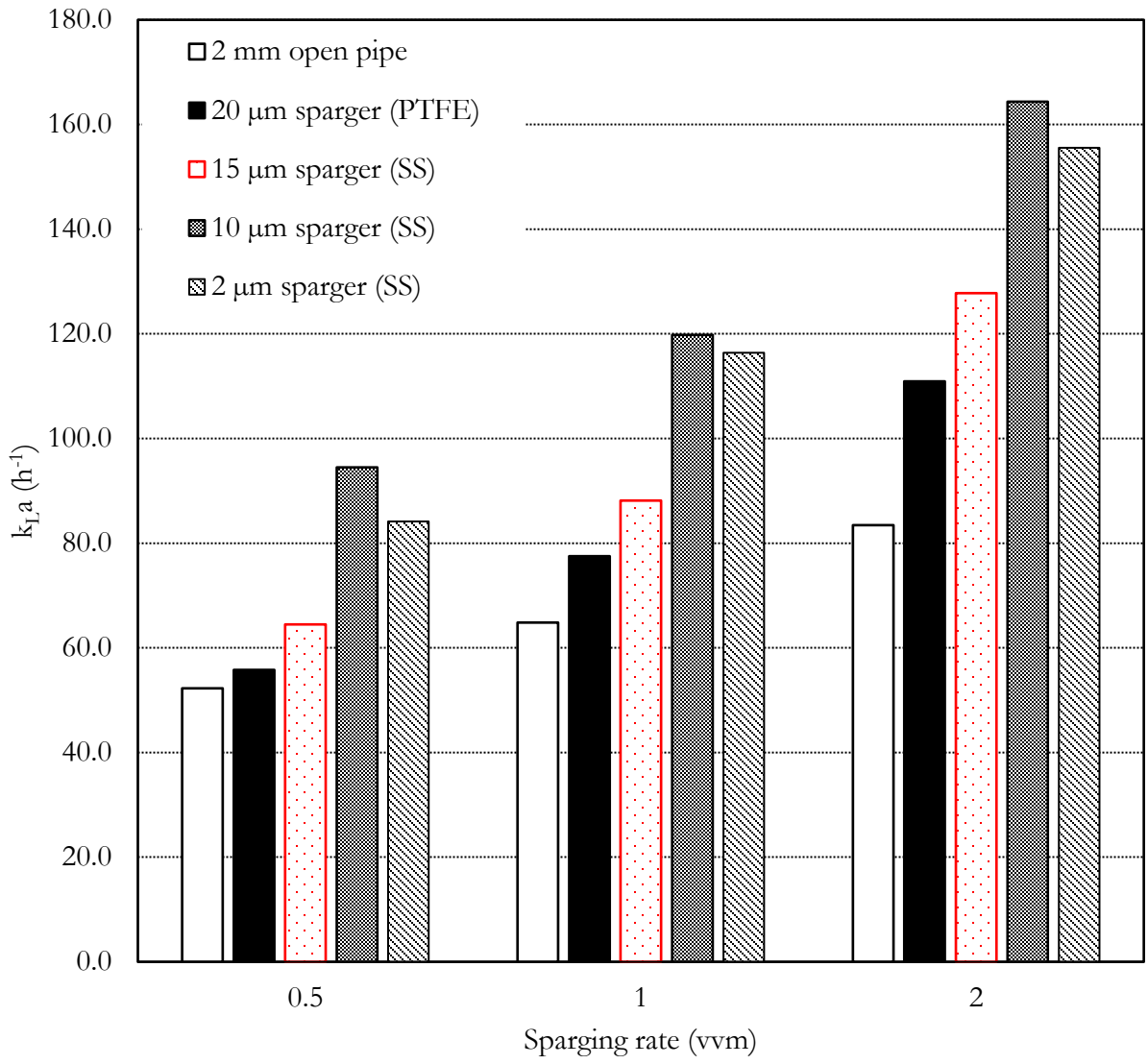

Figure 7.6. Values of k_La estimated in distilled water using different spargers and gas flowrates. The sparger used in Chapters 4 and 5 is highlighted in red.

The estimated k_La values for each sparger increase proportionally with sparging rate, which affects gas hold-up. The slopes of these linear relations were nearly identical for all spargers except that of the open pipe, which was 2-fold lower. This may have resulted from flooding of the impeller, which negatively impacts k_La due to a reduction of power input. It is often assumed that bubbles in a stirred tank are spherical, with an initial diameter proportional to that of the orifice or pore of the sparger.[155] Thus, since the surface-to-volume ratio of a sphere is inversely proportional to its diameter, it would be expected that spargers with smaller pore sizes result in proportionally larger interfacial areas. For example, the k_La estimated using a sparger with a pore size of 2 μm should be 5-fold higher than that with a pore size of 10 μm, but this was found not to be the case. As a result of how they are manufactured, sintered frits can often have broad pore size distributions that may even vary significantly between individual spargers of the same type.[154a] As such, the bubbles leaving the frit are often unevenly distributed across its surface, especially at lower gas flowrates (reduced gas pressure).[154a] This is because bubbles form preferentially at larger pores where the capillary pressure that needs to be overcome is lower.[144d] Therefore, at low gas flowrates, larger bubbles are generated but with a narrow bubble size distribution.[144d] In contrast, at high gas flowrates the increased pressure allows bubble formation at all pores, but broadens the size distribution.[144d] Consequently, the smaller the mean pore size of a sparger, the higher the gas pressure must be to make effective use of all of its pores. Therefore, below some 'critical' pressure, the presence of a path of least resistance through the sparger is likely to dramatically reduce its performance.

In addition to this, bubbles at the surface of the frit tend to coalesce before they detach.[154a] Therefore, the actual size of bubbles in the system may be more dependent on the surface tension of the liquid phase, which counteracts bubble detachment[136a], than on the pore size, potentially limiting the effect of reducing pore size indefinitely. This may explain why reducing the pore size of the sparger from 10 to 2 μm had little impact on the estimated k_La in the range of sparging rates that were tested. The sparging rate that can be implemented in the system is limited by the stability of the enzymes, capacity for foam control, as well as the maximum stirring speed to ensure effective gas-liquid dispersion. Compression costs may also limit the sparging rate, especially at higher operating pressures. Nevertheless, these results show that the estimated values of k_La could be further increased by a factor of 1.4 by reducing the mean pore size of the sparger to 10 μm instead of 15 μm.

To determine which combination of improvement strategies to implement, upper limits for enzyme concentration, operating pressure and feed gas composition are required. These can be found by

performing a techno-economic analysis of the system. With these limits in place, the model could be used to independently optimize the operating conditions of each reactor. A basic guideline for determining these limits is outlined in the next chapter.

7.4 Conclusions

In this chapter, nonlinear regression was used to fit a model of two CSTRs in series to experimental data for the purposes of estimating model parameters. A sensitivity and identifiability analysis was used to reduce the number of parameters from 8 to 3, to allow their estimation with a high degree of certainty. The rate constant of GOx was estimated and found to be close to the value determined in a tube-in-tube reactor. The mass transfer coefficients in each reactor were estimated to be much higher than the values measured in distilled water. Additionally, the k_La in the second reactor was significantly larger than that in the first. As both reactors were identical in geometry and operated at the same sparging rate and stirring speed, the difference in k_La appears to be a result of the different media compositions in each reactor. Therefore, this appears to be a good technique for estimating k_La, that takes into account all reactor/reaction properties at the desired operating conditions.

With the estimated values of k_La, the model was used to predict the effect of a number of improvement strategies on the process performance metrics. Increasing the activity of GOx through protein engineering has the same effect as increasing the enzyme concentration, but without reducing the biocatalyst yield. Improving the affinity of GOx towards oxygen does allow for significant performance improvements, although it is not a direct replacement for raising the operating pressure, which raises the driving force for gas-liquid oxygen transfer. It is also possible to raise the oxygen transfer rate by increasing k_La, through the use of a sparger with a smaller mean pore size. However, the effectiveness of this strategy is limited by the maximum allowable sparging rate. A techno-economic analysis can be used to identify the boundaries for each operating condition. With these constraints, the model can be used to identify the most cost-effective combination of operating conditions and set targets for improvement of the enzyme by protein engineering.

Chapter 8

Identifying constraints on operating conditions

In Chapter 2, a methodology for reactor selection was described, based on which CSTRs were proposed as a practical means of achieving the necessary gas-liquid mass transfer rates to operate a biocatalytic oxidation in industry, despite their broad residence time distributions, inability to achieve full conversion and dilution of the feed stream. While alternative reactor technologies for gas-liquid reactions, such as microfluidic tube-in-tube or segmented flow reactors, may avoid these obstacles, some practical limitations currently restrict their scale-up/scale-out. In the meantime, the scale-up of CSTRs is well-researched. Furthermore, many manufacturers already use stirred tank reactors in batch. Transitioning to continuous production in tubular reactors would render this existing infrastructure redundant. But, by retrofitting these stirred tanks to operate continuously, the benefits of continuous processing may be gained with minimal capital expenditure. Of course, blindly retrofitting reactors without first assessing whether they can achieve the desired performance targets when combined with an enzyme of interest is ill-advised. This chapter will discuss the prerequisite knowledge that is required about the process, reactor and enzyme to make such an assessment.

Effectiveness factor

The first step is to determine whether it is possible to achieve the required steady-state reaction rate with the enzyme of interest. The required rate (v_{req}) can be calculated from the target annual production capacity, given the working volume of the reactor. The maximum rate (V_{max}) of the enzyme is the product of its rate constant (k_{cat}) and its concentration (C_E). To determine the rate constant, the enzyme needs to be characterized. Accurate characterization requires measuring the rate of the enzyme across a wide range of substrate concentrations. Depending on the enzyme and substrates, this may prove to be challenging. For example, achieving sufficiently large dissolved oxygen concentrations to saturate an oxidase and measure its maximum rate is often not possible without pressurizing the system, due to the poor water-solubility of molecular oxygen. Likewise, sufficiently low concentrations of dissolved oxygen to precisely assess the affinity of the enzyme towards oxygen (K_{MO}), may be limited by the accuracy of mass flow control. The allowable cost contribution of an enzyme has been estimated to be approximately 5-10% of the product selling price, depending on its value.[7a] Based on these costs, the maximum allowable enzyme concentration can be calculated if the cost of the enzyme

(which factors in any costs related to its production, purification and immobilization, as well as its stability) is known.

With the rate constant and maximum allowable enzyme concentration known, V_{max} can be calculated and compared to v_{req}, which leads to one of three scenarios. If the maximum rate is less than the required rate, the enzyme is too expensive or too slow to achieve the desired production capacity. In such a case, protein engineering could be used to improve its activity and/or stability. If the maximum rate is equal to, or slightly above, the required rate, the enzyme can achieve the target production capacity provided it is used very effectively ($v_{req}/V_{max} \approx 1$). If the maximum rate is significantly larger than the required rate, the enzyme can achieve the desired production capacity even it is used less effectively ($v_{req}/V_{max} < 1$).

Substrate concentrations and operating pressure

Having characterized the enzyme, the required effectiveness factor, η, can now be used to determine the steady-state substrate concentrations needed to achieve it. This is illustrated in Figure 8.1, using GOx as a case study.

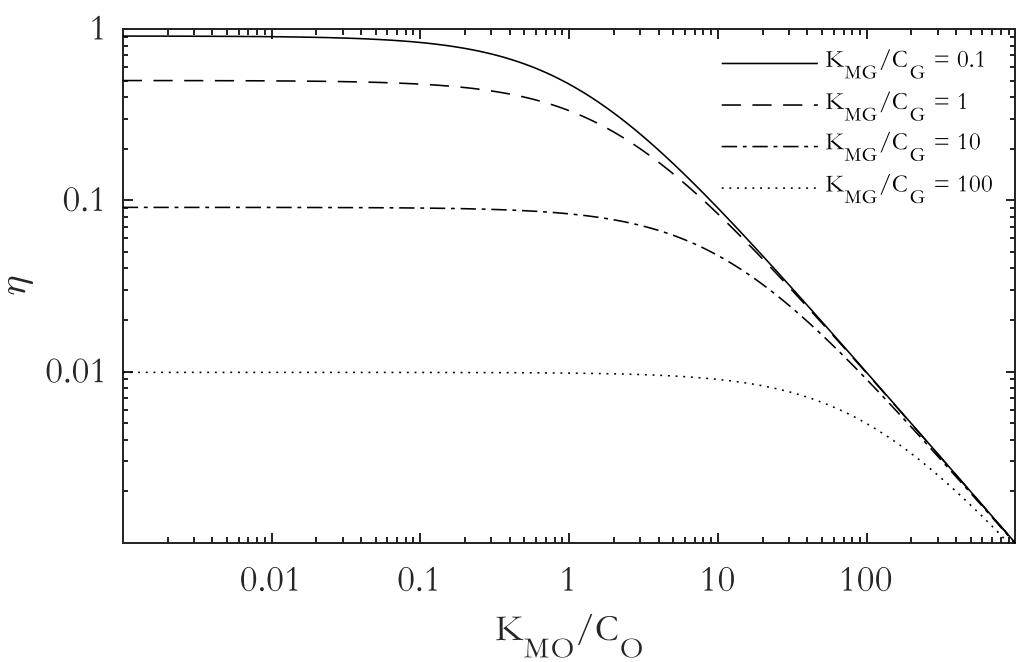

Figure 8.1. GOx effectiveness factor as substrate concentrations change relative to their corresponding affinity constants.

In order to use GOx with an effectiveness of roughly 0.9 at steady state, the glucose and dissolved oxygen concentrations must be at least 10 times higher than K_{MG} and K_{MO}, respectively. This corresponds to a glucose concentration of 752 mM and dissolved oxygen concentration of 5.1 mM at steady state. This glucose concentration can easily be achieved due to its high water-solubility. But, in a CSTR, the same concentration of glucose will be present in the effluent of the reactor. Thus, if a higher substrate conversion is desired, a second reactor can be placed in series, although the effectiveness factor in this reactor may be reduced. In contrast, the poor water-solubility of oxygen prevents the required concentration from being achieved at atmospheric pressure. Using the Henry's law constant of oxygen in water ($1.3x10^{-5}$ $mmol.L^{-1}.Pa^{-1}$), it can be calculated that an oxygen partial pressure of approximately 3.9 bar is required to achieve an oxygen solubility of 5.1 mM. This represents the absolute minimum oxygen partial pressure that would be required to achieve an effectiveness of 0.9, assuming the oxygen transfer rate (OTR) is high enough to fully saturate the reaction media ($C_O \approx C_O^*$). However, in most cases, the k_La in a reactor is not high enough to maintain such a high OTR, especially as the driving force for mass transfer (C_O^* - C_O) becomes smaller. Therefore, during a reaction, the dissolved oxygen concentration in the bulk liquid is substantially lower than the saturation concentration at the bubble interface ($C_O < C_O^*$). Thus, to achieve a bulk dissolved oxygen concentration of 5.1 mM, the partial pressure of oxygen in the gas phase would have to be significantly higher than 3.9 bar. Furthermore, the oxygen content of the gas phase determines the total pressure required to achieve the desired effectiveness factor. For instance, if pure oxygen is used, the reactor has to be operated at a minimum of 3.9 bar, whereas if air is used, the minimum operating pressure is 18.6 bar. The maximum oxygen content of the feed gas is set by the stability limit of the enzyme or, if the enzyme is relatively inexpensive, the allowable cost contribution for substrates.

Mass transfer coefficient

Having determined the minimum required operating pressure (P_{req}), it can now be compared with the maximum allowable pressure of the reactor ($P_{max,R}$). If $P_{max,R} < P_{req}$, then the desired effectiveness cannot be achieved in the chosen reactor. In such cases, protein engineering could be used to improve the affinity of the enzyme towards oxygen so that the required oxygen partial pressure can be reduced. If $P_{max,R} > P_{req}$, it may be possible to achieve the desired effectiveness factor in the reactor. In this case, $P_{max,R}$ sets the maximum oxygen saturation concentration that can be achieved in the reactor ($C_O^*{}_{max}$). Based on the stoichiometry of an oxidase coupled with catalase, the OTR must be equal to half of v_{req}.

With the OTR and C_O required to achieve the desired effectiveness factor known, together with the $C_O^*{}_{max}$ of the reactor, it is possible to calculate the minimum allowable k_La.

Agitation speed and sparging rate

Figure 8.2 illustrates how the k_La varies with agitation speed and sparging rate for a specified reactor. For the purposes of this discussion, the k_La is estimated using the following empirical power law correlation[76] (Equation 8.1). However, it should be noted that the values of the coefficient and exponents must first be determined for the system of interest.[156]

$$k_La = 0.04 \cdot v_s{}^{0.47} \left(\frac{P_G}{V}\right)^{0.6} \tag{8.1}$$

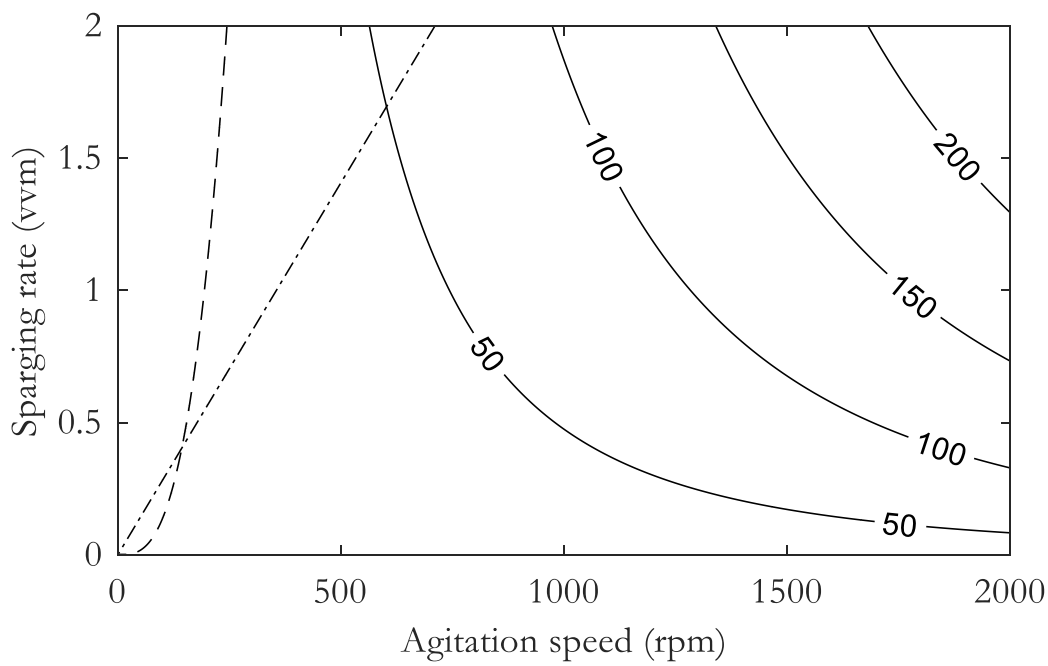

Figure 8.2. k_La in a CSTR as sparging rate and agitation speed are varied. Boundaries above which the impeller becomes flooded and the impeller blades form large cavities are indicated by the dashed line and dash-dot line respectively.

The superficial gas velocity (v_s) and gassed power input (P_G/V) are dependent on the reactor dimensions, operating conditions and the liquid density and viscosity. Detailed calculations can be found in Chapters 6 and 11 of the Handbook of Industrial Mixing.[78] It should be noted that the

resulting k_La values may not account for the effects of media composition discussed in Chapter 6. As expected, the higher the agitation speed and sparging rate, the larger k_La becomes. However, if the sparging rate is too high relative to the agitation speed, the gas cannot be efficiently dispersed, which can allow large cavities to form behind the blades of the impeller and eventually even lead to the impeller becoming completely flooded. This greatly reduces the effectiveness with which power can be transferred to the liquid and so this regime should be avoided. The boundaries for each of these phenomena, below which the gas can be effectively dispersed, are shown in Figure 8.2. Figure 8.3 shows a more generalized version of this plot, with additional limitations included.

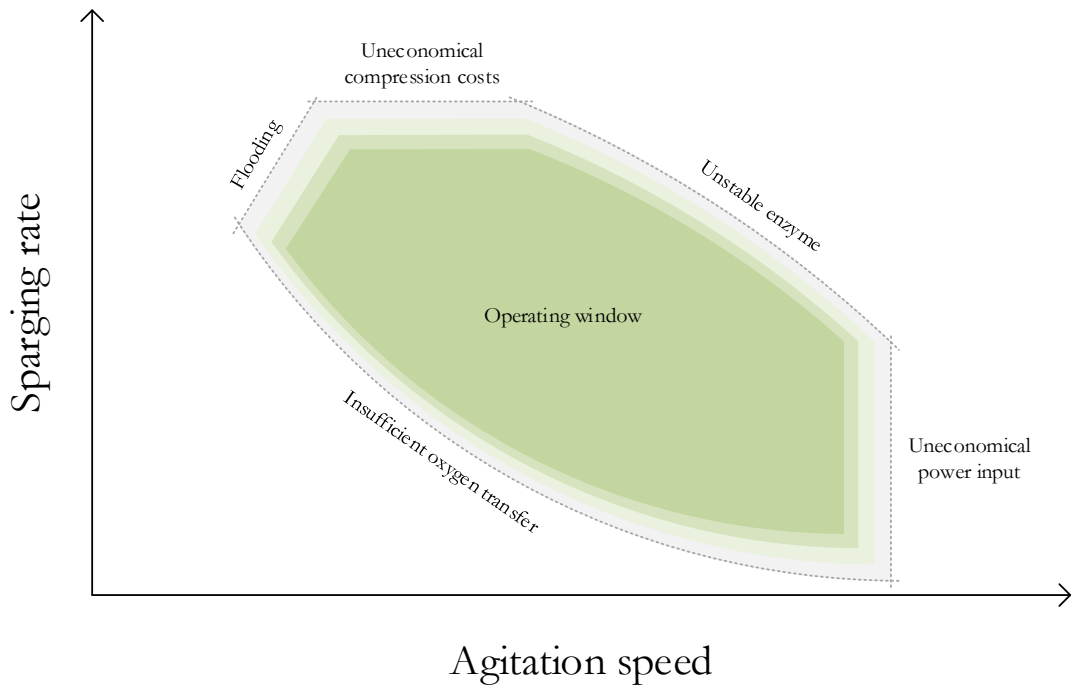

Figure 8.3. Conceptual regime map illustrating possible limitations, which restrict the value of gas-liquid mass transfer coefficient that can be achieved in a continuous stirred tank reactor during a biocatalytic oxidation.

For instance, if the gas sparging rate becomes too high, the cost of gas compression will eventually become uneconomical. The higher the operating pressure, the lower this limit. Similarly, the energy costs required to mix the contents of the reactor will eventually become uneconomical at high agitation speeds. The minimum allowable k_La, calculated previously, sets a minimum limit on the sparging rate and agitation speed to ensure the OTR is high enough to reach the required rate. Lastly, it is possible that the enzyme will become destabilized at high sparging rates and agitation speeds, due to direct

contact with molecular oxygen at the gas-liquid interface, as discussed in Chapter 4. This may be more prevalent at high oxygen partial pressures. These limits create an operating window, within which the k_La is high enough to achieve the required OTR. Since the OTR is dependent on both the k_La as well as the oxygen saturation concentration (C_O^*), the operating pressure, sparging rate and agitation speed can be optimized to find the most economical way of achieving the necessary OTR.

Chapter 9

Conclusions

The majority of chemical processing industries have already embraced or are trending towards the use of continuous manufacturing to reap the benefits of process intensification and reaction telescoping. Oxidations remain an important class of reactions in the synthesis of numerous chemicals of industrial interest. For this reason, oxidases are attractive biocatalysts due to their exceptional selectivity, mild operating conditions and use of molecular oxygen as an environmentally friendly oxidant. Furthermore, protein engineering allows these enzymes to be modified, in principal, according to the limitations of the process. As a result, a number of oxidases have already been implemented in industry for the production of active pharmaceutical ingredients. However, in many cases, the low solubility of oxygen in aqueous media may limit the reaction rates of these enzymes and so a deeper understanding is required to streamline the implementation of these enzymes into industrial scale continuous processes. The main conclusions arrived at in this thesis are presented below:

- A reactor selection methodology for continuous biocatalytic reactions was developed based on analyzing fundamental reactor types with respect to enzyme kinetics and limitations. Plug-flow operation is highly attractive as it enables the simplification of downstream processing by allowing complete conversion and precise control of residence times. However, the lack of mixing in plug-flow reactors restricts their use for multiphase reactions, unless operated at the microscale where surface-to-volume ratios are higher. Continuous stirred tank reactors (CSTRs) were proposed as a practical and scalable alternative, facilitating gas-liquid mass transfer by mechanical mixing and enabling rapid implementation through retrofitting of batch stirred tank reactors that are already prevalent in industry.
- Experiments with glucose oxidase in a laboratory-scale CSTR demonstrated poor performance due to oxygen limitation when supplied with air. Increasing the enzyme concentration does significantly improve reaction rates, but at the cost of reducing how effectively the enzyme is used. Increasing the oxygen partial pressure in the feed gas was found to have a much stronger influence on reaction rate, by virtue of increasing the solubility of oxygen in the liquid phase. However, when feed gas oxygen concentrations were increased above 60-80%, reaction performance began to drop, possibly due to inactivation of the

enzyme. As an alternative, oxygen partial pressure could be increased by raising the overall operating pressure of the system. However, this might also result in enzyme inactivation. Therefore, improving the affinity of glucose oxidase towards oxygen, to enable the use of lower oxygen partial pressures, is a safer approach.

- Conversions in a single CSTR are inevitably limited due to the homogeneity of the reactor contents and the substrate dependence of enzymatic reactions. The conversion can be improved by connecting multiple CSTRs in series, which also allows more cost-effective use of the enzyme. A model of 10 CSTRs in series showed that the overall conversion doubles upon addition of the second reactor, with diminishing returns thereafter. Therefore, a dual-CSTR configuration appears to be the most practical means of raising conversions and enabling more effective enzyme use, without excessive capital expenditure. Experiments in a series of two identical laboratory-scale CSTRs showed that overall conversion was actually tripled by inclusion of a second reactor. This was attributed to higher dissolved oxygen concentrations in the second reactor.
- The volumetric gas-liquid oxygen transfer rate controls the steady-state dissolved oxygen concentration in a CSTR, which predominantly limits the reaction rate of a biocatalytic oxidation. Therefore, accurate estimation of the mass transfer coefficient, k_La, is essential for design, scale-up and operation of these systems. Experiments showed that k_La is highly influenced by the presence and concentrations of a number of media components from the glucose oxidase system, including the buffer, product and enzymes. This was postulated to be a result of the interaction of these components with the gas-liquid interfaces, which may affect the surface tension and subsequent interfacial area within the reactor, or influence the liquid-side mass transfer coefficient by changing the thickness or recirculation of the liquid boundary layer surrounding the bubbles. A factorial design of experiments with two of the components indicated the presence of strong interaction effects, complicating the accurate prediction of k_La based on media composition.
- A model of the laboratory setup was developed and fit to experimental data to estimate k_La in each reactor as well as enzyme kinetic parameters. Initial results showed that the model is capable of fitting the experimental data, but that the dataset was too small to enable estimation of all parameters with certainty. A sensitivity and identifiability analysis was performed to reduce the number of estimated parameters. The rate constant of GOx was estimated and found to validate the value obtained in a tube-in-tube reactor. The mass transfer coefficients

in each reactor were also estimated and found to differ significantly, possibly due to differences in media composition and reaction rates, which may enhance the liquid-side mass transfer coefficient. The model was used to predict the outcome of various changes to the process and protein, indicating that it could be possible to achieve near-complete conversion in a dual-CSTR configuration. The most cost-effective combination of changes can be identified using the model, provided the specific economic constraints of the process are defined.

- A basic guideline for assessing the suitability of a reactor for operating a biocatalytic oxidation was outlined, based on the economic constraints that limit operating conditions. Once the enzyme of interest is characterized, its reaction rate can be assessed to ascertain whether it is sufficient to achieve the target market demand, using a cost-effective amount of enzyme. This sets the effectiveness with which the enzyme must be used, from which it is possible to calculate the required substrate concentrations during operation. For a biocatalytic oxidation, the required concentration of dissolved oxygen and stability of the oxidase towards oxygen can be used to set the required operating pressure, which subsequently fixes the minimum allowable mass transfer coefficient. The sparging rate and agitation speed required to achieve the minimum k_La can then be calculated. A conceptual regime plot was presented to highlight the constraints that limit the feasible range of operation.

Chapter 10

Future perspectives

In this thesis, an attempt has been made at presenting a means of implementing biocatalytic oxidations into industry in a streamlined and practical way. Nevertheless, there remain many areas where a deeper understanding could help to further broaden the applicability of oxidative enzymes.

- While oxidases were selected as the focus of this work, there are other subclasses of enzyme that are able to catalyze oxidation reactions. For example, oxygenases incorporate one or two atoms of oxygen directly into the substrate. However, they require expensive nicotinamide cofactors (NADPH or NADH) to do so. As such, they are typically implemented *in vivo* to benefit from native cofactor regeneration cycles within cells. However, the cells are often susceptible to deactivation or inhibition by industrially attractive substrates or products, which limits the stability of resting whole-cell biocatalysts.[1a, 157] Thus, improvements to either the resilience of the cells or the efficiency of *in vitro* cofactor regeneration are required for continuous operation over prolonged periods to be feasible. Peroxidases and peroxygenases, which use hydrogen peroxide as an oxidant, are also attractive options to avoid requirements for excess catalase or gas-liquid oxygen transfer. However, enzyme deactivation by hydrogen peroxide still limits their use.[158] Therefore, to enable continuous operation, the enzymes must be engineered to be more stable. Alternatively, the substrate must be supplied at more dilute concentrations, which may necessitate engineering the enzymes for greater affinity.
- The effects of catalyst stability can be reduced by continuously supplying a reaction with fresh enzyme, as was done in this work. However, depending on the value of the product, the biocatalyst yield may not be cost-effective. For instance, the biocatalyst yields achieved herein might be suitable for the production of pharmaceuticals or some fine chemicals, but it is estimated that biocatalyst yields in the range of 10^3-10^5 $g_{product} \cdot g_{enzyme}^{-1}$ would be required to produce low value bulk chemicals.[23a] There are cases where protein engineering has been used to increase the activity of enzymes by several orders of magnitude.[159] This would enable the use of much lower enzyme concentrations to maintain the desired performance. However, the use of soluble enzymes will often necessitate their removal downstream. If the cost contribution of downstream processing is large, retention of the enzyme within the reactor by

immobilization or membranes may be preferable, provided the biocatalyst is stable enough for prolonged operation. For gas-liquid reactions in CSTRs, additional research on the optimal configuration for retaining enzymes within the reactor may be required.

- Further studies into the stability of oxidative enzymes when exposed to gaseous oxygen are recommended. Herein it was found that GOx appeared to become inactivated by exposure to gases comprised of more than 60-80% oxygen. Increasing the pressure of the system to raise the solubility of oxygen may exacerbate this phenomenon, by further raising the oxygen partial pressure in the gas phase. Additionally, high dissolved oxygen concentrations may also lead to deactivation. The amino acids which are most susceptible to oxidation are cysteine and methionine.[160] Therefore, it may be possible to prevent deactivation by substituting these enzymes, provided they are not critical to the shape and function of the active site.[161] Alternatively, oxygen must be supplied indirectly through a gas permeable membrane, such as Teflon AF 2400.[162] However, these membranes can be expensive and the surface-to-volume ratios required to facilitate sufficient mass transfer would likely only be possible at the microscale.
- In this work, estimation of k_La by fitting a model to experimental data was proposed to be more practical than predictions based on media composition. Nevertheless, the ability to describe k_La as a function of media composition with relative accuracy would allow more robust dynamic model simulations. It would also facilitate the quantification of any mass transfer enhancements resulting from fast reactions taking place at the bubble surface. This requires an in-depth investigation into the underlying mechanisms by which various media components influence gas-liquid mass transfer.
- Techno-economic analyses of biocatalytic oxidations for the production of low and high value products could be used to set constraints on operating conditions. These constraints would allow the independent optimization of each reactor in a dual-CSTR configuration to achieve desired performance targets while minimizing the largest cost contributor for a specific process. There are already a number of industrially implemented oxidase-catalyzed reactions that could be utilized as case studies. Having up-to-date economic data would greatly facilitate protein engineering efforts towards the industrial implementation of a broader range of oxidases, by setting minimum targets for performance improvements.

References

1. (a) Schrewe, M.; Julsing, M. K.; Buhler, B.; Schmid, A., Whole-cell biocatalysis for selective and productive C-O functional group introduction and modification. *Chem. Soc. Rev.* **2013,** *42*, 6346-6377; (b) Wachtmeister, J.; Rother, D., Recent advances in whole cell biocatalysis techniques bridging from investigative to industrial scale. *Curr. Opin. Biotechnol.* **2016,** *42*, 169-177; (c) Maugeri, Z.; Domínguez de María, P., Whole-Cell Biocatalysis in Deep-Eutectic-Solvents/Aqueous Mixtures. *ChemCatChem* **2014,** *6*, 1535-1537.

2. (a) Fessner, W. D., Systems Biocatalysis: Development and engineering of cell-free "artificial metabolisms" for preparative multi-enzymatic synthesis. *N. Biotechnol.* **2015,** *32* (6), 658-64; (b) Schmid-Dannert, C.; Lopez-Gallego, F., Advances and opportunities for the design of self-sufficient and spatially organized cell-free biocatalytic systems. *Curr. Opin. Chem. Biol.* **2019,** *49*, 97-104; (c) Petroll, K.; Kopp, D.; Care, A.; Bergquist, P. L.; Sunna, A., Tools and strategies for constructing cell-free enzyme pathways. *Biotechnol. Adv.* **2019,** *37* (1), 91-108.

3. (a) Es, I.; Vieira, J. D.; Amaral, A. C., Principles, techniques, and applications of biocatalyst immobilization for industrial application. *Appl. Microbiol. Biotechnol.* **2015,** *99*, 2065-2082; (b) Cipolatti, E. P.; Valério, A.; Henriques, R. O.; Moritz, D. E.; Ninow, J. L.; Freire, D. M. G.; Manoel, E. A.; Fernandez-Lafuente, R.; de Oliveira, D., Nanomaterials for biocatalyst immobilization – state of the art and future trends. *RSC Adv.* **2016,** *6*, 104675-104692; (c) Prakasham, R. S.; Devi, G. S.; Rao, C. S.; Sivakumar, V. S. S.; Sathish, T.; Sarma, P. N., Nickel-impregnated silica nanoparticle synthesis and their evaluation for biocatalyst immobilization. *Appl. Biochem. Biotechnol.* **2010,** *160*, 1888-1895.

4. (a) Bornscheuer, U. T.; Huisman, G. W.; Kazlauskas, R. J.; Lutz, S.; Moore, J. C.; Robins, K., Engineering the third wave of biocatalysis. *Nature* **2012,** *485*, 185-194; (b) Sheldon, R. A.; Woodley, J. M., Role of Biocatalysis in Sustainable Chemistry. *Chem. Rev.* **2017,** *118*, 801-838; (c) Sheldon, R. A.; van Pelt, S., Enzyme immobilisation in biocatalysis: why, what and how. *Chem. Soc. Rev.* **2013,** *42*, 6223-6235.

5. Jensen, V. J.; Rugh, S., Industrial-Scale Production and Application of Immobilized Glucose Isomerase *Methods Enzymol.* **1987,** *136*, 356-370.

6. Hansen, R. B.; Agerbaek, M. A.; Nielsen, P. M.; Rancke-Madsen, A.; Woodley, J. M., Esterification using a liquid lipase to remove residual free fatty acids in biodiesel. *Process Biochem.* **2020,** *97*, 213-221.

7. (a) Tufvesson, P.; Lima-Ramos, J.; Nordblad, M.; Woodley, J. M., Guidelines and Cost Analysis for Catalyst Production in Biocatalytic Processes. *Org. Process Res. Dev.* **2011,** *15*, 266-274; (b) Sheldon, R. A.; Brady, D., Broadening the Scope of Biocatalysis in Sustainable Organic Synthesis. *ChemSusChem* **2019,** *12*, 2859-2881; (c) Sheldon, R. A.; Pereira, P. C., Biocatalysis engineering: the big picture. *Chem. Soc. Rev.* **2017,** *46*, 2678-2691.

8. (a) Britton, J.; Majumdar, S.; Weiss, G. A., Continuous flow biocatalysis. *Chem. Soc. Rev.* **2018,** *47*, 5891-5918; (b) Guo, F.; Berglund, P., Transaminase biocatalysis: optimization and application. *Green Chem.* **2017,** *19* (2), 333-360; (c) Rudroff, F.; Mihovilovic, M. D.; Gröger, H.; Snajdrova, R.; Iding, H.; Bornscheuer, U. T., Opportunities and challenges for combining chemo- and biocatalysis. *Nat. Catal.* **2018,** *1*, 12-22.

9. (a) Sun, H.; Zhang, H.; Ang, E. L.; Zhao, H., Biocatalysis for the synthesis of pharmaceuticals and pharmaceutical intermediates. *Bioorg. Med. Chem.* **2018,** *26* (7), 1275-1284; (b) Truppo, M. D., Biocatalysis in the Pharmaceutical Industry: The Need for Speed. *ACS Med. Chem. Lett.* **2017,** *8* (5), 476-480; (c) Patel, R. N., Biocatalysis: Synthesis of Key Intermediates for Development of Pharmaceuticals. *ACS Catal.* **2011,** *1*, 1056-1074.

10. Patel, R. N., Biocatalysis for synthesis of pharmaceuticals. *Bioorg. Med. Chem.* **2018,** *26* (7), 1252-1274.

11. (a) Heider, P. L.; Born, S. C.; Basak, S.; Benyahia, B.; Lakerveld, R.; Zhang, H.; Hogan, R.; Buchbinder, L.; Wolfe, A.; Mascia, S.; Evans, J. M. B.; Jamison, T. F.; Jensen, K. F., Development of a Multi-Step Synthesis and Workup Sequence for an Integrated, Continuous Manufacturing Process of a Pharmaceutical. *Org. Process Res. Dev.* **2014,** *18* (3), 402-409; (b) Adamo, A.; Beingessner, R. L.; Behnam, M.; Chen, J.; Jamison, T. F.; Jensen, K. F.; Monbaliu, J. M.; Myerson, A. S.; Revalor, E. M.; Snead, D. R.; Stelzer, T.; Weeranoppanant, N.; Wong, S. Y.; Zhang, P., On-demand continuous-flow production of pharmaceuticals in a compact, reconfigurable system. *Science* **2016,** *352*, 61-67; (c) Vaxelaire, C.; Winter, P.; Christmann, M., One-pot reactions accelerate the synthesis of active pharmaceutical ingredients. *Angew. Chem. Int. Ed.* **2011,** *50* (16), 3605-7.

12. (a) Beilin, E.; Baker, L. J.; Aikins, J.; Baryla, N. E., Effect of incomplete removal of the tert-butoxycarbonyl protecting group during synthesis of a pharmaceutical drug substance on the residual solvent analysis. *J. Pharm. Biomed. Anal.* **2010,** *52* (2), 316-9; (b) Acosta, J.; del Arco, J.; Martinez-Pascual, S.; Clemente-Suárez, V.; Fernández-Lucas, J., One-Pot Multi-Enzymatic Production of Purine Derivatives with Application in Pharmaceutical and Food Industry. *Catalysts* **2018,** *8* (1), 9; (c)

Zhao, Y.; Barrera, E. V., Asymmmetric Diamino Functionalization of Nanotubes Assisted by BOC Protection and Their Epoxy Nanocomposites. *Adv. Funct. Mater.* **2010,** *20* (18), 3039-3044.

13. (a) Chen, W.-H.; Vázquez-González, M.; Zoabi, A.; Abu-Reziq, R.; Willner, I., Biocatalytic cascades driven by enzymes encapsulated in metal–organic framework nanoparticles. *Nat. Catal.* **2018,** *1* (9), 689-695; (b) Schrittwieser, J. H.; Sattler, J.; Resch, V.; Mutti, F. G.; Kroutil, W., Recent biocatalytic oxidation-reduction cascades. *Curr. Opin. Chem. Biol.* **2011,** *15* (2), 249-56; (c) Huffman, M. A.; Fryszkowska, A.; Alvizo, O.; Borra-Garske, M.; Campos, K. R.; Canada, K. A.; Devine, P. N.; Duan, D.; Forstater, J. H.; Grosser, S. T.; Halsey, H. M.; Hughes, G. J.; Jo, J.; Joyce, L. A.; Kolev, J. N.; Liang, J.; Maloney, K. M.; Mann, B. F.; Marshall, N. M.; McLaughlin, M.; Moore, J. C.; Murphy, G. S.; Nawrat, C. C.; Nazor, J.; Novick, S.; Patel, N. R.; Rodriguez-Granillo, A.; Robaire, S. A.; Sherer, E. C.; Truppo, M. D.; Whittaker, A. M.; Verma, D.; Xiao, L.; Xu, Y.; Yang, H., Design of an in vitro biocatalytic cascade for the manufacture of islatravir. *Science* **2019,** *366*, 1255-1259.

14. Schrittwieser, J. H.; Velikogne, S.; Hall, M.; Kroutil, W., Artificial Biocatalytic Linear Cascades for Preparation of Organic Molecules. *Chem. Rev.* **2018,** *118* (1), 270-348.

15. Schmidt-Dannert, C.; Lopez-Gallego, F., A roadmap for biocatalysis - functional and spatial orchestration of enzyme cascades. *Microb. Biotechnol.* **2016,** *9* (5), 601-9.

16. France, S. P.; Hepworth, L. J.; Turner, N. J.; Flitsch, S. L., Constructing Biocatalytic Cascades: In Vitro and in Vivo Approaches to de Novo Multi-Enzyme Pathways. *ACS Catal.* **2017,** *7*, 710-724.

17. (a) Arnold, F. H., Directed Evolution: Bringing New Chemistry to Life. *Angew. Chem. Int. Ed.* **2018,** *57*, 4143-4148; (b) Denard, C. A.; Ren, H.; Zhao, H., Improving and repurposing biocatalysts via directed evolution. *Curr. Opin. Chem. Biol.* **2015,** *25*, 55-64; (c) Currin, A.; Swainston, N.; Day, P. J.; Kell, D. B., Synthetic biology for the directed evolution of protein biocatalysts: navigating sequence space intelligently. *Chem. Soc. Rev.* **2015,** *44* (5), 1172-239.

18. (a) Bommarius, A. S.; Blum, J. K.; Abrahamson, M. J., Status of protein engineering for biocatalysts: how to design an industrially useful biocatalyst. *Curr. Opin. Chem. Biol.* **2011,** *15*, 194-200; (b) Bernal, C.; Rodriguez, K.; Martinez, R., Integrating enzyme immobilization and protein engineering: An alternative path for the development of novel and improved industrial biocatalysts. *Biotechnol. Adv.* **2018,** *36* (5), 1470-1480; (c) Behrens, G. A.; Hummel, A.; Padhi, S. K.; Schätzle, S.; Bornscheuer, U. T., Discovery and Protein Engineering of Biocatalysts for Organic Synthesis. *Adv. Synth. Catal.* **2011,** *353* (13), 2191-2215.

19. (a) Lutz, S., Beyond directed evolution--semi-rational protein engineering and design. *Curr. Opin. Biotechnol.* **2010,** *21* (6), 734-43; (b) Güven, G.; Prodanovic, R.; Schwaneberg, U., Protein Engineering - An Option for Enzymatic Biofuel Cell Design. *Electroanalysis* **2010,** *22* (7-8), 765-775; (c) Bottcher, D.; Bornscheuer, U. T., Protein engineering of microbial enzymes. *Curr. Opin. Microbiol.* **2010,** *13* (3), 274-82.

20. (a) Richter, F.; Leaver-Fay, A.; Khare, S. D.; Bjelic, S.; Baker, D., De Novo Enzyme Design Using Rosetta3. *PLoS One* **2011,** *6*, e19230; (b) Kries, H.; Blomberg, R.; Hilvert, D., De novo enzymes by computational design. *Curr. Opin. Chem. Biol.* **2013,** *17* (2), 221-8; (c) Huang, P. S.; Boyken, S. E.; Baker, D., The coming of age of de novo protein design. *Nature* **2016,** *537* (7620), 320-7.

21. (a) Turner, N. J.; O'Reilly, E., Biocatalytic retrosynthesis. *Nat. Chem. Biol.* **2013,** *9* (5), 285-8; (b) de Souza, R.; Miranda, L. S. M.; Bornscheuer, U. T., A Retrosynthesis Approach for Biocatalysis in Organic Synthesis. *Chemistry* **2017,** *23* (50), 12040-12063; (c) Green, A. P.; Turner, N. J., Biocatalytic retrosynthesis: Redesigning synthetic routes to high-value chemicals. *Perspect. Sci.* **2016,** *9*, 42-48.

22. (a) Lima-Ramos, J.; Neto, W.; Woodley, J. M., Engineering of Biocatalysts and Biocatalytic Processes. *Top. Catal.* **2014,** *57*, 301-320; (b) Woodley, J. M., Integrating protein engineering with process design for biocatalysis. *Phil. Trans. R. Soc. A* **2017,** *376*; (c) Tufvesson, P.; Fu, W.; Jensen, J. S.; Woodley, J. M., Process considerations for the scale-up and implementation of biocatalysis. *Food Bioprod. Process.* **2010,** *88*, 3-11.

23. (a) Lima-Ramos, J.; Tufvesson, P.; Woodley, J. M., Application of environmental and economic metrics to guide the development of biocatalytic processes. *Green. Process Synth.* **2014,** *3* (3), 195-213; (b) Tufvesson, P.; Lima-Ramos, J.; Haque, N. A.; Gernaey, K. V.; Woodley, J. M., Advances in the Process Development of Biocatalytic Processes. *Org. Process Res. Dev.* **2013,** *17* (10), 1233-1238.

24. (a) Woodley, J. M., New frontiers in biocatalysis for sustainable synthesis. *Curr. Opin. Green Sustain. Chem.* **2020,** *21*, 22-26; (b) Delgove, M. A. F.; Laurent, A. B.; Woodley, J. M.; De Wildeman, S. M. A.; Bernaerts, K. V.; van der Meer, Y., A Prospective Life Cycle Assessment (LCA) of Monomer Synthesis: Comparison of Biocatalytic and Oxidative Chemistry. *ChemSusChem* **2019,** *12* (7), 1349-1360.

25. (a) Centi, G.; Cavani, F.; Trifiro, F., *Selective Oxidation by Heterogeneous Catalysis*. Springer Science: New York, USA, 2001; (b) Guo, Z.; Liu, B.; Zhang, Q.; Deng, W.; Wang, Y.; Yang, Y., Recent advances in heterogeneous selective oxidation catalysis for sustainable chemistry. *Chem. Soc. Rev.* **2014,** *43* (10), 3480-524.

26. Zope, B. N.; Hibbitts, D. D.; Neurock, M.; Davis, R. J., Reactivity of the Gold/Water Interface During Selective Oxidation Catalysis. *Science* **2010,** *330*, 74-78.

27. Pina, C. D.; Falletta, E.; Rossi, M., Update on selective oxidation using gold. *Chem. Soc. Rev.* **2012,** *41* (1), 350-69.

28. (a) Staudt, S.; Bornscheuer, U. T.; Menyes, U.; Hummel, W.; Groger, H., Direct biocatalytic one-pot-transformation of cyclohexanol with molecular oxygen into varepsilon-caprolactone. *Enzyme Microb. Technol.* **2013,** *53* (4), 288-92; (b) Torres Pazmino, D. E.; Winkler, M.; Glieder, A.; Fraaije, M. W., Monooxygenases as biocatalysts: Classification, mechanistic aspects and biotechnological applications. *J. Biotechnol.* **2010,** *146* (1-2), 9-24; (c) Holtmann, D.; Fraaije, M. W.; Arends, I. W.; Opperman, D. J.; Hollmann, F., The taming of oxygen: biocatalytic oxyfunctionalisations. *Chem. Commun.* **2014,** *50* (87), 13180-200.

29. (a) Tieves, F.; Willot, S. J.; van Schie, M. M. C. H.; Rauch, M. C. R.; Younes, S. H. H.; Zhang, W.; Dong, J.; Gomez de Santos, P.; Robbins, J. M.; Bommarius, B.; Alcalde, M.; Bommarius, A. S.; Hollmann, F., Formate Oxidase (FOx) from Aspergillus oryzae: One Catalyst Enables Diverse H2 O2 -Dependent Biocatalytic Oxidation Reactions. *Angew. Chem. Int. Ed.* **2019,** *58* (23), 7873-7877; (b) Pollegioni, L.; Motta, P.; Molla, G., L-amino acid oxidase as biocatalyst: a dream too far? *Appl. Microbiol. Biotechnol.* **2013,** *97* (21), 9323-41; (c) Habib, M. H. M.; Deuss, P. J.; Lončar, N.; Trajkovic, M.; Fraaije, M. W., A Biocatalytic One-Pot Approach for the Preparation of Lignin Oligomers Using an Oxidase/Peroxidase Cascade Enzyme System. *Adv. Synth. Catal.* **2017,** *359* (19), 3354-3361.

30. (a) Black, W. B.; Zhang, L.; Mak, W. S.; Maxel, S.; Cui, Y.; King, E.; Fong, B.; Sanchez Martinez, A.; Siegel, J. B.; Li, H., Engineering a nicotinamide mononucleotide redox cofactor system for biocatalysis. *Nat. Chem. Biol.* **2020,** *16* (1), 87-94; (b) Wu, X.; Jiang, J.; Chen, Y., Correlation between Intracellular Cofactor Concentrations and Biocatalytic Efficiency: Coexpression of Diketoreductase and Glucose Dehydrogenase for the Preparation of Chiral Diol for Statin Drugs. *ACS Catal.* **2011,** *1* (12), 1661-1664; (c) Baumer, B.; Classen, T.; Pohl, M.; Pietruszka, J., Efficient Nicotinamide Adenine Dinucleotide Phosphate [NADP(H)] Recycling in Closed-Loop Continuous Flow Biocatalysis. *Adv. Synth. Catal.* **2020,** *362* (14), 2894-2901.

31. (a) Lim, J. H.; Seo, S. W.; Kim, S. Y.; Jung, G. Y., Refactoring redox cofactor regeneration for high-yield biocatalysis of glucose to butyric acid in Escherichia coli. *Bioresour. Technol.* **2013,** *135*, 568-73; (b) Hollmann, F.; Arends, I. W. C. E.; Buehler, K., Biocatalytic Redox Reactions for Organic Synthesis: Nonconventional Regeneration Methods. *ChemCatChem* **2010,** *2* (7), 762-782; (c) Kim, J.; Lee, S. H.; Tieves, F.; Choi, D. S.; Hollmann, F.; Paul, C. E.; Park, C. B., Biocatalytic C=C Bond

Reduction through Carbon Nanodot-Sensitized Regeneration of NADH Analogues. *Angew. Chem. Int. Ed.* **2018,** *57*, 13825-13828.

32. (a) Patel, N. R.; Nawrat, C. C.; McLaughlin, M.; Xu, Y.; Huffman, M. A.; Yang, H.; Li, H.; Whittaker, A. M.; Andreani, T.; Levesque, F.; Fryszkowska, A.; Brunskill, A.; Tschaen, D. M.; Maloney, K. M., Synthesis of Islatravir Enabled by a Catalytic, Enantioselective Alkynylation of a Ketone. *Org. Lett.* **2020,** *22* (12), 4659-4664; (b) Mattey, A. P.; Sangster, J. J.; Ramsden, J. I.; Baldwin, C.; Birmingham, W. R.; Heath, R. S.; Angelastro, A.; Turner, N. J.; Cosgrove, S. C.; Flitsch, S. L., Natural heterogeneous catalysis with immobilised oxidase biocatalysts. *RSC Adv.* **2020,** *10* (33), 19501-19505.

33. (a) Wong, K. S.; Fong, W. P.; Tsang, P. W., A single Phe54Tyr substitution improves the catalytic activity and thermostability of Trigonopsis variabilis D-amino acid oxidase. *N. Biotechnol.* **2010,** *27* (1), 78-84; (b) Nohair, B.; Thao, P. t. H.; Nguyen, V. T. H.; Tien, P. Q.; Phuong, D. T.; Hy, L. G.; Kaliaguine, S., Hybrid Periodic Mesoporous Organosilicas (PMO-SBA-16): A Support for Immobilization of d-Amino Acid Oxidase and Glutaryl-7-amino Cephalosporanic Acid Acylase Enzymes. *J. Phys. Chem. C* **2012,** *116* (20), 10904-10912; (c) Pollegioni, L.; Molla, G., New biotech applications from evolved D-amino acid oxidases. *Trends Biotechnol.* **2011,** *29* (6), 276-83.

34. (a) Yuan, B.; Page, A.; Worrall, C. P.; Escalettes, F.; Willies, S. C.; McDouall, J. J.; Turner, N. J.; Clayden, J., Biocatalytic desymmetrization of an atropisomer with both an enantioselective oxidase and ketoreductases. *Angew. Chem. Int. Ed.* **2010,** *49* (39), 7010-3; (b) Zajkoska, P.; Rosenberg, M.; Heath, R.; Malone, K. J.; Stloukal, R.; Turner, N. J.; Rebros, M., Immobilised whole-cell recombinant monoamine oxidase biocatalysis. *Appl. Microbiol. Biotechnol.* **2015,** *99* (3), 1229-36.

35. (a) Jones, E.; McClean, K.; Housden, S.; Gasparini, G.; Archer, I., Biocatalytic oxidase: Batch to continuous. *Chem. Eng. Res. Des.* **2012,** *90*, 726-731; (b) Gasparini, G.; Archer, I.; Jones, E.; Ashe, R., Scaling Up Biocatalysis Reactions in Flow Reactors. *Org. Process Res. Dev.* **2012,** *16*, 1013-1016; (c) Li, G.; Ren, J.; Iwaki, H.; Zhang, D.; Hasegawa, Y.; Wu, Q.; Feng, J.; Lau, P. C.; Zhu, D., Substrate profiling of cyclohexylamine oxidase and its mutants reveals new biocatalytic potential in deracemization of racemic amines. *Appl. Microbiol. Biotechnol.* **2014,** *98* (4), 1681-9; (d) Yao, P.; Cong, P.; Gong, R.; Li, J.; Li, G.; Ren, J.; Feng, J.; Lin, J.; Lau, P. C. K.; Wu, Q.; Zhu, D., Biocatalytic Route to Chiral 2-Substituted-1,2,3,4-Tetrahydroquinolines Using Cyclohexylamine Oxidase Muteins. *ACS Catal.* **2018,** *8* (3), 1648-1652.

36. Scalacci, N.; Black, G. W.; Mattedi, G.; Brown, N. L.; Turner, N. J.; Castagnolo, D., Unveiling the Biocatalytic Aromatizing Activity of Monoamine Oxidases MAO-N and 6-HDNO: Development of Chemoenzymatic Cascades for the Synthesis of Pyrroles. *ACS Catal.* **2017,** *7* (2), 1295-1300.

37. (a) Pedersen, A. T.; de Carvalho, T. M.; Sutherland, E.; Rehn, G.; Ashe, R.; Woodley, J. M., Characterization of a Continuous Agitated Cell Reactor for Oxygen Dependent Biocatalysis. *Biotechnol. Bioeng.* **2017,** *114*, 1222-1230; (b) Decamps, K.; Joye, I. J.; Haltrich, D.; Nicolas, J.; Courtin, C. M.; Delcour, J. A., Biochemical characteristics of Trametes multicolor pyranose oxidase and Aspergillus niger glucose oxidase and implications for their functionality in wheat flour dough. *Food Chem.* **2012,** *131* (4), 1485-1492; (c) Mu, Q.; Cui, Y.; Tian, Y.; Hu, M.; Tao, Y.; Wu, B., Thermostability improvement of the glucose oxidase from Aspergillus niger for efficient gluconic acid production via computational design. *Int. J. Biol. Macromol.* **2019,** *136*, 1060-1068.

38. Perez Galende, P.; Hidalgo Cuadrado, N.; Kostetsky, E. Y.; Roig, M. G.; Villar, E.; Shnyrov, V. L.; Kennedy, J. F., Kinetics of Spanish broom peroxidase obeys a Ping-Pong Bi-Bi mechanism with competitive inhibition by substrates. *Int. J. Biol. Macromol.* **2015,** *81*, 1005-1011.

39. Ringborg, R. H.; Pedersen, A. T.; Woodley, J. M., Automated Determination of Oxygen-Dependent Enzyme Kinetics in a Tube-in-Tube Flow Reactor. *ChemCatChem* **2017,** *9*, 3285-3288.

40. Sander, R., Henry's Law Constants. In *NIST Chemistry WebBook, NIST Standard Reference Database Number 69*, P.J., L.; W.G., M., Eds. National Institute of Standards and Technology: Gaithersburg MD, 2018.

41. Schomburg, I.; Chang, A.; Ebeling, C.; Gremse, M.; Heldt, C.; Huhn, G.; Schomburg, D., BRENDA, the enzyme database: updates and major new developments. *Nucleic Acids Res.* **2004,** *32*, D431-3.

42. Hernandez, K.; Berenguer-Murcia, A.; Rodrigues, R. C.; Fernandez-Lafuente, R., Hydrogen Peroxide in Biocatalysis. A Dangerous Liaison. *Curr. Org. Chem.* **2012,** *16*, 2652-2672.

43. Bao, J.; Furumoto, K.; Yoshimoto, M.; Fukunaga, K.; Nakao, K., Competitive inhibition by hydrogen peroxide produced in glucose oxidation catalyzed by glucose oxidase. *Biochem. Eng. J.* **2003,** *13*, 69-72.

44. (a) He, W.; Zhou, Y. T.; Wamer, W. G.; Hu, X.; Wu, X.; Zheng, Z.; Boudreau, M. D.; Yin, J. J., Intrinsic catalytic activity of Au nanoparticles with respect to hydrogen peroxide decomposition and superoxide scavenging. *Biomaterials* **2013,** *34* (3), 765-73; (b) Rey, A.; Zazo, J. A.; Casas, J. A.; Bahamonde, A.; Rodriguez, J. J., Influence of the structural and surface characteristics of activated carbon on the catalytic decomposition of hydrogen peroxide. *Appl. Catal. A: Gen.* **2011,** *402* (1-2), 146-155; (c) Lee, H.; Lee, H. J.; Sedlak, D. L.; Lee, C., pH-Dependent reactivity of oxidants formed by iron and copper-catalyzed decomposition of hydrogen peroxide. *Chemosphere* **2013,** *92* (6), 652-8.

45. Gebicki, J. M., Oxidative stress, free radicals and protein peroxides. *Arch. Biochem. Biophys.* **2016,** *595*, 33-9.

46. May, S. A., Flow chemistry, continuous processing, and continuous manufacturing: A pharmaceutical perspective. *J. Flow Chem.* **2017,** *7* (3–4), 137-145.

47. Klutz, S.; Magnus, J.; Lobedann, M.; Schwan, P.; Maiser, B.; Niklas, J.; Temming, M.; Schembecker, G., Developing the biofacility of the future based on continuous processing and single-use technology. *J. Biotechnol.* **2015,** *213*, 120-30.

48. Dallinger, D.; Kappe, C. O., Why flow means green – Evaluating the merits of continuous processing in the context of sustainability. *Curr. Opin. Green Sustain. Chem.* **2017,** *7*, 6-12.

49. Porta, R.; Benaglia, M.; Puglisi, A., Flow Chemistry: Recent Developments in the Synthesis of Pharmaceutical Products. *Org. Process Res. Dev.* **2015,** *20*, 2-25.

50. (a) Ceccoli, R. D.; Bianchi, D. A.; Rial, D. V., Flavoprotein monooxygenases for oxidative biocatalysis: recombinant expression in microbial hosts and applications. *Front. Microbiol.* **2014,** *5*, 25; (b) Reetz, M. T., Biocatalysis in Organic Chemistry and Biotechnology: Past, Present, and Future. *J. Am. Chem. Soc.* **2013,** *135*, 12480-12496; (c) Fesko, K.; Gruber-Khadjawi, M., Biocatalytic Methods for C□ C Bond Formation. *ChemCatChem* **2013,** *5* (6), 1248-1272.

51. Woodley, J. M., Scale-Up and Development of Enzyme-Based Processes for Large-Scale Synthesis Applications. In *Science of Synthesis: Biocatalysis in Organic Synthesis*, Faber, K.; Fessner, W. D.; Turner, N. J., Eds. Thieme: Stuttgart, 2015; Vol. 3, pp 515-546.

52. (a) Zhou, X.; Lü, S.; Xu, Y.; Mo, Y.; Yu, S., Improving the performance of cell biocatalysis and the productivity of xylonic acid using a compressed oxygen supply. *Biochem. Eng. J.* **2015,** *93*, 196-199; (b) Dennewald, D.; Hortsch, R.; Weuster-Botz, D., Evaluation of parallel milliliter-scale stirred-tank bioreactors for the study of biphasic whole-cell biocatalysis with ionic liquids. *J. Biotechnol.* **2012,** *157*, 253-257.

53. (a) Zhang, J.; Fang, X.; Zhu, X.-L.; Li, Y.; Xu, H.-P.; Zhao, B.-F.; Chen, L.; Zhang, X.-D., Microbial lipid production by the oleaginous yeast Cryptococcus curvatus O3 grown in fed-batch culture. *Biomass Bioenergy* **2011,** *35* (5), 1906-1911; (b) Gomes, N.; Teixeira, J. A.; Belo, I., Fed-batch versus batch cultures of Yarrowia lipolytica for gamma-decalactone production from methyl ricinoleate. *Biotechnol. Lett.* **2012,** *34* (4), 649-654.

54. Tran, D.-T.; Chen, C.-L.; Chang, J.-S., Continuous biodiesel conversion via enzymatic transesterification catalyzed by immobilized Burkholderia lipase in a packed-bed bioreactor. *Appl. Energ.* **2016,** *168*, 340-350.

55. Xu, Y.; Nordblad, M.; Woodley, J. M., A two-stage enzymatic ethanol-based biodiesel production in a packed bed reactor. *J. Biotechnol.* **2012,** *162* (4), 407-414.

56. (a) Mohr, S.; Fisher, K.; Scrutton, N. S.; Goddard, N. J.; Fielden, P. R., Continuous two-phase flow miniaturised bioreactor for monitoring anaerobic biocatalysis by pentaerythritol tetranitrate reductase. *Lab on a chip* **2010,** *10* (15), 1929-36; (b) Britton, J.; Raston, C. L.; Weiss, G. A., Rapid protein immobilization for thin film continuous flow biocatalysis. *Chem. Commun.* **2016,** *52* (66), 10159-62.

57. Valera, F. E.; Quaranta, M.; Moran, A.; Blacker, J.; Armstrong, A.; Cabral, J. T.; Blackmond, D. G., The flow's the thing... or is it? Assessing the merits of homogeneous reactions in flask and flow. *Angew. Chem. Int. Ed.* **2010,** *49*, 2478-2485.

58. (a) Qiu, Z.; Zhao, L.; Weatherley, L., Process intensification technologies in continuous biodiesel production. *Chem. Eng. Process.* **2010,** *49* (4), 323-330; (b) Tamborini, L.; Fernandes, P.; Paradisi, F.; Molinari, F., Flow Bioreactors as Complementary Tools for Biocatalytic Process Intensification. *Trends Biotechnol.* **2018,** *36*, 73-88; (c) Xu, F.; Sun, J.; Konda, N. V. S. N. M.; Shi, J.; Dutta, T.; Scown, C. D.; Simmons, B. A.; Singh, S., Transforming biomass conversion with ionic liquids: process intensification and the development of a high-gravity, one-pot process for the production of cellulosic ethanol. *Energy Environ. Sci.* **2016,** *9* (3), 1042-1049.

59. Wegner, J.; Ceylan, S.; Kirschning, A., Ten key issues in modern flow chemistry. *Chem. Commun.* **2011,** *47*, 4583-4592.

60. (a) Yuryev, R.; Strompen, S.; Liese, A., Coupled chemo(enzymatic) reactions in continuous flow. *Beilstein J. Org. Chem.* **2011,** *7*, 1449-67; (b) Morales, M.; Dapsens, P. Y.; Giovinazzo, I.; Witte, J.; Mondelli, C.; Papadokonstantakis, S.; Hungerbühler, K.; Pérez-Ramírez, J., Environmental and economic assessment of lactic acid production from glycerol using cascade bio- and chemocatalysis. *Energy Environ. Sci.* **2015,** *8* (2), 558-567; (c) Groger, H.; Hummel, W., Combining the 'two worlds' of chemocatalysis and biocatalysis towards multi-step one-pot processes in aqueous media. *Curr. Opin. Chem. Biol.* **2014,** *19*, 171-9.

61. (a) Gutmann, B.; Cantillo, D.; Kappe, C. O., Continuous-Flow Technology—A Tool for the Safe Manufacturing of Active Pharmaceutical Ingredients. *Angew. Chem. Int. Ed.* **2015,** *54*, 6688-6728; (b) Poechlauer, P.; Manley, J.; Broxterman, R.; Gregertsen, B.; Ridemark, M., Continuous Processing

in the Manufacture of Active Pharmaceutical Ingredients and Finished Dosage Forms: An Industry Perspective. *Org. Process Res. Dev.* **2012,** *16* (10), 1586-1590.

62. Wohlgemuth, R., Biocatalysis-key to sustainable industrial chemistry. *Curr. Opin. Biotechnol.* **2010,** *21*, 713-724.

63. Bordeaux, M.; Galarneau, A.; Fajula, F.; Drone, J., A regioselective biocatalyst for alkane activation under mild conditions. *Angew. Chem.* **2011,** *123*, 2123-2127.

64. Woodley, J. M., Protein engineering of enzymes for process applications. *Curr. Opin. Chem. Biol.* **2013,** *17* (2), 310-6.

65. Abu, R.; Woodley, J. M., Application of Enzyme Coupling Reactions to Shift Thermodynamically Limited Biocatalytic Reactions. *ChemCatChem* **2015,** *7*, 3094-3105.

66. Savile, C. K.; Janey, J. M.; Mundorff, E. C.; Moore, J. C.; Tam, S.; Jarvis, W. R.; Colbeck, J. C.; Krebber, A.; Fleitz, F. J.; Brands, J.; Devine, P. N.; Huisman, G. W.; Hughes, G. J., Biocatalytic Asymmetric Synthesis of Chiral Amines from Ketones Applied to Sitagliptin Manufacture. *Science* **2010,** *329*, 305-309.

67. Planchestainer, M.; Contente, M. L.; Cassidy, J.; Molinari, F.; Tamborini, L.; Paradisi, F., Continuous flow biocatalysis: production and in-line purification of amines by immobilised transaminase from Halomonas elongata. *Green Chem.* **2017,** *19*, 372-375.

68. Cerioli, L.; Planchestainer, M.; Cassidy, J.; Tessaro, D.; Paradisi, F., Characterization of a novel amine transaminase from Halomonas elongata. *J. Molec. Catal. B Enzym.* **2015,** *120*, 141-150.

69. Rakmai, J.; Cheirsilp, B., Continuous production of β-cyclodextrin by cyclodextrin glycosyltransferase immobilized in mixed gel beads: Comparative study in continuous stirred tank reactor and packed bed reactor. *Biochem. Eng. J.* **2016,** *105*, 107-113.

70. (a) Magano, J.; Dunetz, J. R., Large-scale applications of transition metal-catalyzed couplings for the synthesis of pharmaceuticals. *Chem. Rev.* **2011,** *111* (3), 2177-250; (b) Sanchez, S.; Demain, A. L., Enzymes and Bioconversions of Industrial, Pharmaceutical, and Biotechnological Significance. *Org. Process Res. Dev.* **2011,** *15*, 224-230; (c) Kelly, S. A.; Pohle, S.; Wharry, S.; Mix, S.; Allen, C. C. R.; Moody, T. S.; Gilmore, B. F., Application of omega-Transaminases in the Pharmaceutical Industry. *Chem. Rev.* **2018,** *118* (1), 349-367.

71. Xue, R.; Woodley, J. M., Process technology for multi-enzymatic reaction systems. *Bioresour. Technol.* **2012,** *115*, 183-195.

72. (a) Schmolzer, K.; Madje, K.; Nidetzky, B.; Kratzer, R., Bioprocess design guided by in situ substrate supply and product removal: process intensification for synthesis of (S)-1-(2-chlorophenyl)ethanol. *Bioresour. Technol.* **2012,** *108*, 216-23; (b) Gruber, P.; Marques, M. P. C.; O'Sullivan, B.; Baganz, F.; Wohlgemuth, R.; Szita, N., Conscious coupling: The challenges and opportunities of cascading enzymatic microreactors. *Biotechnol. J.* **2017,** *12* (7).

73. Karande, R.; Schmid, A.; Buehler, K., Miniaturizing Biocatalysis: Enzyme-Catalyzed Reactions in an Aqueous/Organic Segmented Flow Capillary Microreactor. *Adv. Synth. Catal.* **2011,** *353*, 2511-2521.

74. (a) O'Brien, M., An automated colorimetric inline titration of CO 2 concentrations in solvent flow streams using a Teflon AF-2400 tube-in-tube device. *J. CO2 Util.* **2017,** *21*, 580-588; (b) Brzozowski, M.; O'Brien, M.; Ley, S. V.; Polyzos, A., Flow Chemistry: Intelligent Processing of Gas-Liquid Transformations Using a Tube-in-Tube Reactor. *Acc. Chem. Res.* **2015,** *48*, 349-362; (c) Mastronardi, F.; Gutmann, B.; Kappe, C. O., Continuous Flow Generation and Reactions of Anhydrous Diazomethane Using a Teflon AF-2400 Tube-in-Tube Reactor. *Org. Lett.* **2013,** *15*, 5590-5593.

75. (a) Yang, L.; Nieves-Remacha, M. J.; Jensen, K. F., Simulations and analysis of multiphase transport and reaction in segmented flow microreactors. *Chem. Eng. Sci.* **2017,** *169*, 106-116; (b) Jovanovic, J.; Rebrov, E. V.; Nijhuis, T. A.; Hessel, V.; Schouten, J. C., Phase-Transfer Catalysis in Segmented Flow in a Microchannel: Fluidic Control of Selectivity and Productivity. *Ind. Eng. Chem. Res.* **2010,** *49*, 2681-2687; (c) Bolivar, J. M.; Wiesbauer, J.; Nidetzky, B., Biotransformations in microstructured reactors: more than flowing with the stream? *Trends Biotechnol.* **2011,** *29*, 333-342.

76. Kapic, A.; Heindel, T. J., Correlating Gas-Liquid Mass Transfer in a Stirred-Tank Reactor. *Chem. Eng. Res. Des.* **2006,** *84* (3), 239-245.

77. Ferreira, A.; Ferreira, C.; Teixeira, J. A.; Rocha, F., Temperature and solid properties effects on gas–liquid mass transfer. *Chem. Eng. J.* **2010,** *162* (2), 743-752.

78. Paul, E. L.; Atiemo-Obeng, V. A.; Kresta, S. M., Handbook of Industrial Mixing - Science and Practice. John Wiley & Sons: 2004.

79. Stocks, S. M., Industrial enzyme production for the food and beverage industries: process scale up and scale down. In *Microbial Production of Food Ingredients, Enzymes and Nutraceuticals*, Woodhead Publishing Limited: Cambridge, UK, 2013; pp 144-172.

80. (a) Krischan, J.; Makaruk, A.; Harasek, M., Design and scale-up of an oxidative scrubbing process for the selective removal of hydrogen sulfide from biogas. *J. Hazard. Mater.* **2012,** *215-216*, 49-56; (b) Wang, X.; Ding, J.; Guo, W.-Q.; Ren, N.-Q., Scale-up and optimization of biohydrogen production reactor from laboratory-scale to industrial-scale on the basis of computational fluid dynamics simulation. *Int. J. Hydrog. Energy* **2010,** *35* (20), 10960-10966; (c) Bashiri, H.; Bertrand, F.; Chaouki, J., Development of a multiscale model for the design and scale-up of gas/liquid stirred tank reactors. *Chem. Eng. J.* **2016,** *297*, 277-294.

81. Ye, X.; Johnson, M. D.; Diao, T.; Yates, M. H.; Stahl, S. S., Development of Safe and Scalable Continuous-Flow Methods for Palladium-Catalyzed Aerobic Oxidation Reactions. *Green Chem.* **2010,** *12* (8), 1180-1186.

82. Nordblad, M.; Gomes, M. D.; Meissner, M. P.; Ramesh, H.; Woodley, J. M., Scoping Biocatalyst Performance Using Reaction Trajectory Analysis. *Org. Process Res. Dev.* **2018,** *22* (9), 1101-1114.

83. Doukyu, N.; Ogino, H., Organic solvent-tolerant enzymes. *Biochem. Eng. J.* **2010,** *48* (3), 270-282.

84. Lee, A.; Chaibakhsh, N.; Rahman, M. B. A.; Basri, M.; Tejo, B. A., Optimized enzymatic synthesis of levulinate ester in solvent-free system. *Ind. Crops Prod.* **2010,** *32* (3), 246-251.

85. Luo, J.; Morthensen, S. T.; Meyer, A. S.; Pinelo, M., Filtration behavior of casein glycomacropeptide (CGMP) in an enzymatic membrane reactor: fouling control by membrane selection and threshold flux operation. *J. Memb. Sci.* **2014,** *469*, 127-139.

86. Bezerra, R. M.; Neto, D. M. A.; Galvão, W. S.; Rios, N. S.; Carvalho, A. C. L. d. M.; Correa, M. A.; Bohn, F.; Fernandez-Lafuente, R.; Fechine, P. B. A.; de Mattos, M. C.; dos Santos, J. C. S.; Gonçalves, L. R. B., Design of a lipase-nano particle biocatalysts and its use in the kinetic resolution of medicament precursors. *Biochem. Eng. J.* **2017,** *125*, 104-115.

87. (a) Popat, A.; Hartono, S. B.; Stahr, F.; Liu, J.; Qiao, S. Z.; Qing Max Lu, G., Mesoporous silica nanoparticles for bioadsorption, enzyme immobilisation, and delivery carriers. *Nanoscale* **2011,** *3* (7), 2801-18; (b) Palomo, J. M.; Munoz, G.; Fernandez-Lorente, G.; Mateo, C.; Fernandez-Lafuente, R.;

Guisan, J. M., Interfacial adsorption of lipases on very hydrophobic support (octadecyl–Sepabeads): immobilization, hyperactivation and stabilization of the open form of lipases. *J. Mol. Catal. B: Enzym.* **2002,** *19-20*, 279-286; (c) Rios, N. S.; Pinheiro, M. P.; dos Santos, J. C. S.; de S. Fonseca, T.; Lima, L. D.; de Mattos, M. C.; Freire, D. M. G.; da Silva, I. J.; Rodríguez-Aguado, E.; Gonçalves, L. R. B., Strategies of covalent immobilization of a recombinant Candida antarctica lipase B on pore-expanded SBA-15 and its application in the kinetic resolution of (R , S)-Phenylethyl acetate. *J. Mol. Catal. B: Enzym.* **2016,** *133*, 246-258.

88. (a) Magner, E., Immobilisation of enzymes on mesoporous silicate materials. *Chem. Soc. Rev.* **2013,** *42* (15), 6213-22; (b) Manoel, E. A.; Dos Santos, J. C.; Freire, D. M.; Rueda, N.; Fernandez-Lafuente, R., Immobilization of lipases on hydrophobic supports involves the open form of the enzyme. *Enzyme Microb. Technol.* **2015,** *71*, 53-57.

89. Jesionowski, T.; Zdarta, J.; Krajewska, B., Enzyme immobilization by adsorption: a review. *Adsorption* **2014,** *20* (5-6), 801-821.

90. Matosevic, S.; Lye, G. J.; Baganz, F., Immobilised enzyme microreactor for screening of multi-step bioconversions: characterisation of a de novo transketolase-omega-transaminase pathway to synthesise chiral amino alcohols. *J. Biotechnol.* **2011,** *155* (3), 320-9.

91. Nunes, M. A.; Rosa, M. E.; Fernandes, P. C.; Ribeiro, M. H., Operational stability of naringinase PVA lens-shaped microparticles in batch stirred reactors and mini packed bed reactors-one step closer to industry. *Bioresour. Technol.* **2014,** *164*, 362-70.

92. Sheldon, R. A., Cross-Linked Enzyme Aggregates as Industrial Biocatalysts. *Org. Process Res. Dev.* **2011,** *15* (1), 213-223.

93. (a) Xu, D. Y.; Yang, Z., Cross-linked tyrosinase aggregates for elimination of phenolic compounds from wastewater. *Chemosphere* **2013,** *92* (4), 391-8; (b) Xu, D.-Y.; Chen, J.-Y.; Yang, Z., Use of cross-linked tyrosinase aggregates as catalyst for synthesis of l-DOPA. *Biochem. Eng. J.* **2012,** *63*, 88-94.

94. (a) Lage, F. A.; Bassi, J. J.; Corradini, M. C.; Todero, L. M.; Luiz, J. H.; Mendes, A. A., Preparation of a biocatalyst via physical adsorption of lipase from Thermomyces lanuginosus on hydrophobic support to catalyze biolubricant synthesis by esterification reaction in a solvent-free system. *Enzyme Microb. Technol.* **2016,** *84*, 56-67; (b) Manoel, E. A.; Ribeiro, M. F. P.; dos Santos, J. C. S.; Coelho, M. A. Z.; Simas, A. B. C.; Fernandez-Lafuente, R.; Freire, D. M. G., Accurel MP 1000 as

a support for the immobilization of lipase from Burkholderia cepacia : Application to the kinetic resolution of myo -inositol derivatives. *Process Biochem.* **2015,** *50* (10), 1557-1564.

95. (a) Kazi, F. K.; Fortman, J. A.; Anex, R. P.; Hsu, D. D.; Aden, A.; Dutta, A.; Kothandaraman, G., Techno-economic comparison of process technologies for biochemical ethanol production from corn stover. *Fuel* **2010,** *89*, S20-S28; (b) Li, S.; Yang, X.; Yang, S.; Zhu, M.; Wang, X., Technology prospecting on enzymes: application, marketing and engineering. *Comput. Struct. Biotechnol. J.* **2012,** *2*, e201209017; (c) Chapman, J.; Ismail, A.; Dinu, C., Industrial Applications of Enzymes: Recent Advances, Techniques, and Outlooks. *Catalysts* **2018,** *8* (6), 238.

96. Chen, B.; Li, K.; Liao, L.; Wang, R.; Li, P., Ammonium Gluconate Production from Potato Starch Wastewater Using a Multi-Enzyme Process. *Am. J. Potato Res.* **2019,** *96* (5), 447-456.

97. Çetinus, Ş. A.; Öztop, H. N., Immobilization of catalase into chemically crosslinked chitosan beads. *Enzyme Microb. Technol.* **2003,** *32* (7), 889-894.

98. Colpa, D. I.; Loncar, N.; Schmidt, M.; Fraaije, M. W., Creating Oxidase–Peroxidase Fusion Enzymes as a Toolbox for Cascade Reactions. *Chembiochem : a European journal of chemical biology* **2017,** *18*, 2226-2230.

99. (a) Quijano, G.; Chávez-Avila, R.; Muñoz, R.; Thalasso, F.; Ordaz, A., KLa measurement in two-phase partitioning bioreactors: new insights on potential errors at low power input. *J. Chem. Technol. Biotechnol.* **2010,** *85* (10), 1407-1412; (b) Gabelle, J. C.; Jourdier, E.; Licht, R. B.; Ben Chaabane, F.; Henaut, I.; Morchain, J.; Augier, F., Impact of rheology on the mass transfer coefficient during the growth phase of Trichoderma reesei in stirred bioreactors. *Chem. Eng. Sci.* **2012,** *75*, 408-417; (c) Klockner, W.; Gacem, R.; Anderlei, T.; Raven, N.; Schillberg, S.; Lattermann, C.; Buchs, J., Correlation between mass transfer coefficient kLa and relevant operating parameters in cylindrical disposable shaken bioreactors on a bench-to-pilot scale. *J. Biol. Eng,* **2013,** *7*, 28.

100. (a) Pinelli, D.; Liu, Z.; Magelli, F., Analysis of KLa Measurement Methods in Stirred Vessels: The Role of Experimental Techniques and Fluid Dynamic Models. *Int. J. Chem. React. Eng.* **2010,** *8*; (b) Scargiali, F.; Busciglio, A.; Grisafi, F.; Brucato, A., Simplified dynamic pressure method for measurement in aerated bioreactors. *Biochem. Eng. J.* **2010,** *49* (2), 165-172.

101. Bolivar, J. M.; Mannsberger, A.; Thomsen, M. S.; Tekautz, G.; Nidetzky, B., Process intensification for O2 -dependent enzymatic transformations in continuous single-phase pressurized flow. *Biotechnol. Bioeng.* **2019,** *116* (3), 503-514.

102. Nicholls, P., Classical catalase: ancient and modern. *Arch. Biochem. Biophys.* **2012,** *525* (2), 95-101.

103. Chapman, M. R.; Cosgrove, S. C.; Turner, N. J.; Kapur, N.; Blacker, A. J., Highly Productive Oxidative Biocatalysis in Continuous Flow by Enhancing the Aqueous Equilibrium Solubility of Oxygen. *Angew. Chem.* **2018,** *57* (33), 10535-10539.

104. Garcia-Galan, C.; Berenguer-Murcia, Á.; Fernandez-Lafuente, R.; Rodrigues, R. C., Potential of Different Enzyme Immobilization Strategies to Improve Enzyme Performance. *Adv. Synth. Catal.* **2011,** *353* (16), 2885-2904.

105. (a) Greenfield, P. F.; Kittrell, J. R.; Laurence, R. L., Inactivation of Immobilized Glucose Oxidase by Hydrogen Peroxide. *Anal. Biochem.* **1975,** *65*, 109-124; (b) Yoshimoto, M.; Takaki, N.; Yamasaki, M., Catalase-conjugated liposomes encapsulating glucose oxidase for controlled oxidation of glucose with decomposition of hydrogen peroxide produced. *Colloids Surf. B: Biointerfaces* **2010,** *79* (2), 403-8.

106. Milton, R. D.; Giroud, F.; Thumser, A. E.; Minteer, S. D.; Slade, R. C., Hydrogen peroxide produced by glucose oxidase affects the performance of laccase cathodes in glucose/oxygen fuel cells: FAD-dependent glucose dehydrogenase as a replacement. *Phys. Chem. Chem. Phys.* **2013,** *15* (44), 19371-9.

107. Milton, R. D.; Giroud, F.; Thumser, A. E.; Minteer, S. D.; Slade, R. C., Bilirubin oxidase bioelectrocatalytic cathodes: the impact of hydrogen peroxide. *Chem. Commun.* **2014,** *50* (1), 94-6.

108. (a) Nidetzky, B., Stability and stabilization of d-amino acid oxidase from the yeast *Trigonopsis variabilis*. *Biochem. Soc. Trans.* **2007,** *35*, 1588-1592; (b) Ju, S.-S.; Lin, L.-L.; Chien, H. R.; Hsu, W.-H., Substitution of the critical methionine residues in *Trigonopsis variabilis* D-amino acid oxidase with leucine enhances its resistance to hydrogen peroxide. *FEMS Microb. Lett.* **2000,** *186*, 215-219; (c) Slavica, A.; Dib, I.; Nidetzky, B., Single-site oxidation, cysteine 108 to cysteine sulfinic acid, in D-amino acid oxidase from Trigonopsis variabilis and its structural and functional consequences. *Appl. Environ. Microbiol.* **2005,** *71* (12), 8061-8.

109. Das, S.; Glenn, J. H. t.; Subramanian, M., Enantioselective oxidation of 2-hydroxy carboxylic acids by glycolate oxidase and catalase coexpressed in methylotrophic Pichia pastoris. *Biotechnol. Prog.* **2010,** *26* (3), 607-15.

110. Vasudevan, P. T.; Weiland, R. H., Deactivation of Catalase by Hydrogen Peroxide. *Biotechnol. Bioeng.* **1990,** *36*, 783-789.

111. (a) Miyaji, A.; Suzuki, M.; Baba, T.; Kamachi, T.; Okura, I., Hydrogen peroxide as an effecter on the inactivation of particulate methane monooxygenase under aerobic conditions. *J. Mol. Catal. B: Enzym.* **2009,** *57* (1-4), 211-215; (b) Sukyai, P.; Rezic, T.; Lorenz, C.; Mueangtoom, K.; Lorenz, W.; Haltrich, D.; Ludwig, R., Comparing soluble and co-immobilized catalysts for 2-ketoaldose production by pyranose 2-oxidase and auxiliary enzymes. *J. Biotechnol.* **2008,** *135* (3), 281-90; (c) Nordkvist, M.; Nielsen, P. M.; Villadsen, J., Oxidation of lactose to lactobionic acid by a Microdochium nivale carbohydrate oxidase: kinetics and operational stability. *Biotechnol. Bioeng.* **2007,** *97* (4), 694-707.

112. Damm, M.; Gutmann, B.; Kappe, C. O., Continuous-flow synthesis of adipic acid from cyclohexene using hydrogen peroxide in high-temperature explosive regimes. *ChemSusChem* **2013,** *6* (6), 978-82.

113. (a) Wu, S.-H.; Chou, H.-C.; Pan, R.-N.; Huang, Y.-H.; Horng, J.-J.; Chi, J.-H.; Shu, C.-M., Thermal hazard analyses of organic peroxides and inorganic peroxides by calorimetric approaches. *J. Therm. Anal. Calorim.* **2011,** *109* (1), 355-364; (b) Chi, J.-H.; Wu, S.-H.; Charpentier, J.-C.; I, Y.-P.; Shu, C.-M., Thermal hazard accident investigation of hydrogen peroxide mixing with propanone employing calorimetric approaches. *J. Loss Prev. Process Ind.* **2012,** *25* (1), 142-147; (c) Zang, N.; Qian, X., Influence of Organic Acid on Thermal Hazard of Hydrogen Peroxide. *Procedia Eng.* **2012,** *45*, 526-532.

114. Sheldon, R. A., Recent advances in green catalytic oxidations of alcohols in aqueous media. *Catal. Today* **2015,** *247*, 4-13.

115. (a) Wijma, H. J.; Floor, R. J.; Janssen, D. B., Structure- and sequence-analysis inspired engineering of proteins for enhanced thermostability. *Curr. Opin. Struct. Biol.* **2013,** *23* (4), 588-94; (b) Singh, R. K.; Tiwari, M. K.; Singh, R.; Lee, J. K., From Protein Engineering to Immobilization: Promising Strategies for the Upgrade of Industrial Enzymes. *Int. J. Mol. Sci.* **2013,** *14*, 1232-1277; (c) Damborsky, J.; Brezovsky, J., Computational tools for designing and engineering enzymes. *Curr. Opin. Chem. Biol.* **2014,** *19*, 8-16.

116. Stepankova, V.; Bidmanova, S.; Koudelakova, T.; Prokop, Z.; Chaloupkova, R.; Damborsky, J., Strategies for Stabilization of Enzymes in Organic Solvents. *ACS Catal.* **2013,** *3* (12), 2823-2836.

117. Bar-Even, A.; Noor, E.; Savir, Y.; Liebermeister, W.; Davidi, D.; Tawfik, D. S.; Milo, R., The moderately efficient enzyme: evolutionary and physicochemical trends shaping enzyme parameters. *Biochemistry* **2011,** *50* (21), 4402-10.

118. Baldwin, C. V. F.; Woodley, J. M., On Oxygen Limitation in a Whole Cell Biocatalytic Baeyer-Villiger Oxidation Process. *Biotechnol. Bioeng.* **2006,** *95*, 362-369.

119. (a) Bhagia, S.; Dhir, R.; Kumar, R.; Wyman, C. E., Deactivation of Cellulase at the Air-Liquid Interface Is the Main Cause of Incomplete Cellulose Conversion at Low Enzyme Loadings. *Sci. Rep.* **2018,** *8* (1), 1350; (b) Lou, H.; Zeng, M.; Hu, Q.; Cai, C.; Lin, X.; Qiu, X.; Yang, D.; Pang, Y., Nonionic surfactants enhanced enzymatic hydrolysis of cellulose by reducing cellulase deactivation caused by shear force and air-liquid interface. *Bioresour. Technol.* **2018,** *249*, 1-8; (c) Van Hecke, W.; Haltrich, D.; Frahm, B.; Brod, H.; Dewulf, J.; Van Langenhove, H.; Ludwig, R., A biocatalytic cascade reaction sensitive to the gas–liquid interface: Modeling and upscaling in a dynamic membrane aeration reactor. *J. Mol. Catal. B: Enzym.* **2011,** *68* (2), 154-161.

120. (a) Plumere, N.; Rudiger, O.; Oughli, A. A.; Williams, R.; Vivekananthan, J.; Poller, S.; Schuhmann, W.; Lubitz, W., A redox hydrogel protects hydrogenase from high-potential deactivation and oxygen damage. *Nat. Chem.* **2014,** *6* (9), 822-7; (b) Darensbourg, M. Y.; Weigand, W., Sulfoxygenation of Active Site Models of [NiFe] and [FeFe] Hydrogenases - A Commentary on Possible Chemical Models of Hydrogenase Enzyme Oxygen Sensitivity. *Eur. J. Inorg. Chem.* **2011,** *2011* (7), 994-1004.

121. (a) Yoshimoto, M.; Yamashita, T.; Yamashiro, T., Stability and reactivity of liposome-encapsulated formate dehydrogenase and cofactor system in carbon dioxide gas-liquid flow. *Biotechnol. Prog.* **2010,** *26* (4), 1047-53; (b) Talbert, J. N.; Goddard, J. M., Enzymes on material surfaces. *Colloids Surf. B: Biointerfaces* **2012,** *93*, 8-19.

122. Pedersen, A. T.; Birmingham, W. R.; Rehn, G.; Charnock, S. J.; Turner, N. J.; Woodley, J. M., Process Requirements of Galactose Oxidase Catalyzed Oxidation of Alcohols. *Org. Process Res. Dev.* **2015,** *19* (11), 1580-1589.

123. Khalesi, M.; Venken, T.; Deckers, S.; Winterburn, J.; Shokribousjein, Z.; Gebruers, K.; Verachtert, H.; Delcour, J.; Martin, P.; Derdelinckx, G., A novel method for hydrophobin extraction using CO2 foam fractionation system. *Ind. Crops Prod.* **2013,** *43*, 372-377.

124. Routledge, S. J.; Poyner, D. R.; Bill, R. M., Antifoams: the overlooked additive? *Pharma. Bioproc.* **2014,** *2*, 103-106.

125. Kulkarni, A. A.; Joshi, J. B., Bubble Formation and Bubble Rise Velocity in Gas-Liquid Systems: A Review. *Ind. Eng. Chem. Res.* **2005,** *44*, 5873-5931.

126. Santos, R. M.; Laranjinha, J.; Barbosa, R. M.; Sirota, A., Simultaneous measurement of cholinergic tone and neuronal network dynamics in vivo in the rat brain using a novel choline oxidase based electrochemical biosensor. *Biosens. Bioelectron.* **2015,** *69*, 83-94.

127. Rosini, E.; Pollegioni, L.; Ghisla, S.; Orru, R.; Molla, G., Optimization of D-amino acid oxidase for low substrate concentrations--towards a cancer enzyme therapy. *FEBS J.* **2009,** *276* (17), 4921-32.

128. Mo, Y.; Jensen, K. F., A miniature CSTR cascade for continuous flow of reactions containing solids. *React. Chem. Eng.* **2016,** *1*, 501-507.

129. (a) Yu, H.; Tan, Z., New Correlations of Volumetric Liquid-Phase Mass Transfer Coefficients in Gas-Inducing Agitated Tank Reactors. *Int. J. Chem. React. Eng.* **2012,** *10*; (b) Mießner, U.; Kück, U. D.; Dujardin, V.; Heithoff, S.; Räbiger, N., Correlation forkLaPrediction of Airlift Loop Reactors Including the Gas Phase Residence Time Effect. *Chem. Eng. Technol.* **2015,** *38* (11), 2002-2010; (c) Kracík, T.; Petříček, R.; Moucha, T., Mass transfer in coalescent batch fermenters with mechanical agitation. *Chem. Eng. Res. Des.* **2020,** *160*, 587-592.

130. Schaepe, S.; Kuprijanov, A.; Sieblist, C.; Jenzsch, M.; Simutis, R.; Lubbert, A., kLa of stirred tank bioreactors revisited. *J. Biotechnol.* **2013,** *168* (4), 576-83.

131. Himabindu, K.; Gummadi, S., Effect of kLa and Fed-batch Strategies for Enhanced Production of Xylitol by Debaryomyces nepalensis NCYC 3413. *Br. Biotechnol. J.* **2015,** *5* (1), 24-36.

132. Gabelle, J. C.; Augier, F.; Carvalho, A.; Rousset, R.; Morchain, J., Effect of tank size on kLa and mixing time in aerated stirred reactors with non-newtonian fluids. *Can. J. Chem. Eng.* **2011,** *89* (5), 1139-1153.

133. Li, G.; Li, H.; Wei, G.; He, X.; Xu, S.; Chen, K.; Ouyang, P.; Ji, X., Hydrodynamics, mass transfer and cell growth characteristics in a novel microbubble stirred bioreactor employing sintered porous metal plate impeller as gas sparger. *Chem. Eng. Sci.* **2018,** *192*, 665-677.

134. Damiani, A. L.; Kim, M. H.; Wang, J., An Improved Dynamic Method to Measure kLa in Bioreactors. *Biotech. Bioeng.* **2014,** *111*, 2120-2125.

135. (a) Leroy, P.; Lassin, A.; Azaroual, M.; André, L., Predicting the surface tension of aqueous 1:1 electrolyte solutions at high salinity. *Geochim. Cosmochim. Acta* **2010,** *74* (19), 5427-5442; (b) Song, J.; Kim, M. W., Excess charge density and its relationship with surface tension increment at the air-electrolyte solution interface. *J. Phys. Chem. B* **2011,** *115* (8), 1856-62; (c) Wang, P.; Anderko, A.; Young,

R. D., Modeling Surface Tension of Concentrated and Mixed-Solvent Electrolyte Systems. *Ind. Eng. Chem. Res.* **2011,** *50* (7), 4086-4098.

136. (a) Sieblist, C.; Jenzsch, M.; Pohlscheidt, M., Influence of pluronic F68 on oxygen mass transfer. *Biotechnol. Prog.* **2013,** *29* (5), 1278-88; (b) Samaras, K.; Kostoglou, M.; Karapantsios, T. D.; Mavros, P., Effect of adding glycerol and Tween 80 on gas holdup and bubble size distribution in an aerated stirred tank. *Colloids Surf. A: Physicochem. Eng. Asp.* **2014,** *441*, 815-824; (c) Ramezani, M.; Legg, M. J.; Haghighat, A.; Li, Z.; Vigil, R. D.; Olsen, M. G., Experimental investigation of the effect of ethyl alcohol surfactant on oxygen mass transfer and bubble size distribution in an air-water multiphase Taylor-Couette vortex bioreactor. *Chem. Eng. J.* **2017,** *319*, 288-296.

137. (a) Marcus, Y., Surface Tension of Aqueous Electrolytes and Ions. *J. Chem. Eng. Data* **2010,** *55*, 3641-3644; (b) Yuan, Y.; Zhan, W.; Yi, H.; Zhao, Y.; Song, S., Molecular dynamics simulations study for the effect of cations hydration on the surface tension of the electrolyte solutions. *Colloids Surf. A: Physicochem. Eng. Asp.* **2018,** *539*, 80-84.

138. (a) Slavchov, R. I.; Novev, J. K., Surface tension of concentrated electrolyte solutions. *J. Colloid Interface Sci.* **2012,** *387* (1), 234-43; (b) Markovich, T.; Andelman, D.; Podgornik, R., Surface tension of electrolyte interfaces: Ionic specificity within a field-theory approach. *J. Chem. Phys.* **2015,** *142*, 044702.

139. (a) Alexandrov, N. A.; Marinova, K. G.; Gurkov, T. D.; Danov, K. D.; Kralchevsky, P. A.; Stoyanov, S. D.; Blijdenstein, T. B.; Arnaudov, L. N.; Pelan, E. G.; Lips, A., Interfacial layers from the protein HFBII hydrophobin: dynamic surface tension, dilatational elasticity and relaxation times. *J. Colloid Interface Sci.* **2012,** *376* (1), 296-306; (b) Xiong, T.; Xiong, W.; Ge, M.; Xia, J.; Li, B.; Chen, Y., Effect of high intensity ultrasound on structure and foaming properties of pea protein isolate. *Food Res. Int.* **2018,** *109*, 260-267; (c) Fang, Z.; Bhandari, B., Comparing the efficiency of protein and maltodextrin on spray drying of bayberry juice. *Food Res. Int.* **2012,** *48* (2), 478-483; (d) Gakhar, L.; Bartlett, J. A.; Penterman, J.; Mizrachi, D.; Singh, P. K.; Mallampalli, R. K.; Ramaswamy, S.; McCray, P. B., PLUNC Is a Novel Airway Surfactant Protein with Anti-Biofilm Activity. *PloS ONE* **2010,** *5(2)*, e9098.

140. (a) Hasanien, H. M.; Abd-Rabou, A. S.; Sakr, S. M., Design Optimization of Transverse Flux Linear Motor for Weight Reduction and Performance Improvement Using Response Surface Methodology and Genetic Algorithms. *IEEE Trans. Energy Convers.* **2010,** *25* (3), 598-605; (b) Homem, V.; Alves, A.; Santos, L., Amoxicillin degradation at ppb levels by Fenton's oxidation using design of experiments. *Sci. Total Environ.* **2010,** *408* (24), 6272-80; (c) Sakkas, V. A.; Islam, M. A.; Stalikas, C.;

Albanis, T. A., Photocatalytic degradation using design of experiments: a review and example of the Congo red degradation. *J. Hazard. Mater.* **2010,** *175* (1-3), 33-44.

141. (a) Hollis, P. G.; Clarke, K. G., A systematic quantification and correlation of oxygen transfer coefficients and interfacial area in simulated model hydrocarbon-based bioprocesses in stirred tank reactors. *J. Chem. Technol. Biotechnol.* **2016,** *91* (10), 2720-2728; (b) Reynoso-Cereceda, G. I.; Garcia-Cabrera, R. I.; Valdez-Cruz, N. A.; Trujillo-Roldán, M. A., Shaken flasks by resonant acoustic mixing versus orbital mixing: Mass transfer coefficient kLa characterization and Escherichia coli cultures comparison. *Biochem. Eng. J.* **2016,** *105*, 379-390.

142. Clarke, K. G.; Manyuchi, M. M., Methodology for advanced measurement accuracy of the overall volumetric oxygen transfer coefficient with application to hydrocarbon-aqueous dispersions. *J. Chem. Technol. Biotechnol.* **2012,** *87* (11), 1615-1618.

143. Baquero-Rodríguez, G. A.; Lara-Borrero, J. A., The Influence of Optic and Polarographic Dissolved Oxygen Sensors Estimating the Volumetric Oxygen Mass Transfer Coefficient (KLa). *Mod. Appl. Sci.* **2016,** *10* (8), 142.

144. (a) Yang, L.; Dietrich, N.; Hébrard, G.; Loubière, K.; Gourdon, C., Optical methods to investigate the enhancement factor of an oxygen-sensitive colorimetric reaction using microreactors. *AIChE J.* **2016,** *63* (6), 2272-2284; (b) Zıraman, D. U.; Doğan, Ö. M.; Uysal, B. Z., Mass transfer enhancement factor for chemical absorption of carbon dioxide into sodium metaborate solution. *Korean J. Chem. Eng.* **2018,** *35* (9), 1800-1806; (c) Felis, F.; Strassl, F.; Laurini, L.; Dietrich, N.; Billet, A.-M.; Roig, V.; Herres-Pawlis, S.; Loubière, K., Using a bio-inspired copper complex to investigate reactive mass transfer around an oxygen bubble rising freely in a thin-gap cell. *Chem. Eng. Sci.* **2019,** *207*, 1256-1269; (d) Khanchezar, S.; Hashemi-Najafabadi, S.; Shojaosadati, S. A.; Babaeipour, V., Hydrodynamics and mass transfer in miniaturized bubble column bioreactors. *Bioprocess Biosyst. Eng.* **2019,** *42* (2), 257-266.

145. (a) Braun, M.; Link, H.; Liu, L.; Schmid, R. D.; Weuster-Botz, D., Biocatalytic process optimization based on mechanistic modeling of cholic acid oxidation with cofactor regeneration. *Biotechnol. Bioeng.* **2011,** *108* (6), 1307-17; (b) Al-Haque, N.; Santacoloma, P. A.; Neto, W.; Tufvesson, P.; Gani, R.; Woodley, J. M., A robust methodology for kinetic model parameter estimation for biocatalytic reactions. *Biotechnol. Prog.* **2012,** *28* (5), 1186-96; (c) Wohlgemuth, R.; Plazl, I.; Znidarsic-Plazl, P.; Gernaey, K. V.; Woodley, J. M., Microscale technology and biocatalytic processes: opportunities and challenges for synthesis. *Trends Biotechnol.* **2015,** *33*, 302-314.

146. (a) Schuh, G.; Jussen, P.; Harland, T., The Digital Shadow of Services: A Reference Model for Comprehensive Data Collection in MRO Services of Machine Manufacturers. *Procedia CIRP* **2018,** *73*, 271-277; (b) Stecken, J.; Ebel, M.; Bartelt, M.; Poeppelbuss, J.; Kuhlenkotter, B., Digital Shadow Platform as an Innovative Business Model. *Procedia CIRP* **2019,** *83*, 204-209; (c) Kritzinger, W.; Karner, M.; Traar, G.; Henjes, J.; Sihn, W., Digital Twin in manufacturing: A categorical literature review and classification. *IFAC-PapersOnLine* **2018,** *51*, 1016-1022.

147. (a) Tao, F.; Cheng, J.; Qi, Q.; Zhang, M.; Zhang, H.; Sui, F., Digital twin-driven product design, manufacturing and service with big data. *Int. J. Adv. Manuf. Technol.* **2017,** *94* (9-12), 3563-3576; (b) Schleich, B.; Anwer, N.; Mathieu, L.; Wartzack, S., Shaping the digital twin for design and production engineering. *CIRP Annals* **2017,** *66* (1), 141-144; (c) Haag, S.; Anderl, R., Digital twin – Proof of concept. *Manuf. Lett.* **2018,** *15*, 64-66.

148. Yekta, R.; Dehghan, G.; Rashtbari, S.; Ghadari, R.; Moosavi-Movahedi, A. A., The inhibitory effect of farnesiferol C against catalase; Kinetics, interaction mechanism and molecular docking simulation. *Int. J. Biol. Macromol.* **2018,** *113*, 1258-1265.

149. (a) Sin, G.; Gernaey, K. V., Data handling and parameter estimation. In *Experimental Methods in Wastewater Treatment*, van Loosdrecht, M. C. M.; Nielsen, P. H.; Lopez-Vazquez, C. M.; Brdjanovic, D., Eds. IWA Publishing: London, 2016; pp 201-234; (b) Sin, G.; Meyer, A. S.; Gernaey, K. V., Assessing reliability of cellulose hydrolysis models to support biofuel process design—Identifiability and uncertainty analysis. *Comput. Chem. Eng.* **2010,** *34* (9), 1385-1392.

150. (a) Ringborg, R. H.; Woodley, J. M., The application of reaction engineering to biocatalysis. *React. Chem. Eng.* **2016,** *1* (1), 10-22; (b) Van Daele, T.; Gernaey, K. V.; Ringborg, R. H.; Borner, T.; Heintz, S.; Van Hauwermeiren, D.; Grey, C.; Kruhne, U.; Adlercreutz, P.; Nopens, I., Application of iterative robust model-based optimal experimental design for the calibration of biocatalytic models. *Biotechnol. Prog.* **2017,** *33* (5), 1278-1293.

151. (a) Zavrel, M.; Michalik, C.; Schwendt, T.; Schmidt, T.; Ansorge-Schumacher, M.; Janzen, C.; Marquardt, W.; Büchs, J.; Spiess, A. C., Systematic determination of intrinsic reaction parameters in enzyme immobilizates. *Chem. Eng. Sci.* **2010,** *65* (8), 2491-2499; (b) Eisenkolb, I.; Jensch, A.; Eisenkolb, K.; Kramer, A.; Buchholz, P. C. F.; Pleiss, J.; Spiess, A.; Radde, N. E., Modeling of biocatalytic reactions: A workflow for model calibration, selection, and validation using Bayesian statistics. *AIChE J.* **2019**; (c) Aguilar-Garnica, E.; Silva-Romero, Y. E.; Hernández-Montelongo, R.; García-Sandoval, J. P.; Aceves-Lara, C.-A., Kinetic analysis for the esterification of high free fatty acid feedstocks with a structural identifiability approach. *Eur. J. Lipid Sci. Technol.* **2014,** *116* (11), 1598-1607.

152. (a) Dormann, C. F.; Elith, J.; Bacher, S.; Buchmann, C.; Carl, G.; Carré, G.; Marquéz, J. R. G.; Gruber, B.; Lafourcade, B.; Leitão, P. J.; Münkemüller, T.; McClean, C.; Osborne, P. E.; Reineking, B.; Schröder, B.; Skidmore, A. K.; Zurell, D.; Lautenbach, S., Collinearity: a review of methods to deal with it and a simulation study evaluating their performance. *Ecography* **2013,** *36* (1), 27-46; (b) Lencastre Fernandes, R.; Bodla, V. K.; Carlquist, M.; Heins, A. L.; Eliasson Lantz, A.; Sin, G.; Gernaey, K. V., Applying mechanistic models in bioprocess development. *Adv. Biochem. Eng. Biotechnol.* **2013,** *132*, 137-66; (c) Liao, D.; Valliant, R., Condition indexes and variance decompositions for diagnosing collinearity in linear model analysis of survey data *Surv. Methodol.* **2012,** *38* (2), 189-202.

153. (a) Zhang, X.; Bao, D.; Huang, Y.; Dong, H.; Zhang, X.; Zhang, S., Gas-liquid mass-transfer properties in CO2absorption system with ionic liquids. *AIChE J.* **2014,** *60* (8), 2929-2939; (b) Bhosale, G. S.; Vaidya, P. D.; Joshi, J. B.; Patil, R. N., Kinetics of Ozonation of Phenol and Substituted Phenols. *Ind. Eng. Chem. Res.* **2019,** *58* (18), 7461-7466; (c) Dragan, S., Determining the Effective Mass Transfer Area in Three-Phase Fluidized Bed with Low Density Inert Solids. *Rev. Chim.* **2019,** *70*, 4040-4046.

154. (a) Sieblist, C.; Aehle, M.; Pohlscheidt, M.; Jenzsch, M.; Lubbert, A., A test facility for fritted spargers of production-scale-bioreactors. *Cytotechnology* **2011,** *63* (1), 49-55; (b) Ansari, S.; Jalili, H.; Bizukojc, M.; Amrane, A., Influence of the construction of porous spargers on lovastatin production by *Aspergillus terreus* ATCC 20,542 in a laboratory bubble column. *Bioprocess Biosyst. Eng.* **2019,** *42* (7), 1205-1213.

155. Amer, M.; Feng, Y.; Ramsey, J. D., Using CFD simulations and statistical analysis to correlate oxygen mass transfer coefficient to both geometrical parameters and operating conditions in a stirred-tank bioreactor. *Biotechnol. Prog.* **2019,** *35* (3), e2785.

156. (a) Xie, M.; Xia, J.; Zhou, Z.; Chu, J.; Zhuang, Y.; Zhang, S., Flow Pattern, Mixing, Gas Hold-Up and Mass Transfer Coefficient of Triple-Impeller Configurations in Stirred Tank Bioreactors. *Ind. Eng. Chem. Res.* **2014,** *53* (14), 5941-5953; (b) Labík, L.; Moucha, T.; Kordač, M.; Rejl, F. J.; Valenz, L., Gas-Liquid Mass Transfer Rates and Impeller Power Consumptions for Industrial Vessel Design. *Chem. Eng. Technol.* **2015,** *38* (9), 1646-1653; (c) Karimi, A.; Golbabei, F.; Neghab, M.; Mehrnia, M. R.; Mohammad, K.; Pourmand, M. R.; Nikpey, A., Investigation of Oxygen Transfer in a Two-phase Partition Stirred Tank Bioreactor in the Presence of Silicone Oil. *Chem. Biochem. Eng. Q.* **2011,** *25*, 209-219; (d) Petříček, R.; Moucha, T.; Rejl, F. J.; Valenz, L.; Haidl, J.; Čmelíková, T., Volumetric mass transfer coefficient, power input and gas hold-up in viscous liquid in mechanically agitated fermenters. Measurements and scale-up. *Int. J. Heat Mass Transf.* **2018,** *124*, 1117-1135.

157. Karande, R.; Debor, L.; Salamanca, D.; Bogdahn, F.; Engesser, K.; Buehler, K.; Schmid, A., Continuous Cyclohexane Oxidation to Cyclohexanol Using a Novel Cytochrome P450 Monooxygenase From *Acidovorax* sp. CHX100 in Recombinant *P. taiwanensis* VLB120 Biofilms. *Biotech. Bioeng.* **2016,** *113*, 52-61.

158. (a) Hartmann, M.; Jung, D., Biocatalysis with enzymes immobilized on mesoporous hosts: the status quo and future trends. *J. Mater. Chem.* **2010,** *20*, 844-857; (b) Ma, Y.; Li, Y.; Ali, S.; Li, P.; Zhang, W.; Rauch, M. C. R.; Willot, S. J. P.; Ribitsch, D.; Choi, Y. H.; Alcalde, M.; Hollmann, F.; Wang, Y., Natural Deep Eutectic Solvents as Performance Additives for Peroxygenase Catalysis. *ChemCatChem* **2020,** *12* (4), 989-994.

159. Siloto, R. M. P.; Weselake, R. J., Site saturation mutagenesis: Methods and applications in protein engineering. *Biocatal. Agric. Biotechnol.* **2012,** *1* (3), 181-189.

160. Zhang, W.; Xiao, S.; Ahn, D. U., Protein oxidation: basic principles and implications for meat quality. *Crit. Rev. Food Sci. Nutr.* **2013,** *53* (11), 1191-201.

161. Kovačević, G.; Ostafe, R.; Fischer, R.; Prodanović, R., Influence of methionine residue position on oxidative stability of glucose oxidase from Aspergillus niger. *Biochem. Eng. J.* **2019,** *146*, 143-149.

162. O'Brien, M.; Baxendale, I. R.; Ley, S. V., Flow Ozonolysis Using a Semipermeable Teflon AF-2400 Membrane To Effect Gas-Liquid Contact. *Org. Lett.* **2010,** *12*, 1596-1598.